

# **The Synthesis, Stability and Structures of Two Novel Macrocyclic Ligands and Their Complexes**

by

**B.F. Barnard**

Thesis presented in full fulfillment of the requirements for the degree of Master of Chemistry

at the

UNIVERSITY of STELLENBOSCH



Promoter: Dr. R.C. Luckay

*Co-promoter: Prof. H.G. Raubenheimer*

March 2008

## Declaration

I, the undersigned, hereby declare that the work contained in this thesis is my own original work and that I have not previously in its entirety or in part submitted it at any university for a degree.

Signature:.....

Date:.....

Copyright ©2008 Stellenbosch University

All rights reserved

## Abstract

This study comprises the synthesis and full characterization of two novel pendant-arm donor macrocyclic ligands. The stability and structure of the complexes of these two ligands with a series of metals ions [Mn(II), Co(II), Zn(II), Cd(II), Pb(II)], was subsequently investigated.

The two parent macrocyclic ligands, 1,4,7-triazacyclodecane ([10]-ane-N<sub>3</sub>) and 1,4,8-triazacycloundecane ([11]-ane-N<sub>3</sub>) were synthesized by means of the "direct synthesis" method using tosylates as protecting groups. Pendant arms were then added to the parent molecules to create hexadentate ligands. The two macrocyclic ligands are asymmetric because of the different lengths of the carbon bridges between the N-donor atoms of the rings. This feature gives the ligands the possibility to form both five- and six-membered rings when coordinated to metal centers. The ligands were fully characterized by means of NMR, mass spectrometry and elemental-analysis. Melting points were also determined.

These two novel (trianza macrocyclic) ligands now complete the series between 9-ane-N<sub>3</sub> [with its 2-(*S*)-hydroxypropyl pendant arms] and 12-ane-N<sub>3</sub> [with its 2-(*S*)-hydroxypropyl pendant arms].

Protonation data of the ligands were determined using potentiometric titrations. The respective protonation constants for both ligands in 0.1000 mol dm<sup>-3</sup> NaNO<sub>3</sub> are:

$$\text{THTD} \quad \log K_1^{\text{H}} = 9.176 \text{ and } \log K_2^{\text{H}} = 4.20$$

$$\text{THTUD} \quad \log K_1^{\text{H}} = 11.32 \text{ and } \log K_2^{\text{H}} = 5.87$$

A third protonation constant for both ligands (THTD and THTUD) was observed, but the use of potentiometric methods could not produce reliable values at very low pH values.

The stability constants of the new ligands with a series of metal ions were determined using 0.1000 mol dm<sup>-3</sup> NaNO<sub>3</sub> as ionic medium. The log(*K*) values at 25°C with THTD are:

Co(II) 22.93

Zn(II) 14.82

Cd(II) 19.38

Pb(II) 15.47

The log(*K*) values at 25°C with THTUD are:

Co(II) 17.52

Zn(II) 16.43

Cd(II) 18.05

Pb(II) 14.63

Very stable complexes were obtained with the larger Cd(II) ion when compared to other similar ligands.

Crystal structures of some of the metal complexes were determined by X-ray crystallography. Metal perchlorates were used in the preparation of the metal complexes with THTD and THTUD, and various methods were utilized for the crystallization process. The general formula for these complexes is  $[M(L)]^{2+} \cdot 2(ClO_4)^-$  where M=metal ion and L= neutral ligand. The bond lengths between the nitrogen atom and the metal ion, and the oxygen atom and the metal ion are very much the same in the respective crystal structures. This means that the metal ion lies almost halfway between the nitrogen and the oxygen atoms. The Mn(II)-THTD complex featured both a distorted octahedral and distorted trigonal prismatic configuration in the unit cell. Co(II)-THTUD contains three molecules per unit cell all having a distorted octahedral configuration. Zn(II)-THTUD crystallizes with six molecules per unit cell.

## Opsomming

Hierdie studie behels die bereiding en volledige karakterisering van twee oorspronklike hangkroonarmdonor makrosikliese ligande. Die stabiliteite en struktuur van komplekse van hierdie twee ligande met 'n reeks metaalione [Mn(II), Co(II), Zn(II), Cd(II), Pb(II)] is ondersoek.

Die twee basis ligande 1,4,7-triazasiklodekaan (10-ane-N<sub>3</sub>) en 1,4,8-triazasikloundekaan (11-ane-N<sub>3</sub>) is gesintetiseer deur middel van die "direkte bereidingsmetode" met tosilate as beskermingsgroepe. Hangkroonsyarms is aangeheg om die vorming van 'n heksadentate ligand te bewerkstellig. Die twee makrosikliese ligande is asimmetries as gevolg van die verskillende lengtes van die koolstofbrûe tussen die N-donor atome van die ringe. Hierdie eienskap gee aan die ligande die vermoë om beide vyf- en seslidringe te vorm wanneer komplekse gevorm word met metaalione. Die ligande is ten volle gekarakteriseer deur middel van KMR-metings, massa-spektroskopie en element analise. Smeltpuntbepalings is ook uitgevoer.

Die twee nuwe ligande voltooi nou die homoloë reeks tussen 9-ane-N<sub>3</sub> [en sy 2-(S)-hidroksiepropiel hangkroonarms] en 12-ane-N<sub>3</sub> [en sy 2-(S)-hidroksiepropiel hangkroonarms].

Protonasiedata van die ligande is bepaal deur middel van potensiometriese titrasie. Die onderskeie protonasiekonstantes vir beide ligande in 0.1000 mol dm<sup>-3</sup> NaNO<sub>3</sub> is:

$$\text{THTD} \quad \log K_1^{\text{H}} = 9.176 \text{ en } \log K_2^{\text{H}} = 4.20$$

$$\text{THTUD} \quad \log K_1^{\text{H}} = 11.32 \text{ en } \log K_2^{\text{H}} = 5.87$$

'n Duidelik-waarneembare derde protonasiekonstante vir beide ligande (THTD en THTUD) is opgemerk, maar potensiometriese metodes kon nie betroubare waardes lewer by die uitsers lae pH-lesings nie.

Vormingskonstantes van die ligande met 'n reeks oorgangsmetale is bepaal deur gebruik te maak van 'n 0.1000 mol dm<sup>-3</sup> NaNO<sub>3</sub> as ioniese medium. Die log(*K*) waardes by 25°C vir THTD is:

Co(II) 22.93

Zn(II) 14.82

Cd(II) 19.38

Pb(II) 15.47

Die log(*K*) waardes by 25°C met THTUD is:

Co(II) 17.52

Zn(II) 16.43

Cd(II) 18.05

Pb(II) 14.63

Uiters stabiele komplekse is verkry met die groter Cd(II) ioon in vergelyking met ander soortgelyke ligande.

Kristalstrukture van sommige van die metaalkomplekse is bepaal deur middel van X-straal kristallografie. Metaalperchlorate is gebruik om metal komplekse met THTD en THTUD te berei, en 'n verskeidenheid kristallasieprosesse is gebruik. Die algemene formule vir hierdie komplekse is  $[M(L)]^{2+} \cdot 2(ClO_4)^-$  waar M = metaal ioon en L = neutrale ligand is. Die bindingslengtes tussen die stikstof atoom en die metaalioon, en die suurstof atoom en die metaalioon is nagenoeg dieselfde in die onderskeie kristalstrukture. Dit beteken dat die metaalioon ongeveer halfpad tussen die stikstof en die suurstof atome voorkom. Die Mn(II)-THTD-kompleks vertoon beide oktahedrale - en trigonaal prismaatiese konfigurasie in die eenheidsel. Co(II)-THTUD het drie molekule per eenheidsel, almal verwronge oktahedrale konformasies. Zn(II)-THTUD het gekristaliseer met ses molekule per eenheidsel.

## **To my Parents**

## Acknowledgements

I would like to acknowledge the following people for their contributions to my studies:

Dr. Luckay and Prof Raubenheimer, for all the support, guidance, inspiration and encouragement.

Thank you to all my colleagues, especially Adélé le Roux, for your support and help in the laboratory; Christoff Strasser and Dr. Clive Oliver, for all the support in solving some of the crystal structures.

Jean McKenzie and Elsa Malherhe in the NMR laboratory, for all the work you have done for me and the many times you went out of your way to help and accommodate me. Dr Stefan Louw, for the work done on the MS; Eric Ward (glass blower) and all the technical staff for always being helpful.

To my entire family, especially my dad and my mom for all their prayers and support.

To my friends Jessica and Markus who helped me with all my computer problems. My best friend, Ilse Rootman, with whom I drank lots of hot chocolate while having interesting discussions. Thank you for all the nice conversations - (not just about chemistry and "Abby") - that we shared.

The NRF and Stellenbosch University, for financial support.

Lastly, and most important, I wish to thank Our Lord and Heavenly Father, for giving me the ability, opportunity, love and grace to complete this study.



## Poster Presentations

South African Chemical Institute (SACI), University of Kwa-Zulu Natal, Durban, October 2006: "Novel bi-functional medium sized cyclic triamines as DNA cross-linking alkylating agents as potential anti-cancer drugs", B.F. Barnard, H.G. Raubenheimer and R.C. Luckay

South African Chemical Institute (SACI), Club Mykonos, West Coast, July 2007: "Novel bi-functional medium sized macrocycles as complexing agents and potential anti-cancer drugs"  
B.F. Barnard, H.G. Raubenheimer and R.C. Luckay

## Abbreviations

[9]-ane-N <sub>3</sub> .....	1,4,7-triazacyclononane
[10]-ane-N <sub>3</sub> .....	1,4,7-triazacyclodecane
[11]-ane-N <sub>3</sub> .....	1,4,8-triazacycloundecane
[12]-ane-N <sub>3</sub> .....	1,5,9-triazacyclododecane
[12]-ane-N <sub>4</sub> .....	1,4,7,10-tetraazacyclododecane
[13]-ane-N <sub>4</sub> .....	1,4,7,10-tetraazacyclotridecane
[14]-ane-N <sub>4</sub> .....	1,4,8,11-tetraazacyclotetradecane
[15]-ane-N <sub>4</sub> .....	1,4,8,12-tetraazacyclopentadecane
Å .....	Ångstrom ( $1 \times 10^{-10}$ m)
CFSE .....	Crystal field stabilization energy
DIEN .....	Diethylenetriamine
DMF .....	Dimethylformamide
DMSA .....	Dimercaptosuccinic acid
DNA .....	Deoxyribonucleic acid
DOTA .....	1,4,7,10-tetraazacyclododecane-N,N',N'',N'''-tetraacetic acid
MRI .....	Magnetic resonance imaging
NOTA .....	1,4,7-triazacyclononane-N,N',N''-triacetic acid
NTA .....	Nitrilotriacetate
SHAB .....	Soft-Hard Acid-Base
STDEV .....	Standard deviation
TACI .....	1,3,5-triamino-1,3,5-trideoxy-cis-inositol
TACNTA .....	Triazacyclononane triacetate
TACN-TB .....	Triazacyclononane tris(5-tert-butyl-2-hydroxy benzyl)
TETA .....	1,4,8,11-tetraazacyclotetradecane-N,N',N'',N'''-tetra acetic acid
THETAC .....	N,N',N''-tris(hydroxyethyl)-1,4,7-triazacyclononane
THTD .....	1,4,7-tris-[(S)-2-hydroxypropyl]-1,4,7-triazacyclodecane
THTUD .....	1,4,7-tris-[(S)-2-hydroxypropyl]-1,4,7-triazacycloundecane
Ts .....	Tosylate
$\Delta \log(K)_{MAC}$ .....	Thermodynamic macrocyclic effect

# Table of Contents

<b>Abstract</b> .....	iii
<b>Opsomming</b> .....	v
<b>Acknowledgements</b> .....	viii
<b>Abbreviations</b> .....	x
<b>Table of Contents</b> .....	xi
<b>Chapter 1 Introduction</b> .....	<b>1</b>
1.1 General introduction .....	1
1.2 What are macrocycles? .....	2
1.3 History .....	3
1.4 Why are macrocyclic molecules of interest? .....	5
1.4.1 Biological interest and medical applications .....	7
1.4.2 Industrial applications .....	11
1.4.3 Selectivity of macrocyclic ligands for metal ions .....	13
1.4.3.1 Metal ion selectivity of crown ethers (oxygen donor atoms) .....	14
1.4.3.2 Metal ion selectivity of nitrogen donor macrocycles .....	14
1.5 The stability of complexes .....	20
1.6 The explanation of high protonation constants .....	21
1.7 Crystallographic studies with comparative macrocycles and Fe(III) as common metal ion .....	22
1.8 The chelate, macrocyclic and cryptate effects .....	23
1.9 Ligand design principles .....	26
1.10 Aim .....	28
<b>Chapter 2 The Preparation and Characterization of THTD and     THTUD</b> .....	<b>30</b>
2.1 Introduction .....	30
2.2 Aim .....	30
2.3 Methods of synthesis and pathways .....	31
2.3.1 Template synthesis .....	31
2.3.2 High dilution technique .....	32
2.3.3 Direct synthesis .....	33

2.4	Experimental .....	34
2.4.1	Materials .....	34
2.4.2	Instrumentation .....	34
2.4.3	Experimental procedure of the preparation of THTD and THTUD .....	34
2.4.3.1	Protection of the amines by means of tosylation .....	34
2.4.3.1.1	Tosylation of diethylenetriamine .....	34
2.4.3.1.2	Tosylation of bis-(3-aminopropyl)-amine .....	35
2.4.3.2	Protection of the diol by means of tosylation .....	35
2.4.3.2.1	Tosylation of 1,3-propanediol .....	35
2.4.3.2.2	Tosylation of ethylene glycol .....	36
2.4.4	Preparation of the tosylated triamine disodiumsalt (diethylenetriamine and the bis-(3-aminopropyl)-amine) .....	36
2.4.5	Synthesis of the macrocycles .....	36
2.4.5.1	Synthesis of the tosylated 1,4,7-triazacyclodecane .....	36
2.4.5.2	Synthesis of the tosylated 1,4,8-triazacycloundecane.....	37
2.4.6	De-tosylation and formation of the HBr-salt of the macrocycles .....	37
2.4.7	The addition of the pendant arms .....	37
2.5	Results and discussion .....	39
2.5.1	NMR spectra .....	39
2.5.1.1	NMR spectra of the tosylated diethylenetriamine (DIEN) .....	39
2.5.1.1.1	<sup>13</sup> C spectrum of the tosylated DIEN .....	40
2.5.1.1.2	<sup>1</sup> H spectrum of the tosylated DIEN .....	40
2.5.1.2	NMR spectra of the tosylated bis-(3-aminopropyl)amine .....	41
2.5.1.2.1	<sup>13</sup> C spectrum of the tosylated bis-(3-aminopropyl)-amine .....	42
2.5.1.2.2	<sup>1</sup> H spectrum of the tosylated bis-(3-aminopropyl)-amine .....	42
2.5.1.3	NMR spectra of the tosylated 1,3-propanediol.....	42
2.5.1.3.1	<sup>13</sup> C spectrum of the tosylated 1,3-propanediol .....	43
2.5.1.3.2	<sup>1</sup> H spectrum of the tosylated 1,3-propanediol.....	43
2.5.1.4	NMR spectra of the tosylated ethylene glycol.....	44
2.5.1.4.1	<sup>13</sup> C spectrum of the tosylated ethylene glycol .....	44
2.5.1.4.2	<sup>1</sup> H spectrum of the tosylated ethylene glycol .....	45
2.5.1.5	NMR spectra of the tosylated 1,4,7-triazacyclodecane .....	45
2.5.1.5.1	<sup>1</sup> H spectrum of the tosylated 1,4,7-triazacyclodecane.....	45
2.5.1.6	NMR spectra of the tosylated 1,4,8-triazacycloundecane .....	46

2.5.1.6.1	<sup>1</sup> H spectrum of the tosylated 1,4,8-triazacycloundecane .....	46
2.5.1.7	NMR spectra of THTD .....	47
2.5.1.7.1	<sup>13</sup> C spectrum of THTD .....	48
2.5.1.7.2	<sup>1</sup> H spectrum of THTD .....	49
2.5.1.8	NMR spectra of THTUD .....	49
2.5.1.8.1	<sup>13</sup> C spectrum of THTUD .....	50
2.5.1.8.2	<sup>1</sup> H spectrum of THTUD .....	51
2.5.2	Elemental analysis .....	51
2.5.2.1	The analysis of THTD .....	51
2.5.2.2	The analysis of THTUD .....	52
2.5.3	Mass spectrometry analysis .....	53
2.5.3.1	Mass spectrum of THTD .....	53
2.5.3.2	Mass spectrum of THTUD .....	53
2.5.4	Melting point .....	54
2.5.4.1	Melting point – THTD .....	54
2.5.4.2	Melting point – THTUD .....	54
2.5.5	Physical characteristics of THTD and THTUD .....	54
2.5.5.1	Physical characteristics of THTD .....	54
2.5.5.2	Physical characteristics of THTUD .....	54
2.6	Conclusion .....	55

### **Chapter 3 Determination of the Protonation Constants of THTD and THTUD .....**

	<b>56</b>	
3.1	Introduction .....	56
3.2	Aim .....	57
3.3	Experimental .....	58
3.3.1	Materials .....	58
3.3.2	Instrumentation .....	58
3.3.3	Procedure for the determination of the protonation constants of THTD and THTUD .....	59
3.4	Results and Discussion .....	61
3.4.1	THTD and THTUD .....	62
3.5	Conclusion .....	65

<b>Chapter 4</b>	<b>The Determination and interpretation of Stability Constants of THTD and THTUD with <math>\text{Co}^{2+}</math>, <math>\text{Zn}^{2+}</math>, <math>\text{Cd}^{2+}</math> and <math>\text{Pb}^{2+}</math></b>	<b>66</b>
4.1	Introduction	66
4.2	Aims of this particular study	67
4.3	Experimental Methods	68
4.3.1	Materials	68
4.3.2	Instrumentation	69
4.3.3	Procedure for the determination of the formation constants of the metal complexes with THTD and THTUD	69
4.4	Results and discussion	70
4.4.1	THTD with a series of metal ions	71
4.4.1.1	$\text{Pb}^{2+}$	72
4.4.1.2	$\text{Zn}^{2+}$	72
4.4.1.3	$\text{Cd}^{2+}$	73
4.4.1.1	$\text{Co}^{2+}$	74
4.4.2	THTUD with a series of metal ions	75
4.4.2.1	$\text{Pb}^{2+}$	75
4.4.2.2	$\text{Zn}^{2+}$	75
4.4.1.3	$\text{Co}^{2+}$	76
4.4.1.1	$\text{Cd}^{2+}$	76
4.5	Conclusion	78
<b>Chapter 5</b>	<b>The Determination of Crystal Structures</b>	<b>79</b>
5.1	Introduction	79
5.2	Aim	79
5.3	Experimental Procedures	80
5.3.1	General preparation of the complexes	80
5.3.2	Methods used in the crystallization of the complexes	81
5.3.3	THTD with a Series of Metal ions	82
5.3.3.1	Manganese(II) perchlorate hexahydrate	82
5.3.3.2	Iron(III) perchlorate hexahydrate	82
5.3.3.3	Cobalt(II) perchlorate hexahydrate	82
5.3.3.4	Nickel(II) perchlorate hexahydrate	83

5.3.3.5	Copper(II) perchlorate hexahydrate .....	83
5.3.3.6	Zinc(II) perchlorate hexahydrate .....	83
5.3.3.7	Cadmium(II) perchlorate hydrate .....	84
5.3.3.8	Lead(II) perchlorate (x)hydrate.....	84
5.4.2	THTUD with a Series of Metal ions .....	84
5.4.2.1	Manganese(II) Perchlorate Hexahydrate .....	84
5.4.2.2	Iron(III) Perchlorate (x)hydrate .....	85
5.4.2.3	Cobalt(II) Perchlorate Hexahydrate .....	85
5.4.2.4	Nickel(II) Perchlorate Hexahydrate .....	85
5.4.2.5	Copper(II) Perchlorate Hexahydrate .....	86
5.4.2.6	Zinc(II) Perchlorate Hexahydrate .....	86
5.4.2.7	Cadmium(II) Perchlorate Hydrate .....	86
5.4.1.8	Lead Perchlorate (x)hydrate .....	87
5.3.5	Instrumentation .....	87
5.4	Results and discussion .....	87
5.4.1	Attempted structure determinations of the free ligands.....	87
5.4.2	The unusual complexation during the crystallization of compound X - [Mn <sub>2</sub> (THTD)(THTD-H <sup>+</sup> )-3(ClO <sub>4</sub> ) <sup>-</sup> .....	88
5.4.3	The crystal and molecular structure of [Co(THTUD)](ClO <sub>4</sub> ) <sub>2</sub> .....	94
5.4.4	The crystal and molecular structure of [Zn(THTUD)](ClO <sub>4</sub> ) <sub>2</sub> .....	98
5.5	Conclusion .....	102
<b>Chapter 6</b>	<b>Conclusion .....</b>	<b>104</b>
<b>Appendices</b>	<b>.....</b>	<b>106</b>

# Chapter 1

## *Introduction*

### 1.1 General introduction

The uses of chelating agents have increased dramatically in recent years. These chelating agents were primarily used in the medical field, but new fields of application have emerged; for instance, the selective extraction of precious metals in hydrometallurgy.<sup>1</sup> Synthetic chelating agents are now also used on a large scale in plant nutrition to form soluble metal complexes whereby nutrients are made bio-available to plants. Chelating agents are also used in analytical chemistry, biological systems, corrosion and chemical cleaning, detergents and many more areas of science and industry. Stability constants are needed to determine the nature and efficiency of these artificial carriers.<sup>2</sup>

The use of chelating agents in detergents requires that formation constants must be determined, not only to understand the action of the detergent, but also to see the effect of the chelating agent on sewage treatment and the impact that these detergents might have when released in the environment. Some new chelating agents show very high metal ion affinity and have been tested as detergent agents (e.g., NTA, polyphosphates). This action has been attributed to the high stabilities of these ligands with transition metals in the soil deposits, which would otherwise result in the formation of stain-producing metal deposits on fabrics.<sup>2</sup>

Chelating agents in the electroplating industry is another area of interest. Chelators strongly influence the rate and efficiency of the electroplating process. The electrode positions of the metals are controlled by the stabilities of the complexes which are

---

<sup>1</sup> B.R. Green and R.D. Hancock, *J. S. Afr. Inst. Min. Metall.*, 1982, **82**, 303-307

<sup>2</sup> A.E. Martell and R.J. Motekaites in *Determination and use of Stability Constants*, VCH Publishers, Inc., New York, 1988, pp. 213-216



formed in the plating solution which frequently contain a number of chelating agents. The new types of chelating agents are very important, for they are less toxic than the cyanide baths that are used. Again stability constants provide valuable information to the understanding of the multi-component electroplating solution.<sup>2</sup> Wainwright<sup>3</sup> identified other areas of interest e.g. bioinorganic applications – hydrolytic enzyme models, synthetic ribonucleases, nucleobase recognition reagents and oxygenase promoters. Magnetic resonance imaging (MRI) and tumour-directed radioisotope carriers are of high interest in the medical field.

## 1.2 What are macrocycles?

Macrocycles are large cyclic molecules which contain donor atoms which are part of the cyclic backbone. These donor atoms are important to form coordinate bonds with metal centers. A macrocycle consists of at least nine atoms of which three or more are donor atoms in the ring itself. Because these molecules are cyclic, it means that a metal ion could possibly fit into, or onto the cavity of the ligand that is being used. Depending on the macrocyclic ring size, some metal ions will be too small for the cavity while others may be too big.<sup>4</sup>

Cyclic ring sizes can be categorized into four groups - small, normal, medium and large<sup>5</sup> (Table 1.1). A macrocycle must have at least nine atoms in the ring of which at least three must be donor atoms.

**Table 1.1** The classification of the ring sizes of molecules.

Ring	Size
3,4	Small
5-7	Normal
8-11	Medium
≥12	Large

<sup>3</sup> K.P. Wainwright, *Adv. Inorg. Chem.*, 2001, **52**, 293-334

<sup>4</sup> E.C. Constable in *Co-ordination Chemistry of Macrocyclic Compounds*, Oxford University Press, New York, 1999, p. 1

<sup>5</sup> E.C. Constable in *Co-ordination Chemistry of Macrocyclic Compounds*, Oxford University Press, New York, 1999, p. 32

The type of donor atoms that are situated in the backbone of the ring also play a huge part in the selection of the metal ion. Nitrogen can be seen as a hard donor and oxygen is classified as a hard donor and will react very differently to sulphur which is considered a soft donor.<sup>6</sup> Other factors that will be discussed later are the "bite size" of the chelate rings, how flexible the ring is, the induction effects of the bridges between the donor atoms, and whether there is further functionalization on the macrocycle.

### 1.3 History

Prior to 1967 there was very little literature on macrocyclic polyethers. Because information was so limited, the possibility that macrocyclic molecules of this type might be extremely useful as coordination agents had not yet been grasped by medical, biological or industrial researchers. The value of macrocyclic molecules impacted only when Pedersen and Frensdorff<sup>7</sup> by chance stumbled on dibenzo[18]crown-6 (Fig. 1.1).

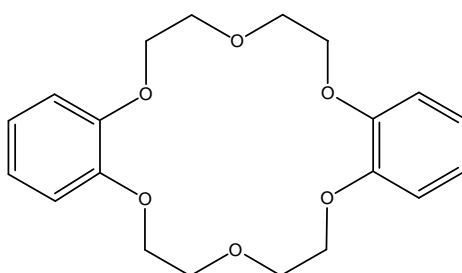


**Fig 1.1** Dibenzo[18]crown-6

Dibenzo[18]crown-6 was the unexpected by-product in the preparation of bis[2-(*o*-hydroxyphenoxyethyl) ether from bis(2-chloroethyl) ether and the Na salt of 2-(*o*-hydroxyphenoxy)-tetrahydropyran which contained a small quantity of catechol. The macrocyclic polyether was recovered as white fibrous crystals as a minor component from the reaction compounds. These crystals would not dissolve in methanol itself, but became soluble on the addition of sodium salts. This observation led to the discovery of the coordination power of crown ethers which then led to the synthesis of other macrocycles with a variety of donor atoms.<sup>6</sup>

<sup>6</sup> J.E. Huheey, E.A. Keiter and R.L. Keiter in *Inorganic Chemistry*, HarperCollins College Publishers, New York, 1993, p. 347

<sup>7</sup> C.J. Pedersen and H.K. Frensdorff, *Angew. Chem. Internat. Edit.*, 1972, **11**, 16-25

The discovery of dibenzo[18]crown-6 evoked an entirely new research area in macrocyclic coordination agents. Researchers moved away from just using oxygen as donor atoms and started to include new donor atoms such as nitrogen, sulphur and phosphorus.<sup>8</sup>

Most studies, however, focused on tetraamine and tetraimine ligands,<sup>9</sup> and to a lesser extent, research was done by Musker and Hussain<sup>10</sup> on complexes containing cyclic diamines (Fig. 1.2). These molecules however are not considered to be proper macrocycles, but rather just as chelating agents because they only possess two donor atoms in the ring and there are less than 9 atoms in total in the ring.

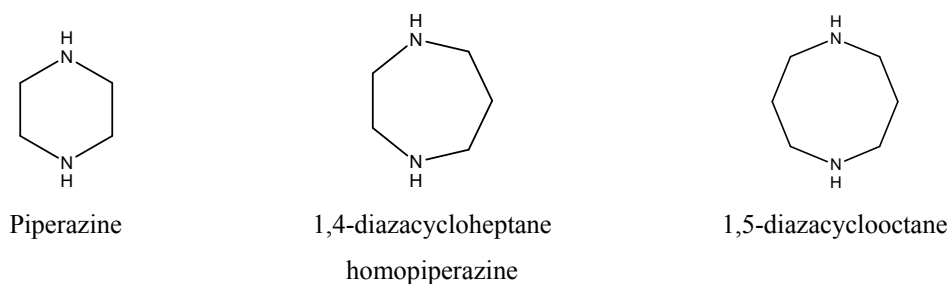


**Fig. 1.2** Cyclic diamines

Pendant donor macrocycles means that a macrocyclic ligand has additional donor groups attached to its periphery. The use of these types of macrocyclic ligands appears to have been reported first in the 1980's,<sup>11</sup> e.g. in 1982 Buøen *et al.* synthesized 1,4,7,10-tetrakis(2-hydroxyethyl)-1,4,7,10-tetraazacyclododecane (Fig. 1.3). These ligands were for the complexation of alkali cations.<sup>12</sup>

<sup>8</sup> J.J Christensen, D.J. Eatough and R.M. Izatt, *Chem. Rev.*, 1974, **74**, 351-360

<sup>9</sup> N.F. Curtis, *Coord. Chem. Rev.*, 1968, **3**, 3-47

<sup>10</sup> W.K. Musker and M.S. Hussain, *Inorg. Chem.*, 1969, **8**, 528-535

<sup>11</sup> K.P. Wainwright, *Coord. Chem. Rev.*, 1997, **166**, 35-90

<sup>12</sup> S. Buøen, J. Dale, P. Groth and J. Krane, *J. Chem. Soc., Chem. Commun.*, 1982, **20**, 1172-1174

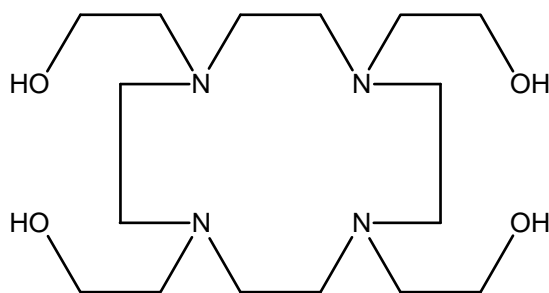


**Fig. 1.3** 1,4,7,10-tetrakis-(2-hydroxyethyl)-1,4,7,10-tetraazacyclododecane

#### 1.4 Why are macrocyclic molecules of interest?

Naturally occurring macrocyclic ligands such as porphyrin, corrin ring systems, and phthalocyanine (not naturally occurring) have been studied intensively over the years. Macrocyclic ligands can be divided into two broad categories namely cyclic polyethers (crown type – Fig. 1.4) and systems containing donor atoms other than oxygen, such as nitrogen, sulphur, and phosphorus. The nitrogen, oxygen and phosphorus containing ligands form strong complexes with transition metals.<sup>13</sup>

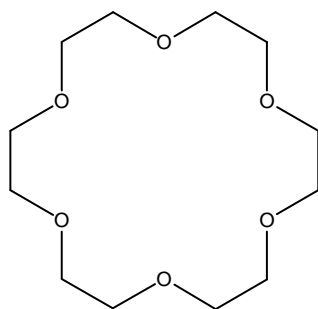


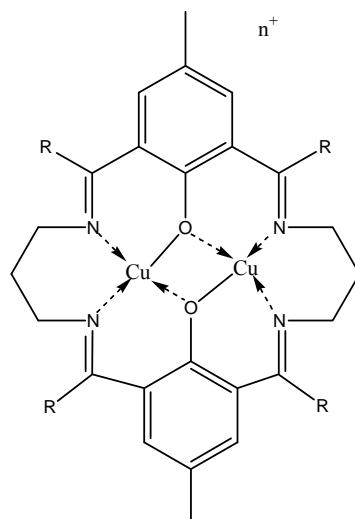
**Fig. 1.4** [18]crown-6 ether.<sup>7, 14</sup>

Macrocyclic ligands can provide transition metals with unusual ligand environments and consequent novel chemical properties. High and low oxidation states are often stabilized, ligand lability is decreased, in other words kinetically stable because of the

<sup>13</sup> L.F. Lindoy, *Chem. Soc. Rev.*, 1975, **4**, 421-441

<sup>14</sup> E.C. Constable in *Coordination Chemistry of Macrocyclic Compounds*, Oxford University Press, New York, 1999, p. 38

chelating effect, and sometimes several metal ions may be held in close proximity within the same molecule such as the binuclear copper(II) complex below (Fig. 1.5).<sup>15</sup>



1. Cu(II)-Cu(II),  $n = 2$ ,  $R = H$
2. Cu(II)-Cu(I),  $n = 1$ ,  $R = H$
3. Cu(II)-Cu(I)(CO),  $n = 1$ ,  $R = H$
4. Cu(II)-Cu(I),  $n = 1$ ,  $R = CH_3$

**Fig. 1.5** Schematic structure of the mixed valence binuclear Cu(II)-Cu(I) complex that was prepared by Gagné, Koval and Smith.<sup>15</sup>

It may also occur that more than one ligand is present when complexed to a metal ion center as can be seen in the Co(II) complexes of triazamacrocycles with pendant alcohol arms  $[Co(H_3L^2)_2(NO_3)_2][PF_6]_2$ .<sup>16</sup> Two ligands were coordinated to the metal ion center in the complexes that were prepared by Al-Sagher and co-workers. L= ligand (Fig. 1.6).

<sup>15</sup> R.R. Gagné, C.A. Koval and T.J. Smith, *J. Am. Chem. Soc.*, 1977, **99**, 8367-8368

<sup>16</sup> H. Al-Sagher, I. Fallas, L.J. Farrugia and R.D. Peacock, *J. Chem. Soc., Chem. Commun.*, 1993, 1499-1500

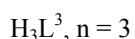
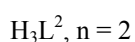
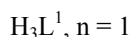
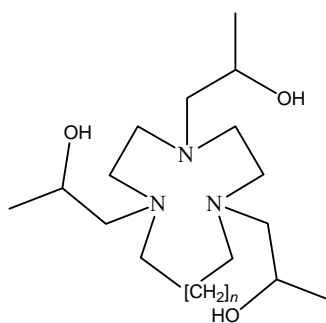


**Fig. 1.6** Schematic structure of the ligand L that was used in the structure of  $[\text{Co}(\text{H}_3\text{L}^2)_2(\text{NO}_3)_2][\text{PF}_6]_2$ .

#### 1.4.1 Biological interest and medical applications

Macrocyclic ligand transition metal complexes are involved in a number of biological systems, for instance the porphyrin ring of the haem-protein (Fe-containing ring - Fig. 1.7), the chlorin ring of chlorophyll (Mg-containing ring - Fig. 1.8) and the corrin ring of vitamin B<sub>12</sub> (Co-containing ring - Fig. 1.9).<sup>17, 18</sup> The above mentioned naturally occurring macrocyclic ligands have been known for a long time, but it is only in the last 30 years that a large number of synthetic macrocyclic compounds have been prepared and investigated. Macrocyclic polyethers, polyamines, polythioethers and related macrocyclic molecules usually have a central hydrophilic cavity while the exterior of the macrocycles are hydrophobic. Macrocyclic ligands therefore have the ability to bind to a wide variety of cations, because of this central hydrophilic cavity that they possess. It is the hydrophobic exterior which allows them to solubilize ionic substances in non-aqueous solvents and in membrane media.<sup>7</sup>

<sup>17</sup> E.C. Constable in *Coordination Chemistry of Macrocyclic Compounds*, Oxford University Press, New York, 1999, pp. 2, 8, 10

<sup>18</sup> L.F. Lindoy in *The Chemistry of Macrocyclic Ligand Complexes*, Cambridge University Press, New York, 1989, p. 3

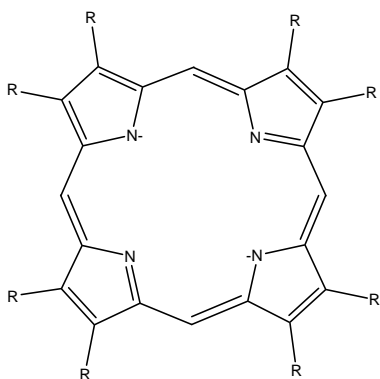


**Fig. 1.7** The porphyrin ring of the heme protein

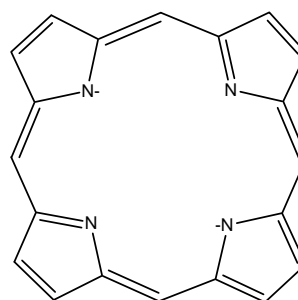


**Fig. 1.8** The chlorin ring of chlorophyll

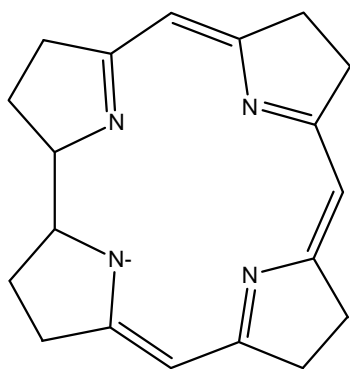


**Fig.1.9** The corrin ring of vitamin B<sub>12</sub>

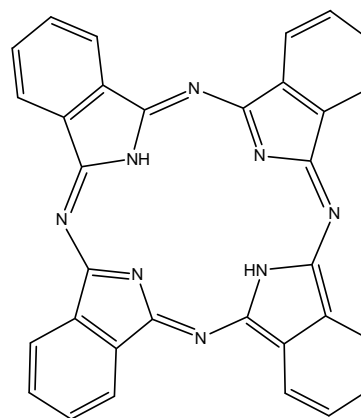


**Fig. 1.10** Phthalocyanine

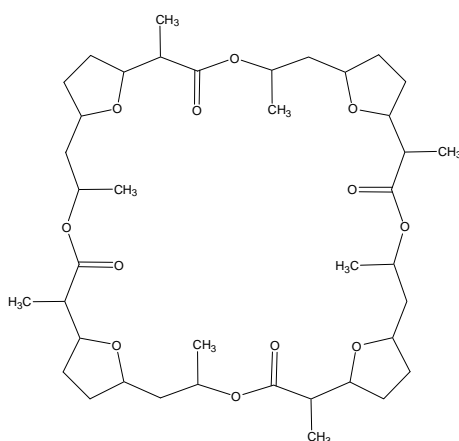


**Fig. 1.11** Nonactin which binds K<sup>+</sup> selectively and acts as a carrier for this ion across cell membranes.

Phthalocyanine (Fig. 1.10) and its derivatives bear a strong resemblance to natural porphyrin systems. The metal ion chemistry of these phthalocyanines is interesting

because of their varied uses. They can, for example, be used as semi-conductors or as catalysts for a number of chemical transformations. They are also commercially used as colouring agents because of their intense colours.<sup>19</sup> Phthalocyanines (Fig. 1.10) and their derivatives can be used very specifically as semi-conductors, catalysts and colouring agents. Copper phthalocyanine produces very intense colours and also shows resistance to degradation and is very stable at high temperatures. It is also inert to acids and bases and can withstand rapid changes in pH.<sup>20</sup>

There are a number of antibiotics such as valinomycin and nonactin (Fig. 1.11) which contain ether, ester and amide bonds in the macrocyclic rings (32 to 36-membered rings). These macrocycles are of interest because they influence the transport of  $\text{Na}^+$  and  $\text{K}^+$  across cell membranes which is one of the fundamental processes in living systems. X-ray structures of the crown ethers showed that the cavity encloses the cation in a manner similar to that found in naturally occurring macrocyclic antibiotics such as valinomycin and nonactin.<sup>21</sup>

There are large numbers of people who suffer from iron overload ( $\beta$ -thalassaemia also known as Cooley's anaemia) when iron in natural storage and transport proteins are overwhelmed, and the iron spills over into other tissues and organs, e.g. the spleen and liver. Desferral, which contains a hard oxygen donor is used to get rid of this overload of iron, since Fe(III) is a hard metal ion.<sup>22</sup>

When designing macrocycles with a medical purpose in mind, various factors must be considered, for instance, method of administration, bio-availability, membrane permeability, toxicity and the rapid elimination of the metal complex before the

---

<sup>19</sup> L.F. Lindoy in *The Chemistry of Macrocyclic Ligand Complexes*, Cambridge University Press, New York, 1989, p. 2

<sup>20</sup> E.C. Constable in *Coordination Chemistry of Macrocyclic Compounds*, Oxford University Press, New York, 1999, pp. 8-9, 11, 30

<sup>21</sup> R.N. Greene, *Tetrahedron Lett.*, 1972, **18**, 1793-1796

<sup>22</sup> A.E. Martell and R.D. Hancock in *Metal Complexes in Aqueous Solutions*, Plenum Press, New York, 1996, pp. 155- 164



spreading of the undesired metal to the rest of the organs in the body.<sup>23</sup> More recently, it was discovered that azamacrocycles have anti-tumour capabilities.<sup>24</sup> Certain nitrogen mustards such as chlorambucil, melphalan, cyclophosphamide and ifosfamide are amongst the most effective and useful clinical agents for the treatment of cancer. All these nitrogen mustards are bifunctional alkylating agents, which alkylate the DNA primarily at the N-7 position of the guanine bases in the major groove after the formation of aziridinium ions. In recent times the coordination chemistry of the polyazamacrocycles has been very well-documented, providing the opportunity for pro-drug formation in the synthesis of a new class of mustard drugs. This also gives rise to their biological evaluation as DNA crosslinking and anti-tumour agents.<sup>24</sup> Fig. 1.11 shows schematically how the polyazamacrocycles with the pendant arms may attach to the DNA. There are two ways in which this can happen, either it can attach in the *cis* direction as in Fig. 1.11a or in the *trans* position as in Fig. 1.11b. Wainwright<sup>3</sup> reported in 2001 that polyazamacrocycles with nitrogen-attached pendant arms are being investigated as tumour-directed radio-isotopes. Weeks *et al.*<sup>25</sup> also stated that the pendant arm polyazamacrocycles show potential as biological tracers and that these macrocyclic molecules may also be used in MRI.

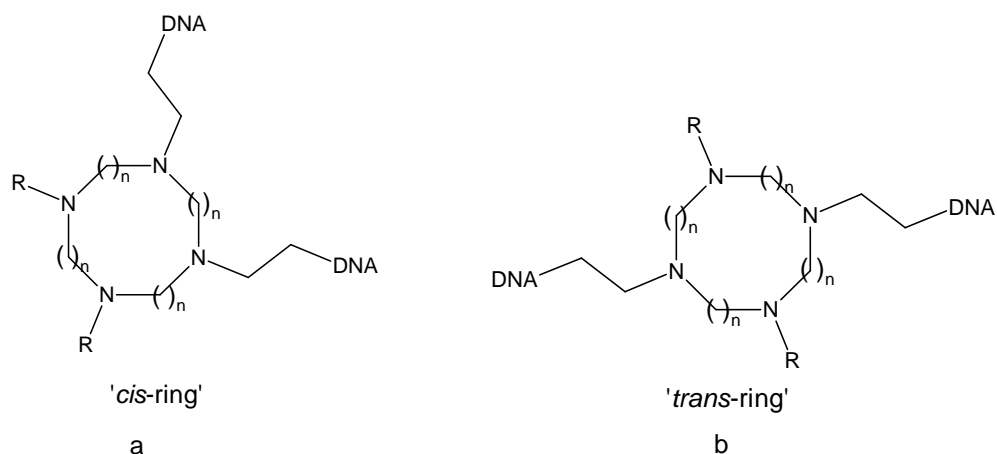


**Fig. 1.12** The possible outcome for bifunctional alkylation<sup>24</sup>.

<sup>23</sup> A.E. Martell and R.D. Hancock in *Metal Complexes in Aqueous Solutions*, Plenum Press, New York, 1996, pp. 149-153

<sup>24</sup> L.L. Parker, F.M. Anderson, C.C. O'Hare, S.M. Lacy, J.P. Bingham, D.J. Robins and J.A. Hartley, *Bio-org. Med. Chem.*, 2005, **13**, 2389-2395

<sup>25</sup> J.M. Weeks, M.A. Butine, S.F. Lincoln, E.R.T. Tiekink and K.P. Wainwright, *J. Chem. Soc., Dalton Trans.*, 2001, 2157-2163

Pendant donor macrocyclic ligands are now being produced to embrace enzyme simulations and also for the attachment to monoclonal antibodies for the purpose of carrying a radionuclide to a targeted cell. It is now widely used as MRI reagents.<sup>3, 10, 26, 27</sup>

### 1.4.2 Industrial applications

Macrocycles are used in solvent extraction of metal salts. They are also used in the recovery of precious metals and the removal of toxic metal ions from the waste streams of industrial plants. Heavy metals such as Cd and Pb are extremely hazardous in water when consumed by people or animals. Pb(II) tends to accumulate in the bone tissue, kidneys and liver. The symptoms of lead poisoning are anaemia, headaches and convulsions, damage to the brain and damage to the central nervous system. Cadmium poisoning occurs even at very low levels and can lead to kidney failure and even tumours. Symptoms of Hg(II) poisoning include headaches, tremors and memory loss. DMSA seems to be the best antidote for Hg poisoning.<sup>28</sup> All these heavy metals are easily absorbed in the gastro intestinal tract and concentrated in the blood stream.

Heavy metals in our surroundings cause extremely serious environmental problems. It is very unfortunate that heavy metals exhibit a strong affinity towards amino -, carboxyl - and thiol groups. These groups are present in proteins and enzymes and can thus complex readily to these heavy metals should they get into the biological system of humans or animals. In other words, to prevent these heavy metals from reaching the vital organs, they are complexed to the macrocycles to form very stable complexes and can be removed from the system. The complexation of the heavy metal ions with the macrocycle will prevent the heavy metals from being absorbed by the organs in the body.<sup>23</sup>

---

<sup>26</sup> A.E. Martell and R.D. Hancock in *Metal Complexes in Aqueous Solutions*, Plenum Press, New York, 1996, pp 168- 191

<sup>27</sup> A.A. Belal, L.J. Farrugia, R.D. Peacock and J. Robb, *J.Chem. Soc. Dalton Trans.*, 1989, 931-935

<sup>28</sup> A.E. Martell and R.D. Hancock in *Metal Complexes in Aqueous Solutions*, Plenum Press, New York, 1996, pp. 163- 164

Macrocyclic ligands can also be used for the recovery of precious metals. Precious metals are recovered through solvent extraction, ion exchange, precipitation and activated carbon adsorption. Reverse osmosis, electrolysis, irradiation and evaporation are also employed, but to a lesser extent. Copper is extracted on an industrial scale through hydrometallurgy which is fairly cost-effective and environmentally friendly. Pyrometallurgy, although widely used, has become very expensive. The alternative is now to use macrocyclic ligands as the preferred method of extraction. Macrocyclic ligands are highly stable when complexed to metals. Macrocyclic ligands are also very selective towards certain metal ions. This means that a specific metal can be selectively isolated from a mixture of metal ions by using tailor-made macrocyclic ligands.<sup>29,30</sup>

ZENECA<sup>31</sup> patented a selective Cu(II) extraction from an acidic solution which can be described by the pH swing method:

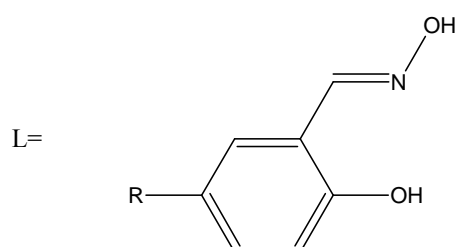
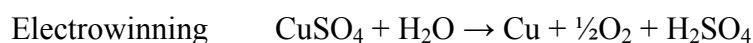
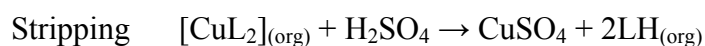
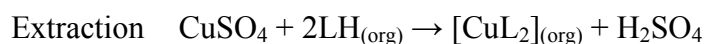
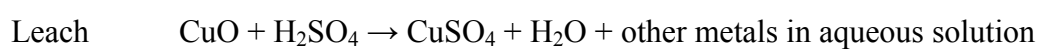


**Fig. 1.13** The schematic view of the ligand that is used in the pH swing method.

<sup>29</sup> P.A. Tasker, P.G. Plieger and L.C. West, *Comprehensive Coordination Chemistry II*, 2004, **9**, 759-808

<sup>30</sup> P.A. Tasker and V. Gasparyov, *Macrocyclic Chemistry*, 2005, 365-382

<sup>31</sup> E.C. Constable in *Coordination Chemistry of Macrocyclic Compounds*, Oxford University Press, New York, 1999, pp. 65-68

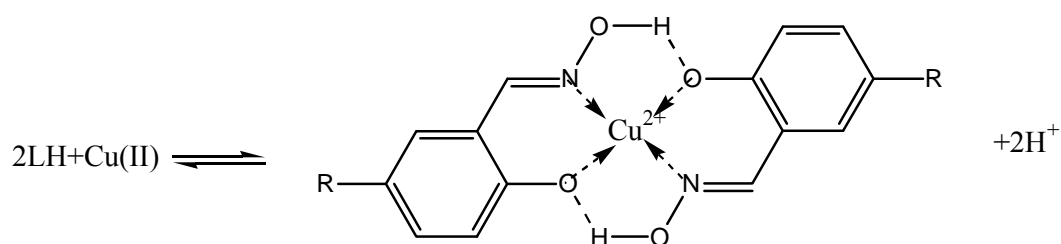


**Fig. 1.14** The complexation of the Cu(II) to the ligand in the pH swing method.

Fig. 1.14 shows the formation of the neutral pseudo-macrocyclic Cu(II) complex with the ligand shown in Fig. 1.13. In the formation of the neutral pseudo-macrocyclic Cu(II) complex, two 5-membered and two 6-membered rings can clearly be seen<sup>29, 31, 32</sup> as they form as a result of the complexation.

Both Gloe *et al.*<sup>33</sup> and Saito *et al.*<sup>34</sup> showed the selectivity of S-containing macrocycles towards Ag(I), Cu(I), Hg(II) and Pd(II).

Pendant donor macrocycles have also been investigated as a basis for cationic surfactants. Other metallosurfactants, where the cationic head group is a poly-azamacrocycle containing a strongly coordinated metal ion and the tail is the pendant arm that is attached to a nitrogen atom of the head group, have also been investigated.<sup>3</sup>

### 1.4.3 Selectivity of macrocyclic ligands for metal ions

Since we are working with ring structures, we have to consider a few factors that will influence the selectivity of the ligands. One such factor is the size-match selectivity. This means that the complex of a metal ion will show maximum stability with a macrocyclic ring when the ionic radius of the metal ion matches the cavity of the macrocyclic ring. There are two ways of increasing the ring size of the

<sup>32</sup> D. Black, A.J. Blake, R.L. Finn, L.F. Lindoy, A. Nezhadali, G. Rougnaghi, P.A. Tasker and M. Schröder, *Chem. Commun.*, 2002, 340-341

<sup>33</sup> K. Gloe, H. Graubaum, M. Wüst, T. Rambusch and W. Seichter, *Coord. Chem. Rev.*, 2001, **222**, 103-126

<sup>34</sup> K. Saito, Y. Masuda and E. Sekido, *Bull. Chem. Soc. Jpn.*, 1984, **57**, 189-193

macrocycle, firstly by varying the number of donor atoms in the ring and secondly, by increasing the size of the bridges between the donor atoms.<sup>35</sup>

A nitrogen containing macrocycle for example, needs between 13 and 16 members in the ring to fully encircle a first row transition metal ion, provided that the nitrogen atoms are situated in such a way that five-, six-, or seven-membered rings will form on coordination.<sup>13</sup>

#### ***1.4.3.1 Metal ion selectivity of crown ethers (oxygen donor atoms)***

Consideration for size match selectivity is best explained with the use of crown ethers (Fig. 1.15 shows some examples of crown ethers). 18-crown-6, for example, has an approximate ionic radius of between 1.8 and 2.2 Å.  $K^+$  has an ionic radius of 1.9 Å. This means that  $K^+$  will best fit into the cavity of 18-crown-6.<sup>36</sup> In this instance we observe that 18-crown-6 definitely shows size-match selectivity. The cavities of 12-crown-4 and 15-crown-5 are too small to allow  $K^+$  within the cavity. In this instance the metal ions lie outside the cavity and factors that govern selectivity are very much the same as for open-chain ligands. Large crown ethers have a tendency to fold and bend around the metal ions. This phenomenon leads to the conclusion that large crown ethers have no real cavity and that they exert their selectivity mainly due to torsional constraints.<sup>37, 38</sup>

---

<sup>35</sup> A.E. Martell and R.D. Hancock in *Metal Complexes in Aqueous Solutions*, Plenum Press, New York, 1996, p. 112

<sup>36</sup> E.C. Constable in *Coordination Chemistry of Macrocyclic Compounds*, Oxford University Press, New York, 1999, pp. 21, 22

<sup>37</sup> E.C. Constable in *Coordination Chemistry of Macrocyclic Compounds*, Oxford University Press, New York, 1999, pp. 22-31

<sup>38</sup> A.E. Martell and R.D. Hancock in *Metal Complexes in Aqueous Solutions*, Plenum Press, New York, 1996, pp. 101-105

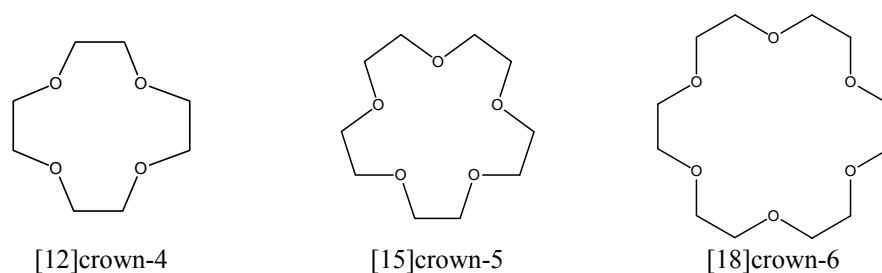


**Fig. 1.15** A few examples of crown ethers.<sup>14</sup>

### 1.4.3.2 Metal ion selectivity of nitrogen donor macrocycles

Nitrogen donor macrocycles do not conform to the idea of size match selectivity. Pb(II) for instance, shows a steady decrease in the  $\Delta\log(K_1)$  as the size of the macrocycle increases and we find that Pb(II) complexes more strongly with [12]-ane-N<sub>4</sub> (Fig. 1.16) which has a cavity much too small for the Pb(II) ion.<sup>39</sup>

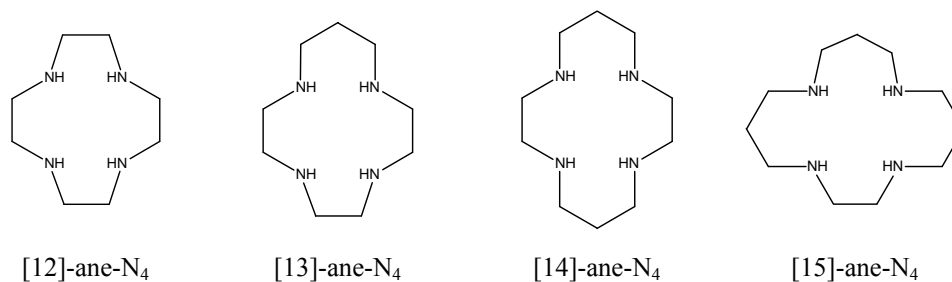


**Fig. 1.16** [12]-ane-N<sub>4</sub> to [15]-ane-N<sub>4</sub>

Zn(II) is a medium-sized metal ion and size match selectivity suggests that it should complex best with [15]-ane-N<sub>4</sub> (Fig. 1.16). Yet, in this instance, Zn(II) shows a weak preference for [12]-ane-N<sub>4</sub> which is fairly small in comparison to [15]-ane-N<sub>4</sub>. The idea of size match selectivity leads us to believe that low spin Ni(II) would best fit into the cavity of [13]-ane-N<sub>4</sub> (Fig. 1.16), yet it complexes better with [14]-ane-N<sub>4</sub> (Fig. 1.16) which has a larger cavity than [13]-ane-N<sub>4</sub>. It is only Cu(II) and the high spin Ni(II) that follow the size match selectivity rule when simple tetraazamacrocycles are used as

<sup>39</sup> A.E. Martell and R.D. Hancock in *Metal Complexes in Aqueous Solutions*, Plenum Press, New York, 1996, pp. 120-131, 164

coordination agents (Fig. 1.16). This observation leads to the conclusion that there are other factors that drive the complexation with metal ions rather than the size of the metal ion and the diameter of the cavity of the macrocycle. Metal ion selection is far more complex when azamacrocycles are used for metal ion selection.<sup>40</sup>

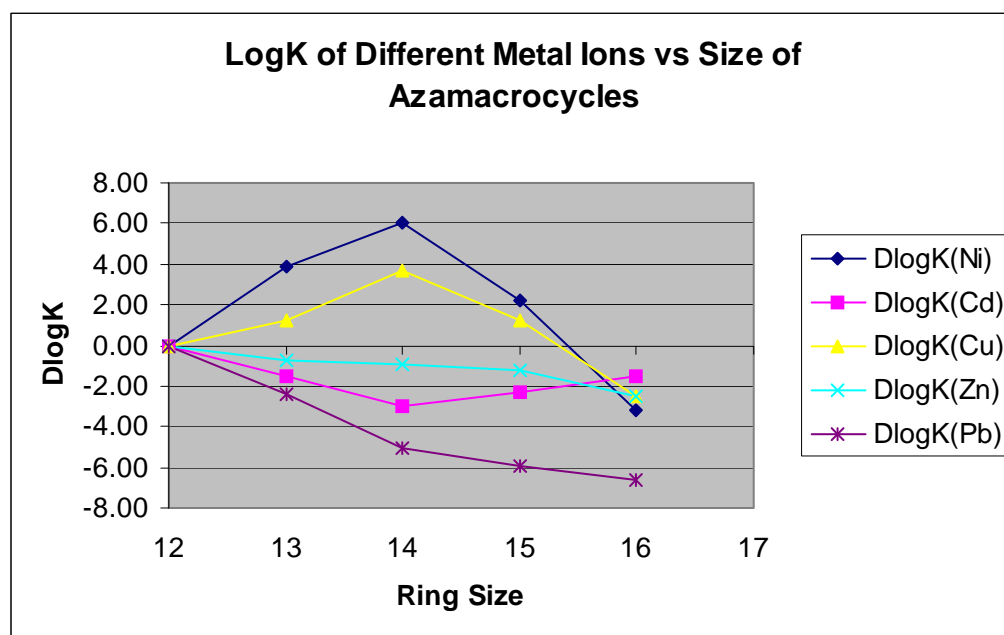


**Fig. 1.17**  $\Delta \log K_1$  of different metal ions vs size of the azamacrocycle. From the graph it is clear that there is no size match selection when nitrogen donor atoms are present in the macrocycle. ( $D\log K = \Delta \log K$ )

Triazamacrocycles differ from tetraazamacrocycles in that the ligands are too small to have a cavity. The triaza rings are also much more rigid than the tetraazamacrocycles. This is the reason why only one type of conformer (either the R,R,R or the S,S,S) has been observed for [9]-ane-N<sub>3</sub>. Because the triaza rings are so small, the metal ions do not lie in the plane of the ring, but above the ring. In this case the [9]-ane-N<sub>3</sub> does not exert size-match selectivity.<sup>40</sup>

<sup>40</sup> A.E. Martell and R.D. Hancock in *Metal Complexes in Aqueous Solutions*, Plenum Press, New York, 1996, pp. 112-131

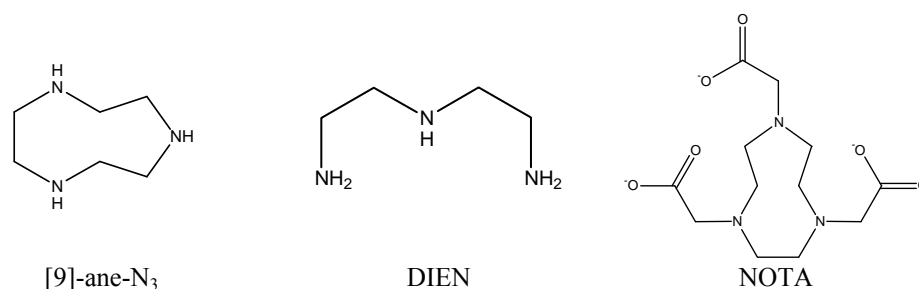


**Fig. 1.18** [9]-ane-N<sub>3</sub>, DIEN and NOTA

Table 1.2 shows a comparative study between [9]-ane-N<sub>3</sub> and DIEN (Fig. 1.18) with a series of metal ions. With Ni(II) there is an improvement in log(*K*) of 5.7 when [9]-ane-N<sub>3</sub> is used, rather than DIEN. With copper there was very little difference. Zn(II), Cd(II) and Pb(II) all showed slight improvements in the log(*K*) values. From the data that is presented it can be seen that [9]-ane-N<sub>3</sub> is a better coordination agent than the open chain analogue DIEN.<sup>40</sup>

**Table 1.2** Δlog(*K*) (MAC) = thermodynamic macrocyclic effect.<sup>40</sup>

Metal Ions	Ni(II)	Cu(II)	Zn(II)	Cd(II)	Pb(II)
Ionic Radius	0.69	0.75	0.74	0.95	1.18
Log( <i>K</i> <sub>1</sub> ) (9-ane-N <sub>3</sub> )	16.2	15.5	11.6	9.4	11.0
Log( <i>K</i> <sub>1</sub> ) (DIEN)	10.5	15.9	8.8	8.1	7.5
ΔLog( <i>K</i> ) (MAC)	5.7	-0.40	2.8	1.3	3.5

Selectivity of macrocycles with pendant donor groups are of great interest because of their potential use in the biomedical field. By adding the pendant arms, the small triazamacrocyclic ligand has been converted into a potential hexadentate ligand. With the tetraazamacrocyclic rings, addition of pendant donor groups leads to potential octadentate ligands. The smaller ligands, it is thought, are best suited for smaller metal ions while the octadentate ligand capability of the larger rings will be better suited for larger metal ions.<sup>40</sup>

Since it was found that the macrocycle is a better coordinating ligand than the open chain equivalent, a comparative study was done between the parent macrocycle and the macrocycle with pendant arms. Three acetate groups were added to the triazamacrocycle 9-ane-[N<sub>3</sub>] to produce NOTA [1,4,7-triazacyclononane-N,N',N''-triacetic acid - (Fig.1.18)]. These acetate groups



that were added gave the ligand a far better chelating capability than the parent ligand on its own<sup>40</sup> (Table 1.3).

**Table 1.3** The  $\Delta\log(K)$  values show that for these specific metal ions the macrocycle with the pendant arms is a better chelating agent than just the parent molecule.<sup>40</sup>

Metal ion	Cu(II)	Zn(II)	Cd(II)	Pb(II)
$\log(K_1)$ (9-ane-N <sub>3</sub> )	15.5	16.2	9.50	11.1
$\log(K_1)$ (NOTA)	21.6	21.1	16.0	16.6
$\Delta\log(K)$	6.10	4.90	6.50	5.50

It was found, in general, that smaller metal ions prefer to bind to a system that would provide 6-membered rings, while larger metal ions prefer to form 5-membered rings.<sup>41</sup>

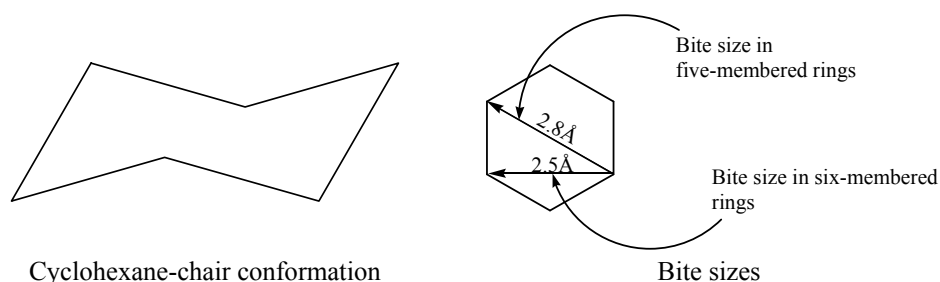


**Fig. 1.19** Cyclohexane in the chair conformation - minimum energy in the ring - and the bite size of the five- and six-membered rings.<sup>41</sup>

Considering cyclohexane (Fig. 1.19) in the chair conformation, the torsion angles are  $60^\circ$  and the bond angles are all ideal at  $109.5^\circ$ . In this conformation the strain energy is at a minimum in the molecule. This gives the ligand a "bite size" of 2.5 Å when forming a six-membered ring (Fig. 1.19 and 1.20) with a metal, and the angle that will form with the metal is  $109.5^\circ$ . The distance between the metal ion and the nitrogen atoms is 1.6 Å (Fig. 1.20). Because of this geometry and these dimensions, the smaller metal ion will prefer the six-membered ring structure.<sup>41</sup>

<sup>41</sup> A.E. Martell and R.D. Hancock in *Metal Complexes in Aqueous Solutions*, Plenum Press, New York, 1996, pp. 77-82, 98-104

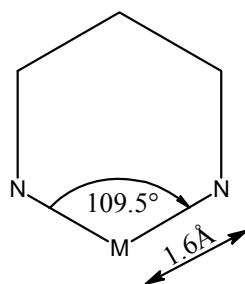


**Fig. 1.20** The ideal geometry for a six-membered ring.<sup>41</sup>

Considering the cyclohexane structure once more (Fig. 1.19), we are able to see what the diagonal dimensions would be for a five-membered chelate ring. In this instance it is easy to see that the "bite size" of the ligand is now 2.8 Å. The distance between the metal ion and the nitrogen atoms is now 2.5 Å (Fig. 1.21). The angle that is formed is 69°. Because of the angle and the longer bond distances, this is more suitable for larger metal ions (Fig. 1.19 and 1.21).<sup>41</sup>

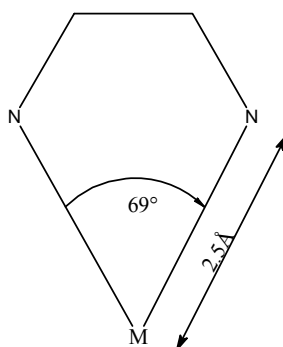


**Fig. 1.21** The ideal geometry for a five-membered ring.<sup>41</sup>

When oxygen donor atoms are considered, the angles for the five-membered rings between the oxygen and the carbon atoms change to 126° while the angle with the metal ion is now 58° (Fig. 1.22). The distance between the oxygen and the metal ion increases up to 3.2 Å.<sup>41</sup>

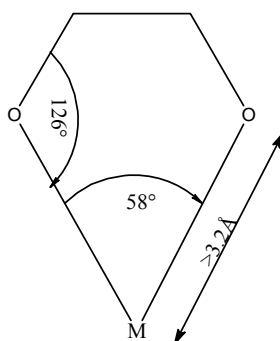


**Fig. 1.22** The ideal geometry for a five-membered ring.<sup>41</sup>

The six-membered rings will have an oxygen-metal-oxygen angle of  $95^\circ$  and the metal-donor distance will increase to approximately  $1.9 \text{ \AA}$  (Fig. 1.23).<sup>41</sup>

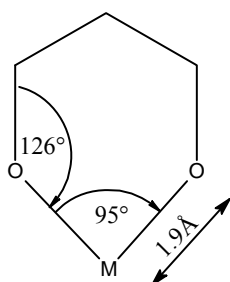


**Fig. 1.23** The ideal geometry for a six-membered ring.<sup>41</sup>

As can be seen from the above discussion, there is quite a variation in the bond lengths, and bond angles when comparing nitrogen and oxygen donor atoms in a macrocycle. The difference between chelate rings containing neutral nitrogen and neutral oxygen donors is that the neutral nitrogen donors will form as close to a tetrahedral structure as possible, while the oxygen will prefer a trigonal planar geometry. The reason for this preferred trigonal planar geometry is probably because the hybridization of the neutral oxygen donors is  $sp^2$ . There will be very little strain in the chelate rings when the neutral oxygen donors form the required trigonal planar geometry with the metal ion.<sup>41</sup>

## 1.5 The stability of complexes

Stability constants are a quotient involving concentrations of, or activities of reacting species in solution at equilibrium.<sup>42</sup> The quantitative description of metal complex stability and equilibria are of concern in a number of fields such as environmental monitoring of toxic metals and in medicinal agents based on metal ions.<sup>43</sup>



$$K_{\text{eq}} = \frac{a_{\text{C}}^{\gamma} a_{\text{D}}^{\delta}}{a_{\text{A}}^{\alpha} a_{\text{B}}^{\beta}} \quad (1.2)$$

Considering the general reaction (1.1), determination of the stability constant will be given by equation (1.2) when concentrations or activities are being used.

This equation is rather cumbersome, so it is common practice now to measure stability constants at a constant ionic strength. The equation (1.2) now changes to equation (1.3):

$$K_{\text{c}} = \frac{[\text{C}]^{\gamma} [\text{D}]^{\delta}}{[\text{A}]^{\alpha} [\text{B}]^{\beta}} \quad (1.3)$$

Stability constants, or equilibrium constants are effective measures of the affinity of ligands for metal ions. The measurement of stepwise stability constants for monodentate ligands basically started with the formation of transition metal-ammonia complexes in aqueous solution. This later led to stability work on chelate compounds.

---

<sup>42</sup> A.E. Martell and R.J. Motekaitis in *Determination and Use of Stability Constants*, VCH Publishers, New York, 1988, pp. 1-31

<sup>43</sup> K.N. Raymond and J.M. McCormick, *J. Coord. Chem.*, 1998, **46**, 51-57

The method described above is also employed in the determination of protonation constants. There is a definite relationship between the overall and the stepwise (successive) protonation constants and this is discussed in detail in chapter three.

## 1.6 The explanation of high protonation constants

The determination of crystal structures of the free ligands is very important, for this will give a good idea of how the protons will attach to the ligand. We will also get a good idea of the pre-organization of the ligand. From this it will be easy to see how the ligand changes its conformation when coordinated to a metal ion. We will be able to see the geometry, bond lengths, bond angles, torsion angles and the strain in the molecule.

Luckay<sup>44</sup> and co-workers determined the unusual high first protonation constant ( $pK_1$ ) of 1,4,7-tris(2-hydroxyethyl)-1,4,7-triazacyclononane (THETAC). By determining the crystal structure of THETAC·HBr, it was possible to determine the position of the proton in the ligand. By analysing the crystal structure together with some computational studies, it was possible to find the reason for the very high protonation constant.

## 1.7 Crystallographic studies with comparative macrocycles and Fe(III) as common metal ion

Comparative studies were also carried out between THETAC, TACNTA, TACN-TB and TACI (Fig.1.24) with Fe(III) as the common metal ion.<sup>44</sup> Metal-oxygen and metal nitrogen bond lengths were compared.

---

<sup>44</sup> R. Luckay, R.D. Hancock, I. Cukrowski and J.H. Reibenspies, *Inorg. Chim. Acta*, 1996, **246**, 159-169

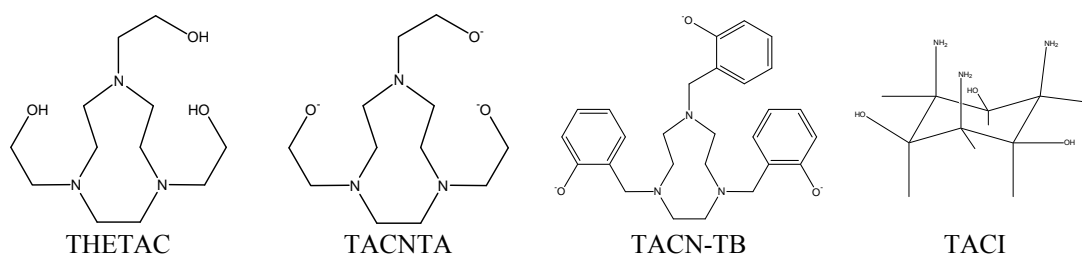


**Fig. 1.24** The ligands used by Luckay and co-workers.

Al-Sagher and co-workers studied the coordination chemistry of 1,4,7-tris[2-(*R*)-2-hydroxypropyl]-1,4,7-triazacyclononane with Co(II). The interesting result was the rare geometry of a six-coordinated trigonal prismatic structure. The vast majority of six-coordinate species are normally octahedral or pseudo-octahedral because the ligand system is very rigid and it cannot distort to conform to a non-octahedral structure.<sup>16</sup>

Another interesting result was obtained by Belal and co-workers.<sup>27</sup> The crystal structure that was obtained in this study was the interesting result of a dimer  $[\text{CoLH}_3\text{LCo}][\text{PF}_6]_3$ . The ligands (L) *N,N',N''*-tris[2-(*S*)-2-hydroxypropyl]-1,4,7-triazacyclononane, were ideally placed to create an octahedral shape. One of the CoL species lost three protons and was then joined by the other CoLH<sub>3</sub> species. These three hydrogen atoms formed hydrogen bonds with the deprotonated CoL. The hydrogen atoms connected the six oxygen atoms to link the CoL and the CoLH<sub>3</sub> and thus completed the dimer.<sup>27</sup>

Rettig and co-workers<sup>45</sup> crystallized  $[\text{Co}(\text{HCONH}_2)_2(\text{HCO}_2)]_x$ . In the structure that they obtained, each Co was connected to four other Co atoms. This generated a square lattice, but the geometry stayed octahedral. Although macrocyclic ligands were never used to form this complex, pseudo-macrocyclic rings were formed. We were interested in the differences or comparisons between these two structures e.g. the bond lengths between the Co and O and the Co and the N.

The Co(II) complex that was obtained in this study will be discussed in chapter 5.

<sup>45</sup> S.J. Rettig, R.C. Thompson, J. Trotter and S. Xia, *Inorg. Chem.*, 1999, **38**, 1360-1363

## 1.8 The chelate, macrocyclic and cryptate effect.

Metal chelates are defined as cyclic metal-organic compounds in which the metal is part of one or more five- or six-membered rings.<sup>46</sup>

The unusual stability of the macrocyclic complexes was attributed to the fixed geometrical placement of the ligand donor atoms according to Busch and co-workers<sup>47</sup> in 1971. This effect was first illustrated with a cyclic triamine by Busch and co-workers in 1970. Yang and Zompa<sup>48</sup> presented further evidence of the coordination strength of cyclic tridentate amines by determining formation constants of the Ni(II), Cu(II) and Zn(II) complexes. Lindoy stated three reasons why macrocyclic ligands often yield complexes which show unusual properties. Firstly, on complex formation geometrical factors, arising from the cyclic nature of the ligands, often impose additional constraints on the positions of the donor atoms. Secondly, if the cycle is fully conjugated and incorporates  $(4n+2)\pi$  electrons then enhanced electron delocalization and ligand stability are characteristic of the resulting Hückel aromatic system. Thirdly, macrocyclic ligand complexes are almost always found to be considerably more stable thermodynamically and kinetically than their corresponding open chain analogues. These properties are intrinsic features related to the cyclic nature of the ligands and have the collective name as the macrocyclic effect<sup>13</sup>. According to Lindoy<sup>13</sup> and Martell and Hancock<sup>38</sup>, there are four factors that play a role:

1. Macrocyclic ligands are pre-organized in comparison to "chainlike" ligands. This means that the macrocycle of the free ligand has only a limited number of conformers. Some of these conformers have structures that are similar to the conformation required to complex to the metal ion.

---

<sup>46</sup> D.A. Skoog, D.M. West and F.J. Holler in *Fundamentals of Analytical Chemistry*, Saunders College Publishing, Fort Worth, 1997, p. 95

<sup>47</sup> D.H. Busch, K. Farmery, V.L. Goedken, V. Katovic, A.C. Melnyk, C.R. Sperati and N. Tokel in *Adv. Chem. Ser.*, **100**, American Chemical Society Publications, Washington D.C., 1971, pp. 44-78

<sup>48</sup> R. Yang and L.J. Zompa, *Inorg. Chem.*, 1976, **15**, 1499-1502

2. Desolvation of the donor atoms in the cavity of the macrocycle, due to the confined space is easier and faster because fewer solvent molecules can be accommodated in the cavity due to the confined space.
3. The intrinsic basicity effects, due to the induction effect of the carbon bridges between the donor atoms; the carbon bridges will have an induction effect on the donor atoms, causing the donor atoms to be more basic.
4. Enforced repulsion between the lone pairs of the donor atoms in the cavity of the macrocycle which is released when the metal complex is formed.<sup>38</sup>

$$\Delta G = \Delta H - T\Delta S$$

$$\Delta G = -RT \ln K$$

$$\frac{d(\ln K)}{dT} = -\frac{\Delta H}{RT^2}$$

From the equations above it is clear that there is a direct relation between  $K$ ,  $\Delta H$  and  $\Delta S$ . It was suggested that the macrocyclic and chelate effect have a common origin, but this suggestion was proven not to be the case for it is not possible to ascribe a single origin to the macrocyclic effect. When the unidentate ligand (Fig. 1.25A ) attaches itself to the metal ion, there is no restriction on the second ligand. The second ammonia ligand is free to move about the entire solution. The chelate effect of a bidentate ligand was proposed by Schwartzenbach in terms of the idea that when the first donor atom had attached itself to the metal ion, the second donor atom is now confined to move only in a restricted volume (Fig. 1.25B). According to this proposal, the entropy of the donor atoms was greatly reduced in comparison to that of the unidentate ligands. The Schwartzenbach model predicted that the chelate effect would prove itself as a more favourable entropy complex formation than would be the case for the analogous unidentate complex formation. From this model it would appear that the stability of complexes with larger chelate rings would be of lower complex stability than those of five membered chelate rings due to the larger volume to which the chelate ring would be restricted when coordinated to the metal ion by only one donor atom. Although this appears to be true in general, the model does not seem to be in agreement with the observation in that it is expected that the decrease in the formation constant



that occurs as the chelate ring size is increased, should be an entropy effect, whereas, at least for chelate ring sizes less than seven it is predominantly an enthalpy effect.<sup>49</sup>

Considering the scheme in Fig. 1.25, it is tempting to think that the entropy effect is the driving force behind the reactions concerning macrocycles. This assumption was proven to be erroneous.

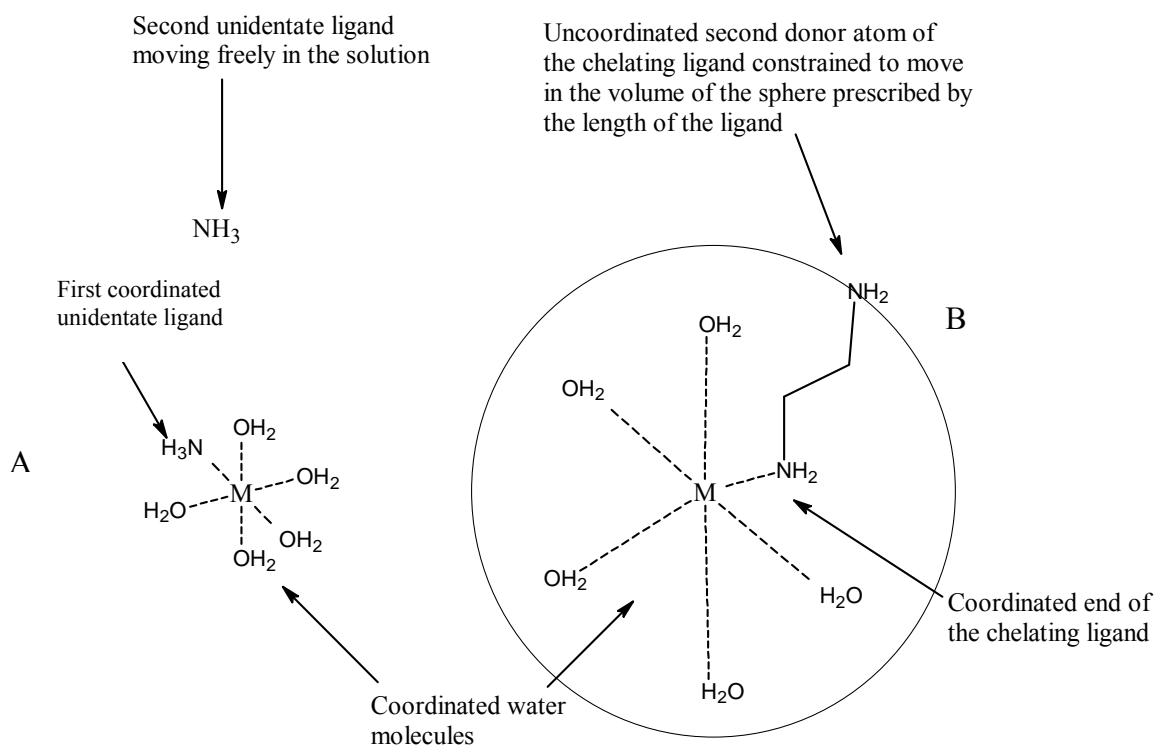


**Fig. 1.25** The diagram illustrates the Schwarzenbach model of the chelate effect. In (A), the second monodentate ligand (ammonia) is free to translate in solution, while in (B) the second donor atom of the chelating ligand (ethylenediamine) is constrained to move in a sphere, the radius of which is prescribed by the length of the bridge connecting the two donor atoms.<sup>49</sup>

From data that was collected it was shown that both the enthalpy and the entropy contributes to the macrocyclic effect. Ring size must also be taken into consideration and so must the solvation of the macrocycle, but this is then again linked to the entropy effect.<sup>50</sup> It is clear that a single factor cannot be considered on its own.

<sup>49</sup> A.E. Martell and R.D. Hancock in *Metal Complexes in Aqueous Solutions*, Plenum Press, New York, 1996, p. 64

<sup>50</sup> E.C. Constable in *Coordination Chemistry of Macrocyclic Compounds*, Oxford University Press, New York, 1999, pp. 55-59

## 1.9 Ligand design principles

When designing new macrocyclic ligands, there are a number of factors to consider:<sup>51</sup>

- the SHAB (soft-hard acid-base) character of the metal ion
- the size of the metal ion (metal ion radius)
- the coordination number and the geometry of the metal ion e.g. square planar or octahedral etc.
- the general affinity of the metal ion with a particular type of ligand, e.g. OH<sup>-</sup>, NH<sub>3</sub>, HOCH<sub>2</sub>, CH<sub>2</sub>S<sup>-</sup> etc.
- the ring size of the ligand, the denticity and the presence of sterically bulky groups on the ligand.
- the induction effects of the bridges between the donor atoms - ethylene bridges or propylene bridges etc.

**Table 1.4** A comparison between the ligand field strength of unidentate ligands, open chain bidentate ligands and macrocyclic ligands.<sup>52</sup>

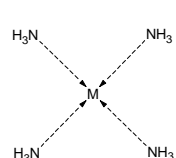
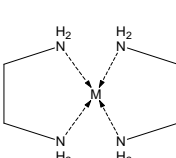
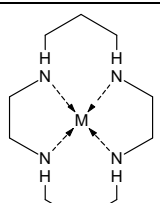
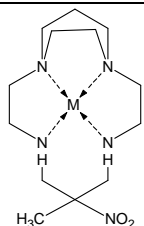
	0°	1°	2°	3°
				
$\Delta H[\text{Cu(II)}](\text{kcalmol}^{-1})$	-22.0	-25.5	-32.4	
$\nu(\text{d-d})(\text{cm}^{-1})\text{Cu(II)}$	17000	18300	19900	21050
$\nu(\text{d-d})(\text{cm}^{-1})\text{Ni(II)}$	~20000	21600	22470	23900

Table 1.4 illustrates how the ligand field strength increases with donor atom basicity along the series 0° < 1° < 2° < 3° and secondly, the increasing power of the N-donor atoms of the ligands along the series 0° < 1° < 2° < 3°. The bridges between the donor

<sup>51</sup> A.E. Martell and R.D. Hancock in *Metal Complexes in Aqueous Solutions*, Plenum Press, New York, 1996, pp. 151-154

<sup>52</sup> A.E. Martell and R.D. Hancock in *Metal Complexes in Aqueous Solutions*, Plenum Press, New York, 1996, p. 52

atoms produce an induction effect which will assist the donor atoms in the donation of their electrons to the metal ion.<sup>49</sup>

By adding pendant arms to the parent macrocycle, the poly-azamacrocyclic ligand now provides the possibility for two or more alkylating moieties to be present in the same molecule. The distance between the donor atoms can be varied by changing the number of carbons in the bridges between the donor atoms.<sup>23</sup> This leads to new possibilities as there can now be hard and soft donor atoms in the same ligand. Longer side chains (or pendant arms) means that the side chains can reach further. This should give the ability for the chelating agent to bind better to even bigger metals although the parent macrocycle may be small.

Pendant arm donor macrocyclic ligands have intrinsically the same purpose as the parent chelating agents. By changing the donor atoms of the pendant arms, they can now provide a non-labile set of donor atoms which serve to immobilize a metal ion along with a set of possibly more labile donor atoms of the macrocyclic ring, which can perturb the metal ion at additional coordination sites, in competition with external substrates, or which can be used as attachment points for other molecules.<sup>11</sup>

The three nitrogen attached pendant donor arms produces a way of forming a six coordinate complex in which there are two pairs of facial donors.<sup>11</sup>

The majority of all nitrogen donor macrocyclic ligands that have been studied are quadridentate.<sup>11</sup> The aim of this study was firstly to synthesize two novel medium-sized triazamacrocycles with pendant arms. Previous work showed that the bridges between the N-atoms were all equal in length, being either 3 ethylene bridges or 3 propylene bridges.<sup>53</sup>

---

<sup>53</sup> E.R. Richman and T.J. Atkins, *J. Am. Chem. Soc.*, 1974, **96**, 2268-2269

## 1.10 Aim

By synthesizing these two new ligands, we will be able to complete the series between the known ligands. In addition to synthesizing the parent molecules, pendant arms were added to create a hexadentate ligand. Each of these molecules would be characterized fully by means of NMR, elemental-analysis, mass spectrometry, melting point determination.

We need to determine the protonation constants (which are also required for the determination of the formation constants) of the ligands by means of potentiometric titration, using a glass electrode with built-in standard electrode.

The third objective is to investigate the formation constants of these ligands with a series of metal ions.

The fourth objective is to complex these ligands to a series of metal ions and to determine their crystal structures through single crystal X-ray diffraction. Each of these structures needs to be examined in detail so that we can achieve a sound understanding of how these molecules react, bond and interact with metal ions of varying sizes.

The macrocyclic ligands will be used as coordination agents with a number of metal ions. The structure of the new ligands creates the opportunity for the metal ions to form both 5- and 6-membered rings in one complex. This means that we would like to see less discrimination in the selection of metal ions when size comes into play. Crystal structures of some of these complexes will be determined by means of single crystal X-ray diffraction. All these results will be discussed and compared to the parent ligand and ligands of similar structure.

## Chapter 2

### *The Preparation and Characterization of THTD and THTUD*

#### 2.1 Introduction

Due to their maximum fixed ring size, macrocyclic ligands can be used in various fields, for instance in mining. Due to their selectivity macrocycles can be used for extraction purposes for specific metal ions.<sup>54</sup> More recently, in the medical field, the usefulness of the parent macrocycle has been extended by adding pendant arms which gives them the ability to act as blocking mechanisms because of the cross linking ability, and so inhibit the pathways of certain reactions. This ability is especially required in medical (cancer) research. Because of the cross linking ability (between DNA stands) of the pendant arms, it can be used as an inhibitor in cancer cells.<sup>24</sup>

#### 2.2 Aim

The first aim of this research project was to synthesize 2 novel, medium sized macrocyclic ligands with pendant arms, 1,4,7-tris[(*S*)-2-hydroxypropyl]-1,4,7-triazacyclodecane (THTD) and 1,4,8-tris[(*S*)-2-hydroxypropyl]-1,4,8-triazacycloundecane (THTUD) and fully characterize these ligands by <sup>1</sup>H and <sup>13</sup>C NMR-, mass spectrometry, elemental analysis and melting point determination.

Previous studies on macrocyclic ligands have shown that when it comes to triazamacrocycles, the bridges between the nitrogen atoms were all equal in length, either being 3 ethylene bridges, [9]-ane-N<sub>3</sub>, or 3 propylene bridges, [12]-ane-N<sub>3</sub>, including all their derivatives. By synthesizing THTD and THTUD, the gap between these ligands, [9]-ane-N<sub>3</sub>, and [12]-ane-N<sub>3</sub> is closed and we also hoped that these two

---

<sup>54</sup> E.C. Constable in *Coordination Chemistry of Macrocyclic Compounds*, Oxford University Press, New York, 1999, pp. 1-5

relatively more unsymmetrical ligands produce an interesting selectivity pattern with a number of transition and post-transition metal ions.

## 2.3 Methods of synthesis and pathways

Over the last three to four decades, various methods and techniques for the synthesis of medium sized cyclic triamines have been reported, e.g. by Koyama and Yoshino in 1972,<sup>55</sup> Yang and Zompa in 1976,<sup>48</sup> Sabatini and Fabbrizzi in 1979<sup>56</sup> and Madeyski and co-workers in 1984.<sup>57</sup> In these publications, the methods and techniques are discussed in great detail. When comparing the various methods, two approaches stand out in the synthesis of macrocycles namely, template synthesis and direct synthesis. A third, the high dilution method, is meant for a particular type of macrocycle and is not applicable to the aza-macrocycles. These types of reactions will be discussed in section 2.3.1 to 2.3.3.

### 2.3.1 Template synthesis

In the template synthesis of macrocycles, it is essential to have a metal ion present to keep the cyclic precursors in position before the formation of the macrocycle<sup>13, 58, 59</sup> (Fig. 2.1). One major problem in the synthesis of macrocycles was how to control the two ends of the chains in order to finalize the cyclization step. The template synthesis method sometimes incorporates an additional donor atom into the chain and the cyclization reaction then takes place in the presence of a metal ion. The metal ion will coordinate to the donor atoms and pre-organize the various intermediates. These pre-organized intermediates will now be in the desired conformation to form the required macrocycle.

---

<sup>55</sup> H. Koyama and T. Yoshino, *Bull. Chem. Soc. Jpn*, 1972, **45**, 481-484

<sup>56</sup> L. Sabatini and L. Fabbrizzi, *Inorg. Chem.*, 1979, **18**, 438-444

<sup>57</sup> C.M. Madeyski, J.P. Michael and R.D. Hancock, *Inorg. Chem.*, 1984, **23**, 1487-1489

<sup>58</sup> P. Comba, N.F. Curtis, G.A. Lawrance, A.M. Sargeson, B.W. Skelton and A.H. White, *Inorg. Chem.*, 1986, **25**, 4260-4267

<sup>59</sup> A.M. Sargeson, *Pure Appl. Chem.*, 1984, **56**, 1603-1619

The advantages of this method are good yields, obtaining a metal complex directly and also mild reaction conditions.<sup>60</sup> There are a few disadvantages to this method. One major disadvantage is that not all metal ions can act as templates for a desired reaction. This means that the reaction will proceed by chance rather than rationally. Another problem is that it is not always possible to predict what the product might be. With template effects involving the group 1 metal ions, it is usually the free ligand that is isolated. When using transition metals, it is more often found that stable metal complexes are formed.

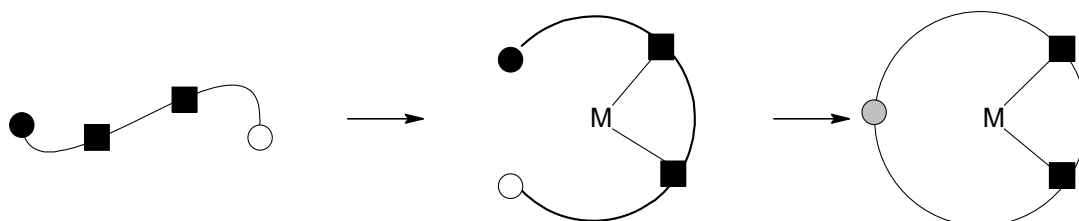


**Fig. 2.1** A schematic view of the cyclization step involved in a templated macrocycle synthesis. The circles represent the mutually reactive functional groups and the squares are the additional donor atoms. The binding of the metal to the donor atoms pre-organize the ligand into the required conformation for cyclization.<sup>68</sup> Not all the donor atoms are shown in the figure.

### 2.3.2 High dilution technique

Stetter and Roos<sup>61</sup> reported that cyclization was obtained in moderate to low yields in the condensation of terminal dihalides with bisulfonamide salts under high dilution conditions. The macrocycles that they synthesized, consisted of a ring system with two benzo rings as part of the macrocyclic ring, connected by carbon bridges (Fig. 2.2).

<sup>60</sup> E.C. Constable in *Coordination Chemistry of Macrocyclic Compounds*, Oxford University Press, 1999, pp. 42-46

<sup>61</sup> H. Stetter and E.-E. Roos, *Chem. Ber.*, 1954, **87**, 566-580

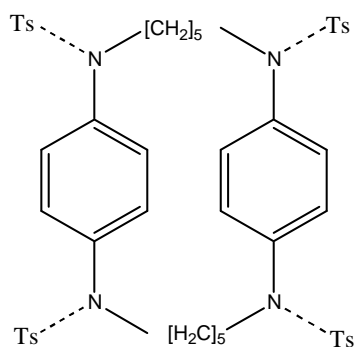


**Fig. 2.2** Bis-[N,N'-ditosyl]-N,N'-pentamethylene-p-phenyldiamine]

### 2.3.3 Direct synthesis

When using the direct method, no metal ions are needed to form the precursor or to keep them in place. The use of protection groups makes it much easier and the conditions are not extreme to perform these reactions. By using the direct method, it is possible to improve the yields substantially. It was found that by using preformed bissulfonamide sodium salts and sulphonate ester leaving groups in a dipolar, aprotic solvent; it is possible to get rid of the high dilution techniques.<sup>53</sup> The method was thoroughly tested by Atkins, Richman and Oettle.<sup>62</sup>

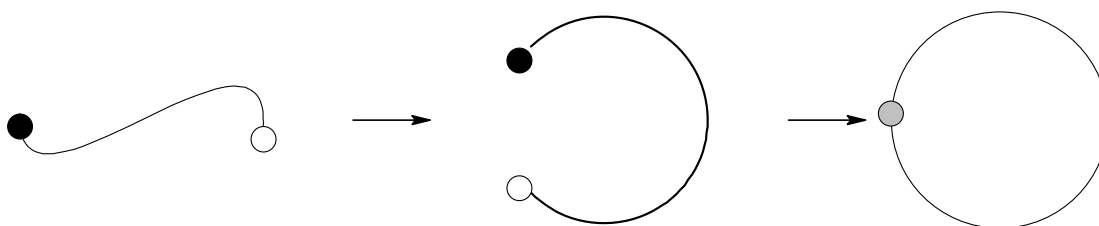


**Fig. 2.3** A schematic view of the cyclization step involved in a non-templated macrocycle synthesis. The circles represent the mutually reactive functional groups. In the first step the appropriate conformation must be adopted so that the reactive functional groups are close to one another and in the correct orientation for reaction. Secondly the new bond is formed and this will complete the macrocycle.<sup>60</sup> The donor atoms have been excluded from the diagram.

<sup>62</sup> T.J. Atkins, J.E. Richman and W.F. Oettle, *Org. Synth.*, 1978, **58**, 86-98



## 2.4 Experimental

The method implemented in this study made use of the direct synthesis method. This method is described by Sabatini and Fabbrizzi,<sup>56</sup> Richman and Atkins,<sup>53</sup> Koyama and Yoshino<sup>55</sup> and Atkins and co-workers.<sup>62</sup>

All reactions were performed under standard atmospheric conditions, unless stated otherwise.

### 2.4.1 Materials

Toluene-4-sulfonyl chloride was obtained from Fluka and the molecular weight was used as indicated on the container. All other chemicals were obtained from Sigma-Aldrich and the molecular weights were used as indicated on the containers.

### 2.4.2 Instrumentation

All NMR spectra were determined on a Varian VNMRS 300 MHz Spectrometer. Electron impact mass spectrometry was done on an AMD 604 High Resolution Mass Spectrometer. The melting points were determined by means of a Stuart Scientific Melting Point Apparatus. The temperature plateau was set to 100°C and the temperature was increased at a rate of 3.5°C per minute. The elemental analysis was carried out at the University of Cape Town.

### 2.4.3 Experimental procedure of the preparation of THTD and THTUD

#### 2.4.3.1 *Protection of the amines by means of tosylation*

##### 2.4.3.1.1 *Tosylation of diethylenetriamine*

Toluene-4-sulfonyl chloride (114.390 g - 0.600 mol,) was dissolved in approximately 700 mL of dry diethyl ether. A solution of NaOH (3.000 mol dm<sup>-3</sup>) was prepared by dissolving NaOH pellets (24.000 g -

0.600 mol) in water (200.0 mL). Diethylenetriamine (20.630 g - 0.200 mol) was then added to the freshly prepared NaOH solution. The solution of toluene-4-sulphonyl chloride was added dropwise over a period of 2 hours to the diethylenetriamine and stirred mechanically for 3 hours. A thick, white precipitate formed. This precipitate was filtered through a no. 4 sintered glass filter and washed, first with water and then with ether to ensure that the product was clean. The tosylated product was dissolved in hot absolute ethanol and left to crystallize at room temperature. The crystals were left in an open atmosphere at room temperature for 3 days to dry completely. A yield of 100% was assumed (mass = 112.950 g).

#### *2.4.3.1.2 Tosylation of bis-(3-aminopropyl)-amine*

The reaction is analogous to the tosylation of the diethylenetriamine as it is described in section 2.4.1.1.1, but differs in that we used bis-(3-aminopropyl)-amine (26.244g - 0.200 mol). A yield of 100% was assumed (mass = 118.760 g).

#### *2.4.3.2 **Protection of the diol by means of tosylation***

##### *2.4.3.2.1 Tosylation of 1,3-propanediol*

1,3-propanediol (15.220 g - 0.200 mol) was added to triethylamine (200 mL). Toluene-4-sulphonyl chloride (76.260 g - 0.400 mol) was dissolved in approximately 400 mL of dry diethylether and added dropwise to the 1,3-propanediol solution over a time period of 2 hours. The mixture was mechanically stirred overnight. A thick, white precipitate was formed. This white precipitate was filtered through a no.4 sintered glass filter and washed first with water, and then with ether. The tosylated product was then crystallized from hot ethanol (99.99%) and the crystals were left for 3 days to dry completely in an open atmosphere at room temperature. A yield of 100% was assumed (mass = 76.894 g).

#### 2.4.3.2.2 *Tosylation of ethylene glycol*

The reaction is analogous to the tosylation of the 1,3-propanediol as it is described in section 2.4.2.1.2, but we used ethylene glycol (12,414g - 0.200 mol). A yield of 100% was assumed (mass = 74.089 g).

#### 2.4.4 Preparation of the tosylated triamine disodiumsalt (diethylenetriamine and the bis-(3-aminopropyl)-amine)

The procedure was carried out under inert conditions (N<sub>2</sub>), in a 2 L round bottom flask, fitted with a CaCl<sub>2</sub> drying tube.

Na (9.196 g - 0.400 mol) was reacted with approximately 1.2 L of ethanol. The tosylated tri-amine (0.200 mol) was then added bit by bit to the Na solution and stirred overnight by means of a mechanical stirrer. A white precipitate formed which is the Na-salt of the tri-amine. This precipitate was filtered through a no. 4 sintered glass filter, and washed with ethanol and diethyl ether. A yield of 90% was obtained (mass = 114.790 g).

The synthesis described is analogous for the tosylated diethylenetriamine as well as the tosylated bis-(3-aminopropyl)-amine. A yield of 92% was obtained (mass = 112.180 g).

#### 2.4.5 Synthesis of the macrocycles

##### 2.4.5.1 *Synthesis of tosylated 1,4,7-triazacyclodecane*

The tosylated diethylenetriamine di-sodium salt was immediately dissolved in approximately 900 mL of DMF and placed in an oil bath at 120°C. The tosylated 1,3-propanediol (114.790 g - 0.180 mol) was dissolved in 450 mL DMF and added dropwise (over a period of 2 hours) to the freshly prepared solution of tosylated diethylenetriamine di-sodium salt while stirring vigorously with an overhead stirrer. This solution was then stirred for a further 8 hours. A clear orange solution had formed. This clear orange

solution was filtered through a no. 4 sintered glass filter and it was then added slowly to approximately 8 L of ice water. A white precipitate formed immediately when added to the water and the solution was left for 24 hours for the maximum amount of product to precipitate. The precipitate was filtered off and recrystallized from ethanol. A 99.99% yield was obtained (mass = 109.040 g).

#### ***2.4.5.2 Synthesis of tosylated 1,4,8- triazacycloundecane***

The reaction is analogous to section 2.4.4.1, using the tosylated bis-(3-aminopropyl)-amine and the tosylated ethylene glycol. A 99.99% yield was obtained (mass = 111.470 g).

#### **2.4.6 De-tosylation and formation of the HBr-salt of the macrocycles**

The reaction described below was applied to both products that were obtained as described in the previous section 2.4.4.

The tosylated macrocycle (15 g, 0.022 mol) was added to 48% HBr (480 mL) and glacial acetic acid (270 mL). The solution turned dark red and was refluxed for 3 days (72 hours). This solution was cooled down to room temperature. After cooling, the solution was filtered through glass wool to get rid of any solids. The volume was then reduced by means of vacuum distillation to approximately 250 mL.

A mixture of ethanol (300 mL - 99.99%) and diethylether (100 mL) was made. The filtrate (detosylated macrocycle) was added to the ethanol/ether mixture and left in an ice bath for 4 hours. A white precipitate formed and this product was filtered through a no.4 sintered glass filter and washed with ether. The product was recrystallized from ethanol (99.99%) and left for 5 days to dry. A yield of 85% was obtained. (mass =  $\pm$  5.2 g)

## 2.4.7 The addition of the pendant arms

The procedure is analogous for both the macrocycles and the reaction must be carried out under inert (N<sub>2</sub>) conditions.

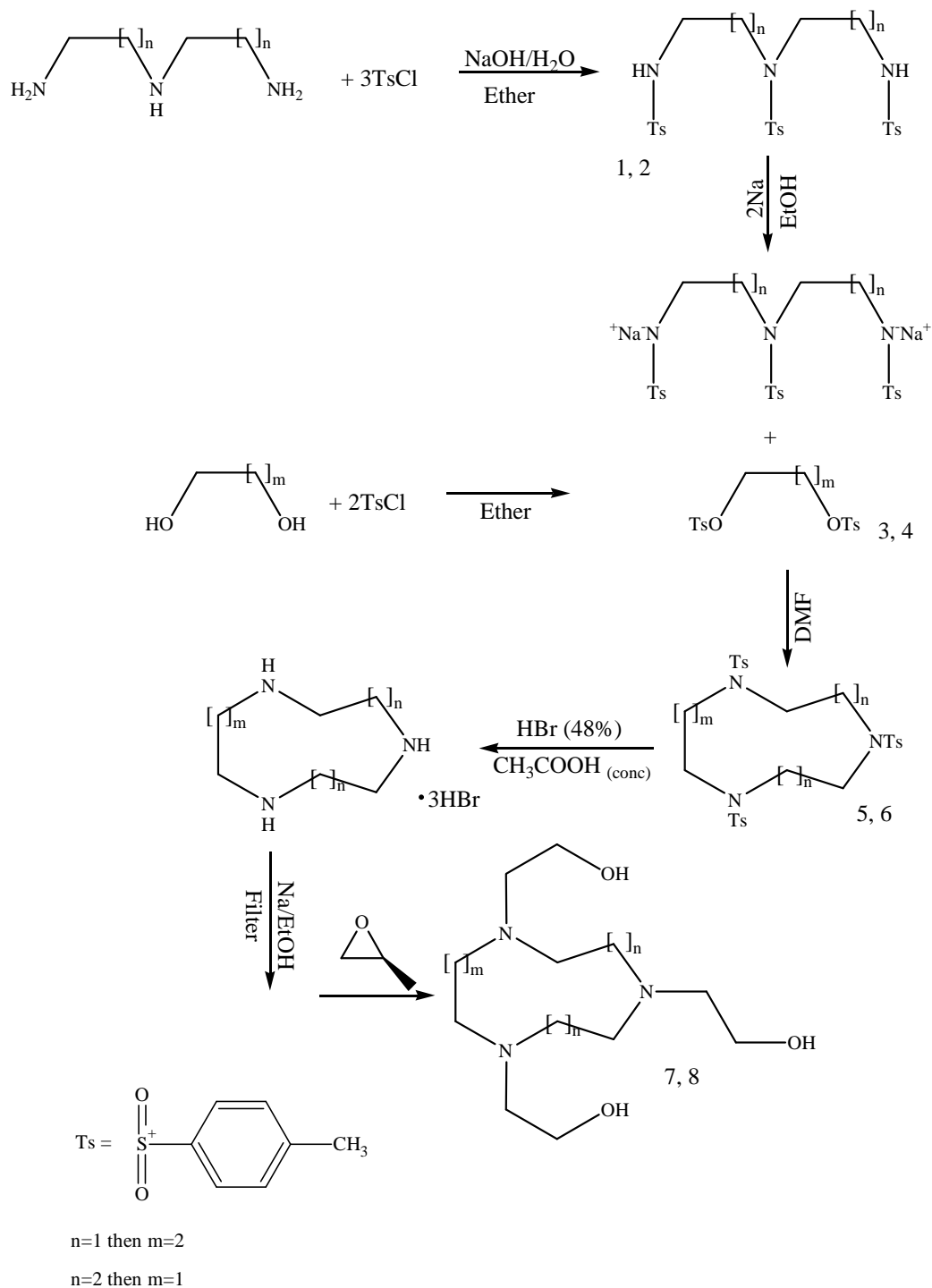


**Fig. 2.4** The synthesis of 1,4,7-tris[(S)-2-hydroxy-propyl]-1,4,7-triazacyclodecane (THTD) and 1,4,8-tris[(S)-2-hydroxy-propyl]-1,4,8-triazacycloundecane (THTUD).

Na metal (0.414 g - 0.018 mol) was reacted with approximately 100 mL ethanol (99.99%). The macrocyclic-HBr-salt (0.006 mol) was then added to the sodium ethoxide solution and stirred for approximately 2 hours. A white precipitate -NaBr- formed which was filtered off by using normal no. 4 filter paper. (*S*)-(-)-propylene oxide (1.5 mL - 0.018 mol) was added to the solution to attach the arms to the macrocycle. This solution was stirred at room temperature for 7 days.

On completion of the reaction, the volume of the solution was reduced with the use of a rotary evaporator. A white precipitate (NaBr) formed which was removed. Since NaBr and the product are soluble in water, it was decided to add CH<sub>2</sub>Cl<sub>2</sub> to the solution because the product is more soluble in the CH<sub>2</sub>Cl<sub>2</sub> than NaBr. The NaBr was removed by filtration through a no. 4 filter paper. This procedure was repeated a few times to ensure that all the NaBr was removed. The product (filtrate) was dried by means of a rotary evaporator and afterwards placed on a vacuum pump to ensure a dry product. A yield of 60% were obtained for both products. (mass: THTD = 3.43 g and THTUD = 3.58 g)

## 2.5 Results and discussion

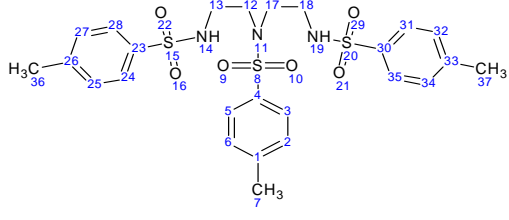
Various analytical methods were used to confirm the formation of the THTD and the THTUD. Apart from the NMR spectra that were collected, we also used elemental analysis and mass spectrometry. Crystal structures of some of the complexes also confirmed the formation of the ligands.

### 2.5.1 NMR spectra

#### 2.5.1.1 NMR spectra of the tosylated diethylenetriamine (DIEN)

An NMR spectrum of the compound was determined (in CDCl<sub>3</sub>) to confirm that the DIEN was indeed tosylated (compound 1). The NMR spectrum was compared to previously-determined NMR-data of similar structures.<sup>27</sup>

**Table 2.1**  $^1\text{H}$  and  $^{13}\text{C}$  NMR data of the tosylated diethylene triamine (compound 1) in  $\text{CDCl}_3$ 

Assignment	$\delta$ / ppm
	
<b><math>^1\text{H}</math> NMR</b>	
$\text{H}^{2, 3, 6, 24, 25, 27, 28, 31, 32, 34, 35, 45}$	7.0-8.0
$\text{H}^{7, 36, 37}$	2.0-2.5
$\text{H}^{12, 13, 17, 18}$	3.0-3.2
$\text{H}^{14, 19}$	1.7-1.9
<b><math>^{13}\text{C}</math> NMR</b>	
$\text{C}^{3, 5}$	130.1
$\text{C}^4$	144.4
$\text{C}^{7, 36, 37}$	21.3
$\text{C}^{23, 30}$	143.8
$\text{C}^{24, 28, 31, 35}$	130.0
$\text{C}^{25, 27, 32, 34}$	127.3
$\text{C}^{26, 33}$	129.3
$\text{C}^{12, 17}$	50.4
$\text{C}^{13, 18}$	42.5

#### 2.5.1.1.1 $^{13}\text{C}$ NMR spectrum of the tosylated DIEN

The  $^{13}\text{C}$  NMR spectrum (Table 2.1, Appendix 1a) of the tosylated intermediate shows the aromatic carbons ( $\text{C}^{2-6}$ ,  $\text{C}^{23-26}$  and  $\text{C}^{30-33}$ ) in the expected region between 126 ppm to 145 ppm. Since there is a slight difference between the terminal tosyl groups and the central tosyl group, there is a very subtle shift downfield for the central tosyl group ( $\text{C}^{2-6}$ ) compared to that of the terminal tosyl groups ( $\text{C}^{23-26}$  and  $\text{C}^{30-33}$ ). The signal for the three methyl groups connected to the tosyl groups ( $\text{C}^7$ ,  $\text{C}^{36}$  and  $\text{C}^{37}$ ) can be found at 21.5 ppm. The resonance for the  $\text{CH}_2$ 's ( $\text{C}^{12}$  and  $\text{C}^{17}$ ) can be seen at 50.5 ppm and the other  $\text{CH}_2$ 's ( $\text{C}^{13}$  and  $\text{C}^{18}$ ) at 42.5 ppm.

#### 2.5.1.1.2 $^1\text{H}$ NMR spectrum of the tosylated DIEN

Table 2.1 gives the chemical shifts of the signals in the  $^1\text{H}$  NMR spectrum of the tosylated DIEN (Appendix 1b). It was found that this data is consistent with a previously published structure.<sup>27, 63</sup>

The range from 7.0 ppm to 8.0 ppm is typical for protons of aromatic rings. The signals in the region from 2.0 ppm to 2.5 correspond to the CH<sub>3</sub>-groups that are attached to the aromatic rings. Integration indicates that the number of protons does indeed correspond to the protons of the methyl groups. Between 3.0 ppm and 3.2 ppm, we see a doublet of doublets. These peaks represent the CH<sub>2</sub>'s of the ethylene bridges. The broad peak between 1.7 ppm and 1.9 ppm is typical of an amine peak. There are traces of unreacted reagents present.

### 2.5.1.2 NMR spectra of the tosylated bis-(3-aminopropyl)-amine

An NMR experiment was carried out (in CDCl<sub>3</sub>) to confirm that the bis-(3-aminopropyl)-amine (compound 2) was indeed tosylated. The NMR spectra were compared to previous NMR-data of similar structures.<sup>27, 63</sup>

**Table 2.2** <sup>1</sup>H and <sup>13</sup>C NMR spectra of the tosylated bis-(3-aminopropyl)-amine (compound 2) in CDCl<sub>3</sub>.

Assignment	δ / ppm
<b><sup>1</sup>H</b>	
H <sup>3, 5, 26, 30, 33, 37</sup>	7.738-7.748
H <sup>2, 6, 27, 29, 34, 36</sup>	7.334-7.344
H <sup>15, 21</sup>	1.555
H <sup>12, 14, 18, 20</sup>	4.044
H <sup>13, 19</sup>	1.966
H <sup>7, 38, 39</sup>	2.425
<b><sup>13</sup>C</b>	
C <sup>1, 28, 35</sup>	145.2
C <sup>4, 25, 32</sup>	132.8
C <sup>2, 6, 27, 29, 34, 36</sup>	130.1
C <sup>3, 5, 26, 30, 33, 37</sup>	128.0
C <sup>12, 14, 18, 20</sup>	65.8
C <sup>13, 19</sup>	28.4
C <sup>7, 38, 39</sup>	21.3

<sup>63</sup> J. Huskens and A.D. Sherry, *Chem. Commun.*, 1997, 845-846



#### 2.5.1.2.1 $^{13}\text{C}$ NMR spectrum of the tosylated bis-(3-aminopropyl)-amine

Table 2.2 gives the chemical shifts of the signals in the  $^{13}\text{C}$  NMR spectrum of the tosylated bis (3-aminopropyl)-amine (Appendix 2a). Four distinct signals occur between 127 ppm and 146 ppm. These are consistent with the aromatic ring carbons of the tosyl groups.

The two resonances at 28 ppm and 66 ppm are respectively assigned to the  $\text{CH}_2$ 's of the propyl bridges.

#### 2.5.1.2.2 $^1\text{H}$ NMR spectrum of the tosylated bis-(3-aminopropyl)-amine

Table 2.2 gives the chemical shifts of the signals in the  $^1\text{H}$  NMR spectrum of the tosylated bis-(3-aminopropyl)-amine (Appendix 2b). The peaks between 7.3 ppm and 7.8 ppm are typical of protons that are situated on aromatic rings. The two doublets indicate that the protons closer to the  $\text{SO}_2$  are shifted further downfield than the neighbouring protons. The peak at 1.56 ppm is consistent with the protons on N15 and N21. The triplet at 4.04 ppm is the  $\text{CH}_2$  ( $\text{C}^{12}$ ,  $\text{C}^{14}$ ,  $\text{C}^{18}$ ,  $\text{C}^{20}$ ) adjacent to the NH. The other  $\text{CH}_2$ 's ( $\text{C}^{13}$ ,  $\text{C}^{19}$ ), split into a quintet at 1.97 ppm because of the four adjacent protons on the neighbouring carbons of the propylene bridges. The 3 methyl groups give a very prominent peak at 2.43 ppm.

#### 2.5.1.3 *NMR spectra of the tosylated 1,3-propanediol*

NMR spectra were recorded (in  $\text{CDCl}_3$ ), to confirm that the 1,3-propanediol was indeed tosylated (compound 3).

**Table 2.3**  $^1\text{H}$  and  $^{13}\text{C}$  NMR data of the tosylated 1,3-propanediol (compound 3) in  $\text{CDCl}_3$ .

Assignment	$\delta$ / ppm
$^1\text{H}$	
$\text{H}^{3, 5, 20, 24}$	7.71-7.78
$\text{H}^{2, 6, 21, 23}$	7.31-7.38
$\text{H}^{10, 12}$	4.00-4.07
$\text{H}^{7, 25}$	2.41-2.44
$\text{H}^{11}$	1.91-2.02
$^{13}\text{C}$	
$\text{C}^{4, 19}$	145.3
$\text{C}^{1, 22}$	132.8
$\text{C}^{3, 5, 20, 24}$	130.1
$\text{C}^{2, 6, 21, 23}$	128.0
$\text{C}^{10, 12}$	65.7
$\text{C}^{11}$	28.5
$\text{C}^{7, 25}$	21.4

#### 2.5.1.3.1 $^{13}\text{C}$ NMR spectrum of the tosylated 1,3-propanediol

Table 2.3 gives the chemical shifts of the  $^{13}\text{C}$  NMR spectrum (Appendix 3a) of the tosylated 1,3-propanediol (compound 3). All the expected carbons are present in the spectrum.

The aromatic ring carbons of the tosyl groups are in the expected chemical environment between 128 ppm and 146 ppm. There are four clearly defined signals that correspond to the four different carbons ( $\text{C}^{1-6}$  and  $\text{C}^{19-24}$ ) of the aromatic rings. At 65.7 ppm we observe the resonances of carbons  $\text{C}^{10}$  and  $\text{C}^{12}$ . These signals of the  $\text{CH}_2$ -groups are shifted downfield because of the two oxygen atoms that are directly connected to them. The signal of the central  $\text{CH}_2$  ( $\text{C}^{11}$ ) can be found at 28.5 ppm. The signals of the methyl groups  $\text{C}^7$  and  $\text{C}^{25}$  are found at 21.4 ppm.

### 2.5.1.3.2 $^1\text{H}$ NMR spectrum of the tosylated 1,3-propanediol

The spectrum (Appendix 3b) shows the proton spectrum of the tosylated 1,3-propanediol (compound 3). Table 2.3 gives the chemical shifts of the  $^1\text{H}$  NMR spectrum.

There are two doublets in the region between 7.3 ppm and 7.8 ppm which correspond to the two CH-groups of the aromatic rings. The protons on  $\text{C}^{10}$  and  $\text{C}^{12}$  are found at 4.04 ppm and appear as a triplet. The quintet at 1.97 ppm represents the protons on  $\text{C}^{11}$ . The two methyl groups,  $\text{C}^7$  and  $\text{C}^{25}$  correspond to the singlet at 2.43 ppm.

### 2.5.1.4 NMR spectra of the tosylated ethylene glycol

NMR spectra were recorded (in  $\text{CDCl}_3$ ) to confirm that the ethylene glycol was indeed tosylated (compound 4).

**Table 2.4**  $^1\text{H}$  and  $^{13}\text{C}$  NMR of the tosylated ethylene glycol (compound 4) in  $\text{CDCl}_3$ .

Assignment	$\delta$ / ppm
$^1\text{H}$	
$\text{H}^{3, 5, 19, 23}$	7.69-7.77
$\text{H}^{2, 6, 20, 22}$	7.31-7.37
$\text{H}^{10, 11}$	4.17
$\text{H}^{7, 24}$	2.43
$^{13}\text{C}$	
$\text{C}^{4, 18}$	145.5
$\text{C}^{21}$	132.6
$\text{C}^{3, 5, 19, 23}$	130.1
$\text{C}^{2, 6, 20, 22}$	128.1
$\text{C}^{10, 11}$	66.6
$\text{C}^{7, 24}$	21.4

#### 2.5.1.4.1 $^{13}\text{C}$ NMR spectrum of the tosylated ethylene glycol

Table 2.4 gives the chemical shifts of the signals in the  $^{13}\text{C}$  NMR spectrum (Appendix 4a) of the tosylated ethylene glycol (compound 4).

The area between 128 ppm and 146 ppm is the typical region for aromatic carbons. The peak at 145.5 ppm is the carbon ( $\text{C}^4$  and  $\text{C}^{18}$ ), closest to the sulphur. At 132.6 ppm we find the peak for  $\text{C}^1$  and  $\text{C}^{21}$ . The peaks at 128.1 ppm and 130.1 ppm are the carbon atoms ( $\text{C}^3$ ,  $\text{C}^5$ ,  $\text{C}^{19}$ ,  $\text{C}^{23}$  and  $\text{C}^2$ ,  $\text{C}^6$ ,  $\text{C}^{20}$ ,  $\text{C}^{22}$ ) of the aromatic rings. The carbon atoms ( $\text{C}^{10}$ ,  $\text{C}^{11}$ ) of the ethylene bridge are at 66.6 ppm. The peak at 21.4 ppm represents the methyl groups ( $\text{C}^7$ ,  $\text{C}^{24}$ ) that are on the aromatic rings.

#### 2.5.1.4.2 $^1\text{H}$ NMR spectrum of the tosylated ethyleneglycol

Table 2.4 gives the chemical shifts of the spectrum for the  $^1\text{H}$  NMR (Appendix 4b) of the tosylated ethylene glycol (compound 4).

Typically, the signals of the aromatic protons appear between 7.3 ppm and 7.8 ppm ( $\text{H}^3$ ,  $\text{H}^5$ ,  $\text{H}^{19}$ ,  $\text{H}^{23}$  and  $\text{H}^2$ ,  $\text{H}^6$ ,  $\text{H}^{20}$ ,  $\text{H}^{22}$ ). There are two doublets, because of the neighbouring protons in the ring. The protons of the ethylene bridges ( $\text{H}^{10}$ ,  $\text{H}^{11}$ ) appear at 4.17 ppm and can be seen as a singlet because there is no differentiation in the adjacent protons. At 2.43 ppm we find the signal representing the methyl groups ( $\text{H}^7$ ,  $\text{H}^{24}$ ).

#### 2.5.1.5 NMR spectrum of tosylated 1,4,7-triazacyclodecane

An NMR spectrum was recorded (in  $\text{CDCl}_3$ ) to confirm that the macrocycle had indeed formed with the protection groups still attached to the ring (compound 5).

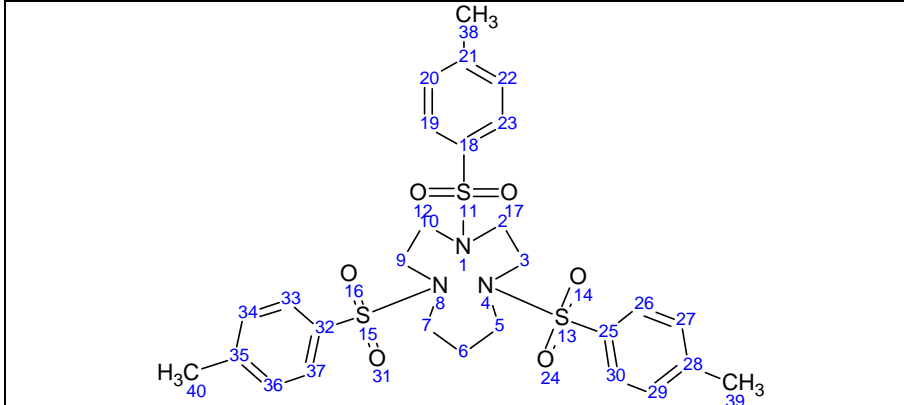
### 2.5.1.5.1 $^1\text{H}$ spectrum of tosylated 1,4,7-triazacyclodecane

Table 2.5 gives the chemical shifts of the  $^1\text{H}$  NMR spectrum of the 1,4,7-triazacyclodecane (Appendix 5).

The signals between 7.2 ppm and 7.9 ppm are in the typical area for the aromatic protons ( $\text{H}^{19, 20, 22, 23, 26, 27, 29, 30, 33, 34, 36, 37}$ ) of the tosyl groups. There are two groups of protons that correspond to the two different protons on the aromatic rings. At 3.30 ppm there is a signal that represents the protons on the propyl bridge at  $\text{H}^6$ . The methyl groups ( $\text{H}^{38, 39, 40}$ ) on the aromatic rings are present at 2.41 ppm as a well defined singlet. The protons of the ethylene bridges ( $\text{H}^{2, 3, 9, 10}$ ) and the remaining two on the propyl bridges ( $\text{H}^{5, 7}$ ) are just a very broad multiplet at 3.10 ppm.

**Table 2.5**  $^1\text{H}$  NMR data of the tosylated 1,4,7-triazacyclodecane (compound 5).

Assignment	$\delta$ / ppm
$^1\text{H}$ $\text{H}^{19, 20, 22, 23, 26, 27, 29, 30, 33, 34, 36, 37}$	7.2-7.9
$\text{H}^6$	3.03-3.23
$\text{H}^{38, 39, 40}$	2.41
$\text{H}^{2, 3, 5, 7, 9, 10}$	1.60



There are traces of unreacted tosylated starting material present.

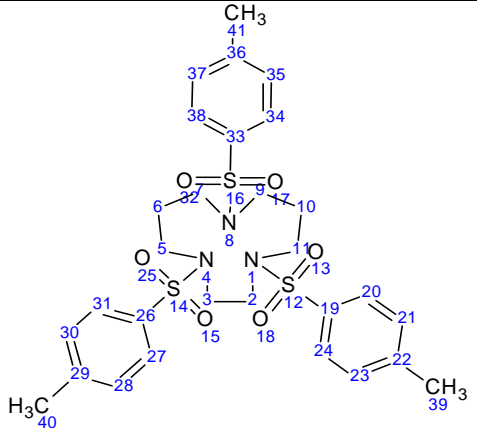
### 2.5.1.6 NMR spectrum of the tosylated 1,4,8-triazacycloundecane

An NMR experiment was carried out in  $\text{CDCl}_3$  to confirm that the tosylated 1,4,8-triazacycloundecane had indeed formed (compound 6).

2.5.1.6.1  $^1\text{H}$  spectrum of the tosylated 1,4,8-triazacycloundecane

Table 2.6 gives the chemical shifts of the proton spectrum of the tosylated 1,4,8-triazacycloundecane (Appendix 6).

**Table 2.6**  $^1\text{H}$  NMR data of the tosylated 1,4,8-triazacycloundecane (compound 6) in  $\text{CDCl}_3$ .

	
Assignment	$\delta$ / ppm
$^1\text{H}$	
$\text{H}^{20, 21, 23, 24, 27, 28, 30, 31, 34, 35, 37, 38}$	7.2-7.8
$\text{H}^{5, 7, 9, 11}$	3.40, 2.97
$\text{H}^{39, 40, 41}$	2.42
$\text{H}^{6, 10}$	1.88
$\text{H}^{2, 3}$	1.53

The protons of the aromatic rings ( $\text{H}^{20, 21, 23, 24, 27, 28, 30, 31, 34, 35, 37, 38}$ ) can be seen in the typical region between 7.2 ppm and 7.8 ppm. Again we can see two distinct sets of resonances which show the two different protons of the phenyl rings. There are two very distinct triplets, first at 3.40 ppm and the second at 2.97 ppm. These two signals are the protons  $\text{H}^5, \text{H}^7, \text{H}^9$  and  $\text{H}^{11}$  that are connected to the protons  $\text{H}^6$  and  $\text{H}^{10}$ . The protons of the methyl groups ( $\text{H}^{39, 40, 41}$ ) can be found at 2.42 ppm. The multiplet at 1.88 ppm are the protons  $\text{H}^6$  and  $\text{H}^{10}$ . These protons are connected to the  $\text{CH}_2$ -groups  $\text{H}^5, \text{H}^7, \text{H}^9$  and  $\text{H}^{11}$  respectively. The broad peak at 1.53 ppm is due to protons  $\text{H}^2$  and  $\text{H}^3$ . They appear as a singlet because of their similarity in their chemical environment.

### 2.5.1.7 NMR spectra of THTD

NMR spectra were recorded in D<sub>2</sub>O. The spectra were compared with previously resolved structures that were published.<sup>27, 63</sup>

**Table 2.7** <sup>1</sup>H and <sup>13</sup>C NMR of the 1,4,7-tris[2(*S*)-hydroxypropyl]-1,4,7-triazacyclodecane (compound 7).

Assignment	$\delta$ / ppm
<b><sup>1</sup>H</b>	
Pendant arms (without the CH <sub>3</sub> - and the OH- groups)	3.11-4.25
Ring structure	2.30-3.02
OH	1.47
CH <sub>3</sub>	0.99-1.22
<b><sup>13</sup>C</b>	
C <sup>12, 15, 18</sup>	76.4
C <sup>11, 14, 17</sup>	66.8
C <sup>2, 3, 5, 7, 9, 10</sup>	66.6
C <sup>6</sup>	18.8
C <sup>20, 21, 22</sup>	15.2

#### 2.5.1.7.1 <sup>13</sup>C NMR spectrum of THTD

The chemical shifts for the signals of the <sup>13</sup>C NMR spectrum of THTD can be seen in Table 2.7. The spectrum is shown in Appendix 7a. Although the signals are fairly weak, they could be assigned unambiguously.

The signal for the CH chiral centre at C<sup>12</sup>, C<sup>15</sup> and C<sup>18</sup> is shifted far downfield due to the OH groups of the pendant arms. This signal can be observed at 76.4 ppm. The resonance at 66.8 ppm are the signal of the CH<sub>2</sub> groups (C<sup>11</sup>, C<sup>14</sup>, C<sup>17</sup>) of the pendant arms, while the signal at

66.6 ppm are the protons of the CH<sub>2</sub> groups (C<sup>2</sup>, C<sup>3</sup>, C<sup>5</sup>, C<sup>7</sup>, C<sup>9</sup>, C<sup>10</sup>) of the carbon bridges. The carbon atom, C<sup>6</sup>, is the lone CH<sub>2</sub> of the propyl bridge at 18.8 ppm and the signal at 15.2 ppm represents the methyl groups (C<sup>20</sup>, C<sup>21</sup>, C<sup>22</sup>) of the pendant arms.

#### 2.5.1.7.2 <sup>1</sup>H NMR spectrum of THTD

The chemical shifts for the <sup>1</sup>H NMR spectrum (Appendix 7b) of THTD can be seen in Table 2.7.

The ligand may appear as a symmetrical molecule, but due to overlapping of the signals, the assignment of the peaks proved to be problematic. A comparative study<sup>27, 63</sup> was made and only chemical environments could be used to identify the different protons. The integration showed that the protons do match the structure of the ligand.

The signals for the CH<sub>2</sub> and CH<sub>3</sub> -groups of the pendant arms are found in the chemical environment between 3.1 ppm and 4.3 ppm. These are shifted downfield because of the OH groups. The region between 2.3 ppm and 3.1 ppm can be divided into two areas. These areas contain the signals for the protons of the parent ligand, the ring itself. The first part is likely to be the propyl bridge while the latter part are the ethylene bridges. Between 0.9 ppm and 1.3 ppm is the signal for the methyl groups. From the integration it can be seen that the number of protons were correct as well as the chemical environment where they were situated.

Based on the <sup>13</sup>C and the <sup>1</sup>H NMR spectra together, it was concluded that the THTD had indeed formed. The proton spectrum on the other hand does not give conclusive evidence. The ligand was thus further characterized by elemental analysis, melting point determination and mass spectrometry to confirm its structure.



### 2.5.1.8 NMR spectra of THTUD

The NMR experiments were carried out in D<sub>2</sub>O. The spectra were compared with previously resolved structures that were published.<sup>27, 63</sup>

#### 2.5.1.8.1 <sup>13</sup>C NMR spectrum of THTUD

**Table 2.8** <sup>13</sup>C NMR data of the 1,4,8-tris[2-(S)-hydroxypropyl]-1,4,8-triazacycloundecane (compound 8).

Assignment	$\delta$ / ppm
<b><sup>1</sup>H</b>	
H <sup>21,22,23</sup>	1.00-1.16
Ring	1.80-2.10
Pendant arms (CH <sub>2</sub> )	3.05-2.80
Pendant arms (CH)	3.86-4.02
<b><sup>13</sup>C</b>	
C <sup>13,16,19</sup>	76.4
C <sup>12,15,18</sup>	66.3, 67.0
C <sup>2,3,5,7,9,11</sup>	64.1
C <sup>21,22,23</sup>	18.8
C <sup>6,10</sup>	15.2

Table 2.8 shows the chemical shifts for the signals of the <sup>13</sup>C NMR spectrum of THTUD. The corresponding NMR can be seen as Appendix 8a.

The CH-groups (C<sup>13</sup>, C<sup>16</sup>, C<sup>19</sup>), attached to the OH groups are furthest downfield and the signal is found at 76.4 ppm. At 66.3 ppm and 67.0 ppm are two resonances that are very similar to each other. These signals are the CH<sub>2</sub>-groups (C<sup>12</sup>, C<sup>15</sup>, C<sup>18</sup>) of the pendant arms that are attached to the nitrogen atoms of the ring. The chemical environment are slightly different for these three groups, splitting them into two signals. The prominent signal at 64.1 ppm are the CH<sub>2</sub>-groups (C<sup>2</sup>,

C<sup>3</sup>, C<sup>5</sup>, C<sup>7</sup>, C<sup>9</sup>, C<sup>11</sup>) of the ring, that are attached to the nitrogen atoms. At 18.8 ppm is the resonance for the CH<sub>2</sub>-groups of the propyl bridges (C<sup>6</sup>, C<sup>10</sup>). The methyl groups (C<sup>21</sup>, C<sup>22</sup>, C<sup>23</sup>) give a signal at 15.2 ppm.

#### 2.5.1.8.2 <sup>1</sup>H NMR spectrum of THTUD

Table 2.8 shows the approximate chemical shifts of the signals of the proton NMR spectrum that can be seen as Appendix 8b.

The resonances for the methyl groups (H<sup>21</sup>, H<sup>22</sup>, H<sup>23</sup>) are found between 1.00 ppm and 1.16 ppm. Between 1.88 ppm and 1.56 ppm the resonances for the ethylene bridge (H<sup>2</sup>, H<sup>3</sup>) of the parent ring can be found. The signal for the protons of the propyl bridges (H<sup>5</sup>, H<sup>7</sup>, H<sup>9</sup>, H<sup>11</sup>) can be observed between 2.00 ppm to 2.74 ppm. This region also includes the OH groups of the pendant arms. The signals of the CH<sub>2</sub>-groups (H<sup>12</sup>, H<sup>15</sup>, H<sup>18</sup>) on the pendant arms can be seen between 2.80 ppm and 3.05 ppm. The CH-groups (H<sup>13</sup>, H<sup>16</sup>, H<sup>19</sup>) of the arms are represented by a broad signal between 3.86 ppm and 4.02 ppm.

Based on the <sup>13</sup>C and the <sup>1</sup>H NMR spectra together, it was concluded that the THTUD had indeed formed. The proton spectrum on the other hand did not give conclusive evidence. The ligand was thus further characterized by elemental analysis, melting point determination and mass spectrometry to confirm its structure.

## 2.5.2 Elemental analysis

### 2.5.2.1 *The analysis of THTD*

The calculated percentages and the experimental results for the ratios of the different atoms, C, H, N and O in the molecule are reported in Table 2.9.

**Table 2.9** The calculated and experimental results of the elemental analysis for THTD. All values are in percentages.

Elements	1		2		3		4	
	Calculated	Experimental	Calculated from 1	Experimental	Calculated from 3	Experimental	Calculated from 3	
C	60.53	49.29	49.33	49.00	49.11			
H	11.11	9.60	11.13	9.89	11.13			
N	13.24	11.47	10.79	11.45	10.74			
O	15.12		28.75		29.03			

The molar mass of anhydrous THTD is 317.47. The mass of the compound according to the elemental analysis is 389.54. The difference between the two masses is thus 72.07. The experimental values obtained are shown in Table 2.9, columns 1 and 3. The experimental data obtained in column 1 was used to calculate the percentage O in the molecule and is shown in column 2 and the data from column 3 was used to calculate the values shown in column 4 (Table 2.9). The values that were calculated from the experimental data showed that the percentage of O was far too high. This leads to the conclusion that the extra weight must be due to water. This means that there are 4.00 H<sub>2</sub>O per molecule.

The ratio C:N/N:C for the calculated and experimental values remain the same, hence confirming that we have obtained the desired ligand and that the extra hydrogen and oxygen is water, showing that the ligand is very hygroscopic. Since the molecule contains OH and N groups, the drying agents available made it very hard to work with because of interaction between these groups.<sup>64</sup>

### 2.5.2.2 The analysis of THTUD

The calculated percentages and the experimental results for the ratios of the different atoms, C, H, N and O in the molecule are reported in Table 2.10.

<sup>64</sup> *Drying in the Laboratory*, E. Merck, Darmstadt, p. 16

**Table 2.10** The calculated and experimental results of the elemental analysis for THTUD. All values are in percentages.

Elements	1		2		3		4	
	Calculated	Experimental	Calculated from 1	Experimental	Calculated from 3	Experimental	Calculated from 3	
C	61.59	53.00	52.96	53.10	53.21	53.10	53.21	
H	11.25	9.66	11.24	9.78	11.24	9.78	11.24	
N	12.68	10.69	10.90	10.90	10.95	10.90	10.95	
O	14.48		24.90		24.60		24.60	

The values of the ratios of the different atoms that are present in the ligand were obtained experimentally (Table 2.10 - columns 1 and 3) and were now used to determine the amount of water that is present in the ligand. The experimental data from column 1 was used to calculate the values in column 2 and the data in column 3 was used to calculate values in column 4 (Table 2.10)

The molar mass of anhydrous THTUD is 331.50. The mass of the compound according to the elemental analysis is 384.65. The difference between the two masses is thus 53.15. The calculated values that were obtained from the experimental data showed that the percentage of O was too high. This leads to the conclusion that the extra weight must be due to water. The data obtained show that there are 3.00 H<sub>2</sub>O per molecule of ligand.

The calculated and experimental values for the ratio C:N/N:C remains the same, hence confirming that we have obtained the desired ligand and that the extra hydrogen and oxygen is water, showing that the ligand is hygroscopic.

### 2.5.3 Mass spectrometric analysis

#### 2.5.3.1 Mass spectrum of THTD

The calculated mass of the THTD is 317.47. The mass spectrum (Appendix 9) of the compound indicates a peak of 318, which corresponds to the molecular mass of THTD. The peak at 302 shows the loss of an OH-group.

The loss of the methyl groups (257, 229, 203) can also be seen.

### **2.5.3.2 Mass spectrum of THTUD**

The calculated mass of the THTUD is 331.50. The mass spectrum (Appendix 10) of the compound indicates 332, which corresponds to the molecular weight of THTUD. The peak at 316 shows the loss of an OH-group.

## **2.5.4 Melting point**

### **2.5.4.1 Melting point - THTD**

THTD	1)	146-149 °C
	2)	147-151 °C

The melting point was determined to be between 146°C and 151°C.

### **2.5.4.2 Melting point - THTUD**

THTUD	1)	167-171 °C
	2)	169-172°C

The melting point was determined to be between 167°C and 172°C

## **2.5.5 Physical characteristics of THTD and THTUD**

### **2.5.5.1 Physical characteristics of THTD**

THTD is ochre in colour. It is extremely hygroscopic and must be kept in a desiccator in the presence of silica gel or under N<sub>2</sub> to prevent it absorbing water. When the temperature is high, the THTD tends to lose some of its water, but does not dry completely. As soon as the humidity rises, the THTD will immediately absorb the water and turn into a slurry. Although THTD is very hydrophilic, it is completely air stable in the sense that it does not

decompose when exposed to air or oxygen. Because it is so hygroscopic, the THTD dissolves very well in water and other polar solvents.

#### ***2.5.5.2 Physical characteristics of THTUD***

THTUD is a dirty white colour. It is hygroscopic, but not to the same extent as THTD. The THTUD should be stored in a desiccator containing dry silica gel or under N<sub>2</sub> to prevent the absorption of water. Although THTUD is hygroscopic, it is completely air stable and does not decompose when exposed to air or oxygen. Because it is so hygroscopic, the THTUD dissolves very well in water and other polar solvents.

## **2.6 Conclusion**

From the NMR-analysis, elemental analysis and the mass spectrometry it is clear that the reactions were successful and that the desired products were obtained. By producing THTD and THTUD successfully, we have now completed the series for this type of ligand between the [9]-ane-N<sub>3</sub> and [12]-ane-N<sub>3</sub>.

## Chapter 3

### *Determination of the Protonation Constants of THTD and THTUD*

#### 3.1 Introduction

Equilibrium constants are important expressions of thermodynamic activity. They are characteristic for a given reaction at a specific temperature and pressure. In a number of natural processes these constants are necessary for the understanding of the functioning of these processes for instance, the oxygen transport by haemoglobin and acid base homeostasis in the human body.<sup>22, 65</sup>

Stability constants, formation constants, binding constants, association and dissociation constants, protonation constants etc., represent different ways of writing various types of equilibrium constants and differences are dependent upon the specific substrate basic and acidic species present. Protonation constants, acid dissociation constants, formation constants, stepwise formation constants etc. for ligands are all related equilibria expressions.<sup>42</sup> The following is a general equation (Eqn. 3.1) showing an equilibrium reaction.

Consider the general chemical reaction:



The equilibrium equation is then defined in terms of the ratios of the activities of the species which can then be simplified to  $K_c$  (Eqn. 3.2) at a constant ionic strength because the activity coefficients are then constant as well.

---

<sup>65</sup> A.E. Martell and R.J. Motekaites in *The Determination and Use of Stability Constants*, VCH Verlagsgesellschaft GmbH, Weinheim, Germany, 1988, p. ix

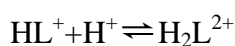
$$K_c = \frac{[S]^\sigma [T]^\tau}{[A]^\alpha [B]^\beta} \quad (3.2)$$

The value of  $K_c$  is dependent on the ionic strength, temperature and pressure.

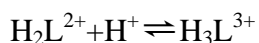
In principle, three protonations are possible for both THTD and THTUD. The stepwise protonation reaction of THTD and THTUD, where L represents the ligands, can be defined in terms of concentrations at a constant ionic strength, as follows:



$$K_1^H = \frac{[HL^+]}{[H^+][L]} \quad (3.3) \quad \beta_{HL^+} = \frac{[HL^+]}{[H^+][L]} \quad (3.6)$$



$$K_2^H = \frac{[H_2L^{2+}]}{[HL^+][H^+]} \quad (3.4) \quad \beta_{H_2L^{2+}} = \frac{[H_2L^{2+}]}{[H^+]^2[L]} \quad (3.7)$$



$$K_3^H = \frac{[H_3L^{3+}]}{[H_2L^{2+}][H^+]} \quad (3.5) \quad \beta_{H_3L^{3+}} = \frac{[H_3L^{3+}]}{[H^+]^3[L]} \quad (3.8)$$

The constant  $\beta_i$  represents overall stability constants. It might be that not all the species are present in significant concentrations in the solution at a given pH-value, but a complete set (Eqn. 3.3 - 3.5) or (Eqn. 3.6 – 3.8) is needed to describe the equilibria in a chosen pH range over which the hydrogen ion concentration is measured.<sup>65</sup>

## 3.2 Aim

The aim of this section of the study was to determine the protonation constants for THTD and THTUD by means of potentiometric titrations. Owing to the basic nature of



these ligands, the stabilities of their metal complexes (Chapter 4) will be pH dependent and thus their affinity for protons should be exactly known.

Various methods can be used for determining the protonation constants for ligands, such as potentiometry, spectrophotometry, NMR spectroscopy etc. In this study we used a potentiometric titration method. Equilibrium constants were determined in terms of overall constants,  $\log(\beta)$  values (which is how they are entered in the ESTAWIN programme), although these constants are easily converted to stepwise values.

### 3.3 Experimental

#### 3.3.1 Materials

The ligands THTD and THTUD were synthesized according to the method described in chapter 2. The concentrations of the ligands were made up precisely to  $0.00500 \text{ mol dm}^{-3}$ . NaOH ( $0.1 \text{ mol dm}^{-3}$  Volucon) was bought from Echalaz & Osborne (Pty.) Ltd. and HNO<sub>3</sub> ( $0.1 \text{ mol dm}^{-3}$  Volucon) was obtained from Merck. The solutions were prepared as described by the suppliers. The NaOH solution was prepared from the Volucon and the concentration was accurately determined ( $0.09687 \text{ mol dm}^{-3}$ ) by means of titration against a standard oxalic acid solution using phenolphthalein as indicator. The HNO<sub>3</sub> solution was prepared from the Volucon and the concentration was accurately determined ( $0.09782 \text{ mol dm}^{-3}$ ) by means of titration against the standardized NaOH solution, using phenol red as indicator.

#### 3.3.2 Instrumentation

The titrations were carried out under standard atmospheric pressure and were carried out in a jacketed glass vessel, equipped with a magnetic stirrer and thermostatted at  $25.0^\circ\text{C}$  ( $\pm 0.5^\circ\text{C}$ ) using a Thermo Orion 420+ pH meter, a 725 Dosimat automatic piston burette and a 9157BN Thermo Orion pH Triode combination Ag/AgCl electrode. The solutions were constantly stirred by a 649

Metrohm magnetic stirrer. A stream of high purity nitrogen was bubbled through the test solution for de-aeration of the sample solutions (Fig. 3.1a and Fig. 3.1b).

### 3.3.3 Procedure for the determination of the protonation constants of THTD and THTUD

The protonation constants for THTD and THTUD were determined according to a similar method. Calibrations were carried out at the beginning of each titration. The graphs can be seen as Appendices 11 and 12.

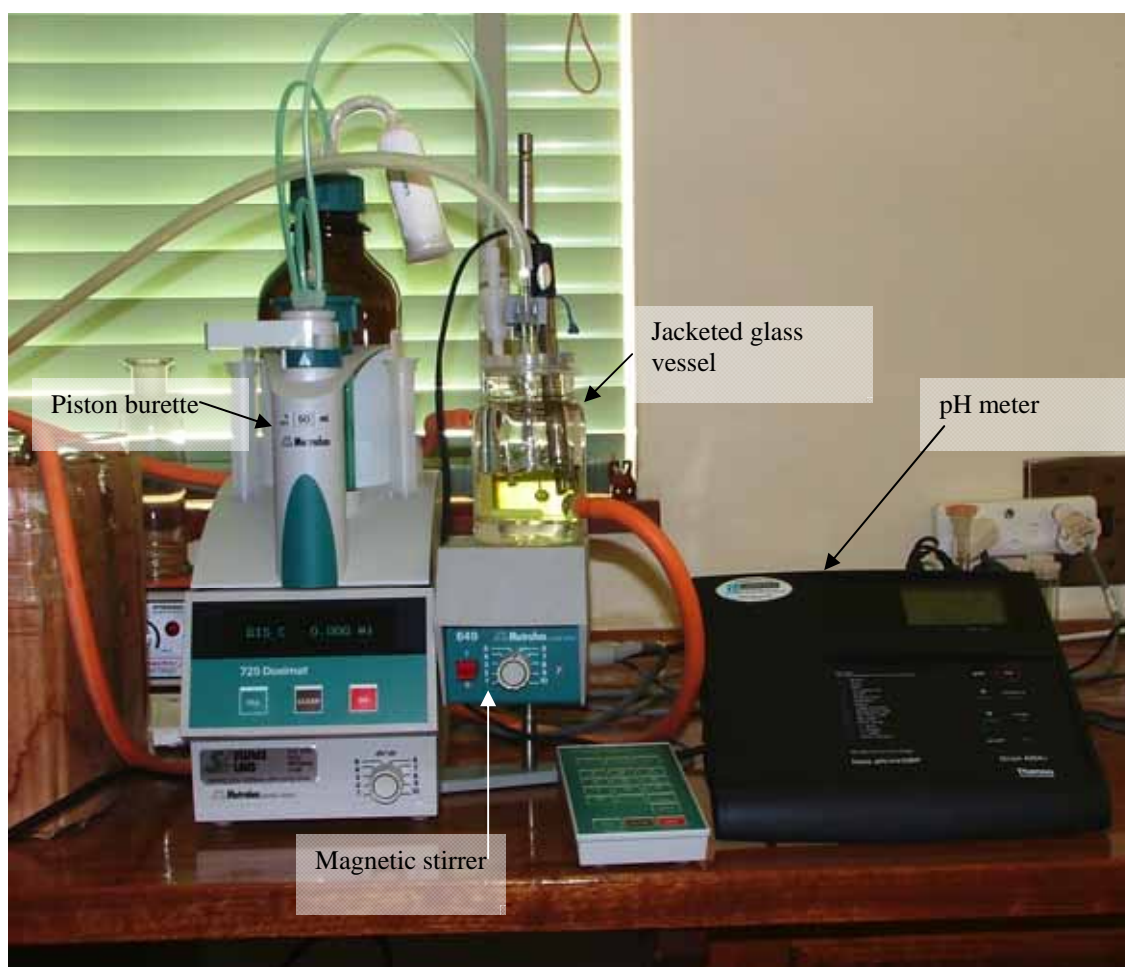


**Fig. 3.1a** The experimental setup for the determination of the protonation constants.

Prior to each potentiometric titration, the cell was calibrated by titration of  $\text{HNO}_3$  with  $\text{NaOH}$ . Points were collected on both sides of the end point. The equation used for the cell calibration is:

$$E_{\text{cell}} = E_{\text{cell}}^0 + k \log[\text{H}^+]$$

$E_{\text{cell}}^0$ , the standard electrode potential, and  $k$ , the response slope of the electrode were determined. The constant  $k$  has a value of approximately the Nernstian value ( $2.303 \times \frac{RT}{F}$ ). The calibration constants  $E_{\text{cell}}^0$  and  $k$  can be calculated from the linear plot of  $E_{\text{cell}}$  versus  $\log[\text{H}^+]$  using a least squares fit of the data.

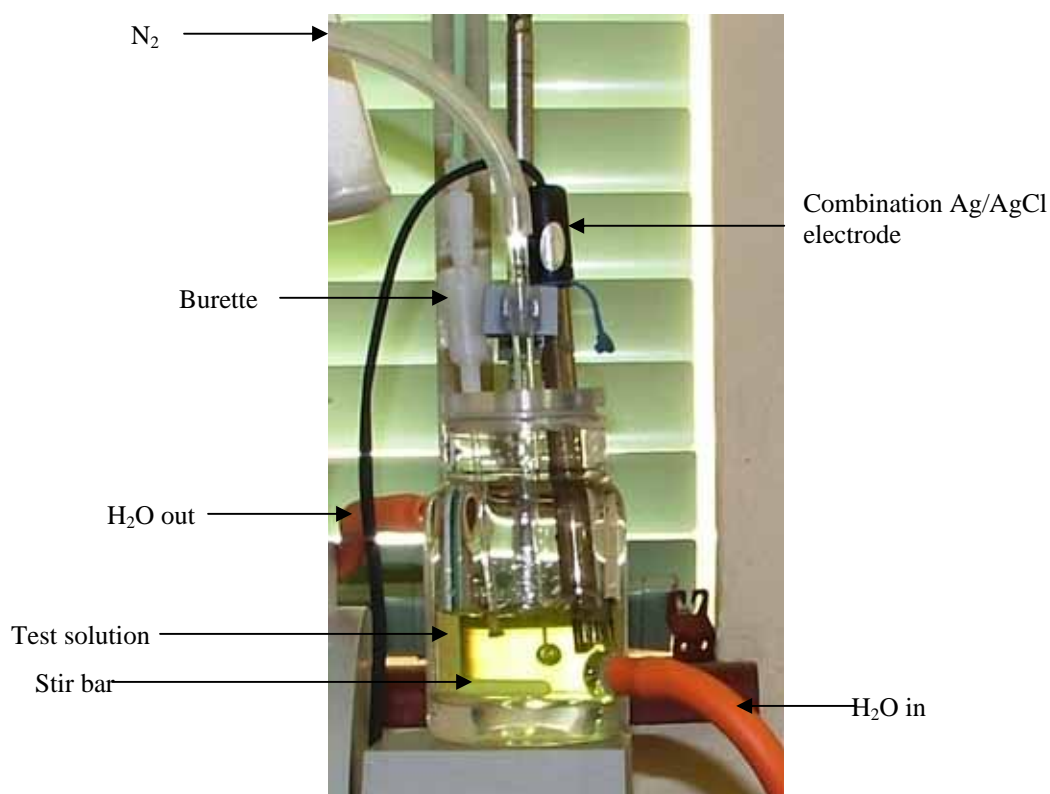


**Fig. 3.1b** The experimental setup for the determination of the protonation constants - the reaction vessel.

To determine the  $E_{\text{cell}}^0$  and  $k$  value,  $\text{HNO}_3$  (30.000 mL) was added to a vessel and was left standing to reach  $25^\circ\text{C}$ . The solution was purged with  $\text{N}_2$ . The  $\text{NaOH}$  was added in increments of 0.250 mL and left to stabilize before the potential readings ( $E_{\text{cell}}$ ) were taken. This was done before a protonation constant titration for the ligands could be done.

For the determination of the protonation constants,  $\text{HNO}_3$  (30.000 mL) was added to the jacketed glass vessel and then the ligand ( $0.05000\text{mol dm}^{-3}$  - 10.000 mL) was added to the  $\text{HNO}_3$  and left for about 30 minutes while the solution was constantly stirred. The  $\text{NaOH}$  was added in increments of 0.250 mL. After each addition, the

solutions were allowed to reach 25°C, and for the potential (mV) to stabilize before any readings were recorded. The data was then processed by using the ESTA-WIN<sup>66</sup> computer program to determine the protonation constants.

### 3.4 Results and discussion

The ESTA-WIN computer program that was used in the determination of the protonation constants, determines the overall protonation constants,  $\log(\beta_i)$ . The calculations used by the computer program are performed by two program modules. The first is the SIMULATION MODULE (ESTA1) and it produces results on a point by point basis. According to the procedure, mass balance equations are solved. The second program, the OPTIMISATION MODULE (ESTA2) is used to optimize the parameters initially entered. This method is based on a least squares procedure over a whole series of titrations.<sup>66</sup>

Initially an excess  $H^+$  was added to the solution which means that the ligand will be fully protonated. The ligands are initially neutral (Fig. 3.2), but the lone pairs of electrons on the nitrogen atoms are responsible for basicity. With three nitrogen atoms in the macrocyclic ring, it is to be expected that the ligand will be protonated three consecutive times. This leaves the ligand with a positive charge of 3; affording  $H_3L^{3+}$ , where L represents the neutral ligands.

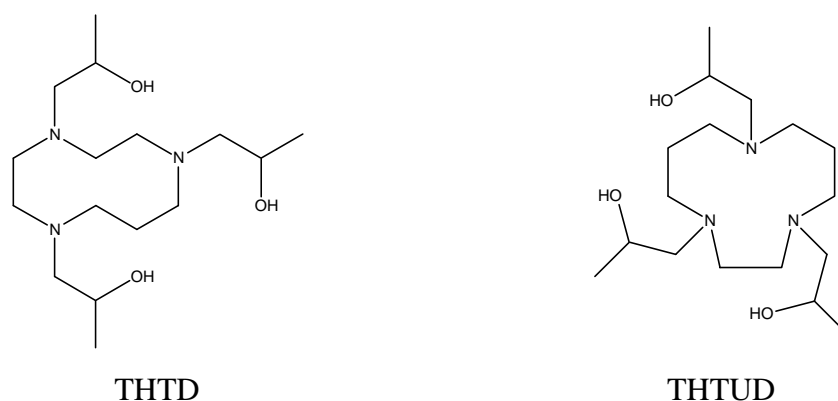


**Fig. 3.2** Structures of the neutral ligands.

<sup>66</sup> P.M. May, K. Murray and D.R. Williams, *Talanta*, 1988, **35**, 825-830

As NaOH is added to the solution, the excess HNO<sub>3</sub> will first be neutralized and the first part of the experiment is nothing else than a straight forward acid base titration. After the excess acid has been neutralized, the stepwise deprotonation occurs.

The results obtained are tabulated in Table 3.1 and are compared to values from the literature for related ligands. Other ligands used for comparison include the simple parent heterocyclic ring, No. 5 and 6, as well as a molecule with pendant arms that are almost similar to the ones that are now used on our new ligands No. 3, THETAC. Also included are the [9]-ane-N<sub>3</sub>, No. 4, [12]-ane-N<sub>3</sub>, No. 7, so as to complete the full series of protonation constants for the macrocycles and to see how they differ with respect to each other.

**Table 3.1** The log(*K*) values of ligands with similar structures as THTD and THTUD.

No.		Log( <i>K</i> <sub>1</sub> )	Log( <i>K</i> <sub>2</sub> )
1	1,4,7-tris[2-( <i>S</i> )-hydroxypropyl]-1,4,7-triazacyclodecane (THTD)	9,18	4,20
2	1,4,8-tris[2-( <i>S</i> )-hydroxypropyl]-1,4,8-triazacycloundecane (THTUD)	11,32	5,87
3	1,4,7-tris(2-hydroxyethyl)-1,4,7-triazacyclononane <sup>67, 68</sup> (THETAC)	11.50	3.42
4	1,4,7-triazacyclononane (9-ane-N <sub>3</sub> ) <sup>68</sup>	10.44	6.81
5	1,4,7-triazacyclodecane (10-ane-N <sub>3</sub> ) <sup>67</sup>	12.00	6.61
6	1,4,8-triazacycloundecane (11-ane-N <sub>3</sub> ) <sup>67</sup>	12.00	7.61
7	1,5,9-triazacyclododecane (12-ane-N <sub>3</sub> ) <sup>67</sup>	12.50	7.54

### 3.4.1 THTD and THTUD

Stepwise protonation constants with standard deviations and R-factors for THTD and THTUD are shown Tables 3.2 and 3.3 respectively.

The value of the first protonation constant of THTD is slightly lower than that of the parent molecule, 1,4,7-triazacyclodecane, log(*K*<sub>1</sub>) = 12.00 ([10]-ane-N<sub>3</sub> - Fig. 3.3). The log(*K*<sub>1</sub>) value of THTD is 9.18, 2.82 log units less than the parent molecule.

In the free ligand [10]-ane-N<sub>3</sub>, a proton is bonded to a nitrogen atom and this proton is most likely stabilized by forming two additional hydrogen bonds with the other

<sup>67</sup> R.M. Smith, A.E. Martell and R.J. Motekaites, *NIST Standard Reference Database 46 (Critically Selected Stability Constants of Metal Complexes)*, Version 8.0, 2004

<sup>68</sup> B.A. Sayer, J.P. Michael and R.D. Hancock, *Inorg. Chim. Acta*, 1983, **77**, L63-L64

nitrogen atoms, similar to [9]-ane-N<sub>3</sub>. When protonating [10]-ane-N<sub>3</sub>, the proton must add onto the outside of the macrocycle, making it easy to protonate this ligand. The result is a very high log(*K*<sub>1</sub>) value of 12.00.<sup>44, 67</sup>

**Table 3.2** Stepwise protonation values log(*K*) of THTD.

	log( <i>K</i> <sub>1</sub> )	log( <i>K</i> <sub>2</sub> )
Values	9.18	4.22
Stdev	0.015	0.020
<b>R-factor</b>		<b>0.0045</b>

The value of the first protonation constant of THTUD is only slightly lower than that of the parent molecule, 1,4,8-triazacycloundecane, log(*K*<sub>1</sub>) = 12.00 ([11]-ane-N<sub>3</sub> - Fig. 3.3). The log(*K*<sub>1</sub>) value of THTUD is 11.32, 0.68 log units less than the parent molecule.

**Table 3.3** Stepwise protonation values log(*K*) of THTUD

	log( <i>K</i> <sub>1</sub> )	log( <i>K</i> <sub>2</sub> )
Values	11.3	5.90
Stdev	0.0251	0.0274
<b>R-factor</b>		<b>0.01007</b>

The log(*K*<sub>1</sub>) for THETAC is higher than that of [9]-ane-N<sub>3</sub>. We expected the same result for THTD and THTUD compared to their parent ligands, but the log(*K*<sub>1</sub>) values for both these ligands were lower.

The log(*K*<sub>1</sub>) value for [9]-ane-N<sub>3</sub> (Table 3.1 - 10.44) can most likely be due to the fact that 2 hydrogen bonds can be formed, lowering the enthalpy in the parent ligand. The entropy in the system however decreases because of the organization of H<sub>2</sub>O around the ligand. Although the entropy decreases, it seems that the enthalpy effect is the driving force when protonating [9]-ane-N<sub>3</sub>. THETAC has pendant arms that have a positive inductive effect on the macrocyclic ring. This makes it easier to protonate the nitrogen atoms which will give rise to a higher log(*K*<sub>1</sub>) value compared to [9]-ane-N<sub>3</sub>. We do however also see that by protonating the ligand, the pendant arms are no longer free to move around the nitrogen atoms, because hydrogen bonding between the OH-groups (of the pendant arms) and the protons occurs. This effect must oppose the enthalpy effect by lowering the log(*K*<sub>1</sub>) value.

The results however showed that the entropy effect does not play a significant role in the protonation of THETAC, but the enthalpy is most likely the driving force in the protonation reaction.

As with THETAC, we expected a positive inductive effect to play a role with THTD and THTUD by yielding a higher  $\log(K_1)$  value. Another factor that again should be considered contributing to a higher  $\log(K_1)$  value is that the protonated ligands now have the ability to form hydrogen bonds, lowering the enthalpy. Because the  $\log(K_1)$  values are lower than those of the parent ligands, this indicates that the enthalpy effect is not the driving force. The  $H_2O$  around the ligand will be more ordered because of hydrogen bonding with the OH-groups (of the pendant arms) and the proton, meaning less entropy in the system. This leads to a further decrease in entropy because the pendant arms are not free to move around the nitrogen atoms any more. As can be seen from the experimental data, the  $\log(K_1)$  values are lower than that of the parent ligands. Hence there is no overwhelming driving force due to enthalpy or entropy in the explanation of the lower protonation constant  $\log(K_1)$ .

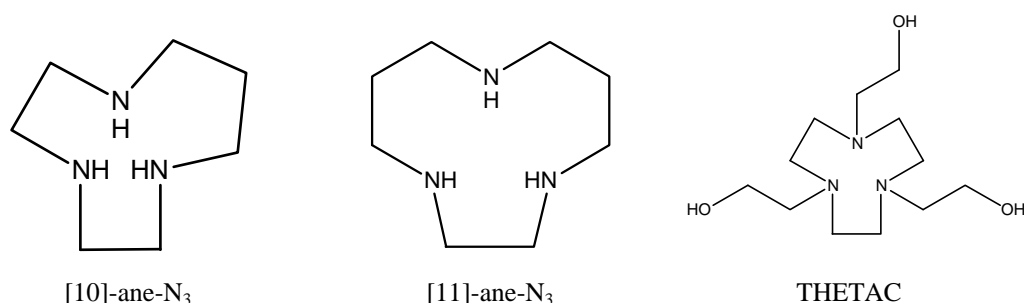


**Fig. 3.3** Schematic view of [10]-ane-N<sub>3</sub>, [11]-ane-N<sub>3</sub> and THETAC.

These arguments are also valid for explaining the second lower protonation constants of both THTD and THTUD.

There is a strong indication of a third protonation constant, but because a glass electrode was used, it is not possible to report this value without a substantial error. This was the same for [10]-ane-N<sub>3</sub> and [11]-ane-N<sub>3</sub>. The values for THETAC were also obtained through NMR. For future studies of the protonation constants, other methods such as e.g. NMR experiments can be used.<sup>44</sup>

### 3.5 Conclusion

There is no easy explanation for the results since there is no definite pattern or rule that has been followed. From the data it was clear that there are three protonation constants. The first two protonation constants were determined with enough certainty and accuracy to be reported. When compared to values from the literature of similar ligands, the values are in the expected regions and correspond well with the values of the known ligands. The pendant arms and the additional methyl groups have some sort of influence on the protonation constants of the ligands but it is difficult with the present information to clarify whether it is an enthalpy or entropy effect that determines the lowering of the  $\log(K)$  values for THPTD and THPTUD.



## Chapter 4

### *The Determination and Interpretation of Stability constants of THTD and THTUD with $\text{Co}^{2+}$ , $\text{Zn}^{2+}$ , $\text{Cd}^{2+}$ and $\text{Pb}^{2+}$*

#### 4.1 Introduction

The selectivity for one metal ion over another is measured as the difference in  $\log K_1$  (stability constant) between two metal ions with a particular ligand.<sup>69</sup> Stability constants or formation constants for metal complexes are in other words a way of determining the affinity of a ligand for a certain metal ion in solution.<sup>42</sup> The pioneers in this field of stability constants were workers such as Von Euler<sup>70</sup> and Bodlander and Storbeck,<sup>71</sup> but they were only interested in empirical formulas and the overall formation constants  $\beta$ . Stability work on chelate compounds began with a seminal paper by Calvin and Wilson,<sup>72</sup> where they used a large excess of ligand to prevent hydrolysis and precipitation. The Irving-Williams series is one of the earliest correlations in the stability between metal complexes for a given ligand. The order for a given ligand is:  $\text{Ba}^{2+} < \text{Sr}^{2+} < \text{Ca}^{2+} < \text{Mg}^{2+} < \text{Mn}^{2+} < \text{Fe}^{2+} < \text{Co}^{2+} < \text{Ni}^{2+} < \text{Cu}^{2+} > \text{Zn}^{2+}$ . Ligands and metals were now being classified as type (a) or type (b) according to their preferential bonding (Table 4.1).<sup>73</sup> Pearson suggested the terms hard, for type (a) and soft, for type (b).<sup>74</sup> Type (a) are the alkali metals, alkaline earth metals and lighter transition metals in higher oxidation states such as  $\text{Ti}^{4+}$ ,  $\text{Cr}^{3+}$ ,  $\text{Fe}^{3+}$ ,  $\text{Co}^{3+}$  and  $\text{H}^+$ . Type (b) metal ions are the heavier transition metals and those in lower oxidation states such as  $\text{Cu}^+$ ,  $\text{Ag}^+$ ,  $\text{Hg}^+$ ,  $\text{Hg}^{2+}$ ,  $\text{Pd}^{2+}$  and  $\text{Pt}^{2+}$ .<sup>73</sup>

<sup>69</sup> R.D. Hancock *et al.*, *Coord. Chem. Rev.*, 2007, **251**, 1678-1689

<sup>70</sup> H. von Euler, *Ber.*, 1903, **36**, 1854-1860

<sup>71</sup> G. Bodlander and O.Z. Storbeck, *Anorg. Chem.*, 1902, **31**, 438-439

<sup>72</sup> M. Calvin and K.W. Wilson, *J. Am. Chem. Soc.*, 1945, **67**, 2003-2007

<sup>73</sup> J.E. Huheey, E.A. Keiter and R.L. Keiter in *Inorganic Chemistry, Principles of Structure and Reactivity*, HarperCollins College Publishers, New York, 1993, 344-346

<sup>74</sup> R.G. Pearson, *J. Am. Chem. Soc.*, 1963, **85**, 3533-3539

**Table 4.1** The table summarizes the stability of a few complexes that are mentioned above.<sup>74</sup>

Tendency to complex with class (a) metal ions	Tendency to complex with class (b) metal ions
N >> P > As > Sb	N << P > As > Sb
O >> S > Se > Te	O << S < Se ~ Te
F > Cl > Br > I	F < Cl < Br < I

Type (a) metal ions prefer to bind to type (a) ligands and type (b) metal ions prefer to bind to type (b) ligands.<sup>74</sup> Since we have donors that are hard and metal ions that are borderline or soft, other factors should be considered such as size-match selectivity. Size-match selectivity of macrocycles means that the cavity of the macrocycle has fairly fixed dimensions and this gives the macrocycle the chance to coordinate to a metal ion whose radius corresponds to that of the cavity.<sup>69</sup>

In recent years, three important developments have occurred in solution coordination chemistry which provides a major role for the stability constant determination and related information, in the further development of the field. These advances are:

- 1 the development of the chemistry of macrocyclic and macrobicyclic (cryptand) complexes;
- 2 the development of the new fields of bioinorganic chemistry and inorganic environmental chemistry;
- 3 the development of computational methods for processing equilibrium data to provide more accurate and more rapid determination of stability constants and the extension of the method to multidentate ligands.<sup>2</sup>

## 4.2 Aims of this particular study

The aim of this study is to determine the formation constants of THTD and THTUD with a series of metal ions. The metals that were used are Co(II), Zn(II), Cd(II), Pb(II). The ligands contain nitrogen donor atoms as part of the cyclic backbone and the pendant arms contain neutral, hydroxy oxygen donor atoms. Oxygen is considered to be a hard donor atom, while nitrogen is considered more hard/ borderline. From Table 4.1 it can be seen that although

nitrogen and oxygen will complex to both classes (*a*) and (*b*) metal ions, they prefer the class (*a*) metals rather than the class (*b*) metals.<sup>74</sup> Co(II), Zn(II) and Pb(II) are considered borderline acids, while Cd(II) is considered a soft acid.

By determining the stability constants, we can establish the affinity of the ligand for the respective metal ions. Although the ligands contain only hard donor atoms, and due to the fact that we are not using hard acids, there are other factors that will also influence the affinity of these ligands for the metal ions such as the size of the macro/hetero cyclic rings, and the size of the chelate rings formed by the pendant arms. It is also known that larger metal ions prefer five-membered chelate rings while smaller metal ions prefer six-membered chelate rings.<sup>69</sup> It was found in a previous study that when a pendant arm incorporates the same chiral centre, one diastereomer of both the ligand and its complexes may be dominantly stable as has been reported for 1,4,7,10-tetrakis[(*R*)-2-hydroxypropyl]- and 1,4,7,10-tetrakis[(*R*)-2-hydroxy-2-phenyl-ethyl]-1,4,7,10-tetraazacyclododecane and their alkali metal complexes.<sup>24</sup> This is a very unusual phenomenon in the eight coordinated complex. THTD and THTUD both incorporate chiral centers in the same position on the pendant arms. It is of great interest to see if the same phenomenon will occur when a hexadentate ligand is used.

## 4.3 Experimental methods

### 4.3.1 Materials

Metal nitrate solutions were used in the determination of the formation constants with THTD and THTUD.  $\text{Co}(\text{NO}_3)_2 \cdot 6\text{H}_2\text{O}$  and  $\text{Pb}(\text{NO}_3)_2$  were bought from Merck Chemicals (PTY) LTD.  $\text{Zn}(\text{NO}_3)_2 \cdot 6\text{H}_2\text{O}$  and  $\text{Cd}(\text{NO}_3)_2 \cdot 4\text{H}_2\text{O}$  were bought from Fluka Riedel- De Haën. THTD and THTUD were prepared according to the method described in Chapter 2.

### 4.3.2 Instrumentation

The titrations were carried out under standard atmospheric pressure, in a jacketed glass vessel, equipped with a magnetic stirrer and thermostatted at 25.0°C ( $\pm 0.5^\circ\text{C}$ ) using a Thermo Orion 420+ pH meter, a 725 Dosimat automatic piston burette and a 9157BN Thermo Orion pH Triode combination Ag/AgCl electrode. The solutions were constantly stirred by a 649 Metrohm magnetic stirrer. A stream of high purity nitrogen was bubbled through the test solution for de-aeration of the sample solutions (Fig. 3.1a and Fig. 3.1b).

### 4.3.3 Procedure for the determination of the formation constants of the metal complexes with THTD and THTUD

To calculate the ionic strength of solutions, the following equation was used:

$$I = \frac{1}{2} \sum Z_i^2 C_i \text{ where} \quad (4.1)$$

I = ionic strength

Z = the charge of an ion i

C = concentration of the ion i

This equation is used when both positive and negative ions are in solution.<sup>75</sup>

An ionic strength of 0.1000 mol dm<sup>-3</sup> was used for all the metal ion solutions. The concentrations of the metal ion solutions were then determined by means of Eqn 4.1. The stability constants were determined by means of potentiometric titration. Two different mol ratios of metal to ligand (1:1.1 and 1:1.5) were used to determine the formation constants.

For the ligand, an ionic strength of 0.1000 mol dm<sup>-3</sup> was used. The ligand was therefore dissolved in a solution of NaNO<sub>3</sub> (0.0999 mol dm<sup>-3</sup>).

---

<sup>75</sup> J.P. Bromberg in *Physical Chemistry*, Allyn and Bacon, Inc., Boston, 1980, p. 300

The pH-meter with a combination glass electrode was calibrated each day before the experiment was carried out. An  $E_{\text{cell}}^0$ -value was determined separately for each of the titrations.  $\text{HNO}_3$  (20.000 mL -  $0.09782 \text{ mol dm}^{-3}$ ) was placed in a jacketed glass vessel and was given sufficient time to stabilize at  $25.0^\circ\text{C}$  ( $\pm 0.5^\circ\text{C}$ ).  $\text{NaOH}$  (40.000 mL -  $0.09687 \text{ mol dm}^{-3}$ ) was then titrated in small increments of 0.200 mL to the  $\text{HNO}_3$ . The potential readings were only taken after the electrode completely stabilized. The equation for the cell calibration is:

$$E_{\text{cell}} = E_{\text{cell}}^0 + k \log[\text{H}^+] \quad (4.2)$$

The data was then manipulated in an EXCELL data sheet and the straight-line graph was extrapolated to determine the  $E^0$ -value as well as the slope according to Eqn 4.2. The method for the determination of the  $E^0$ -value as well as the slope is described in section 3.3.3 of Chapter 3.

For the determination of the formation constants,  $\text{HNO}_3$  (20.000 mL) was added to the jacketed glass vessel. A known volume of the particular ligand solution, and a known volume of the particular metal ion solution (see Appendix 13 to 29), was then added to the  $\text{HNO}_3$ .  $\text{NaOH}$  was then titrated in very small increments of no more than 0.250 mL to the jacketed glass vessel. The change in potential was noted against the change in volume of the solution. This data was then used in the ESTA-WIN<sup>66</sup> computer program to determine the stability constants of the THTD - and THTUD ligands with the various metal ions.

#### 4.4 Results and discussion

The general equation for the reaction can be written as follows:



There is competition between the protons and the metal ion for the ligand. For coordination of the ligand to the metal ion to take place, the ligand and/or the metal ion must be deprotonated. As the solution becomes more basic, the metal ions can form hydroxide complexes because of the excess OH<sup>-</sup>. Other species may also be found when the species distribution is investigated.

Throughout the discussion, all values refer to log(*K*) values.

M = metal ion                      L = ligand

Co(II) is a d<sup>7</sup> system. For a weak ligand field in an octahedral orientation, the e<sup>-</sup>-configuration is  $t_{2g}^5 e_g^2$ . This means that there are 3 unpaired e<sup>-</sup> and thus Co(II) will be a high spin complex with the CFSE = 0.8Δ<sub>o</sub>. The high stability constants of THTD and THTUD suggest that we are dealing with a strong ligand field. Because of this strong ligand field, the splitting between the e<sub>g</sub> and t<sub>2g</sub> levels will be large. The e<sup>-</sup>-configuration for a strong ligand field is  $t_{2g}^6 e_g^1$ . This means that there is only 1 unpaired e<sup>-</sup> and thus Co(II) will be a low spin complex. The CFSE = 1.8Δ<sub>o</sub>.

No electron pairing energy has been considered. Electron pairing energy consists of two components 1) coulombic repulsion – when electrons are forced to occupy the same orbital and 2) the loss of exchange energy – electrons with parallel spins are forced to have antiparallel spins. If one considers the spin pairing to be negligible, Co(II) can be considered a low spin complex in the presence of the strong ligand field created by THTD and THTUD.

#### 4.4.1 THTD with a series of metal ions

From Fig. 4.1 and Table 4.2 it can be seen that even with different mol ratios, the stability constants of the metal ions of the various metals are the same. An average value was determined for the different ratios.

### Stability constants of THTD with various metal ions

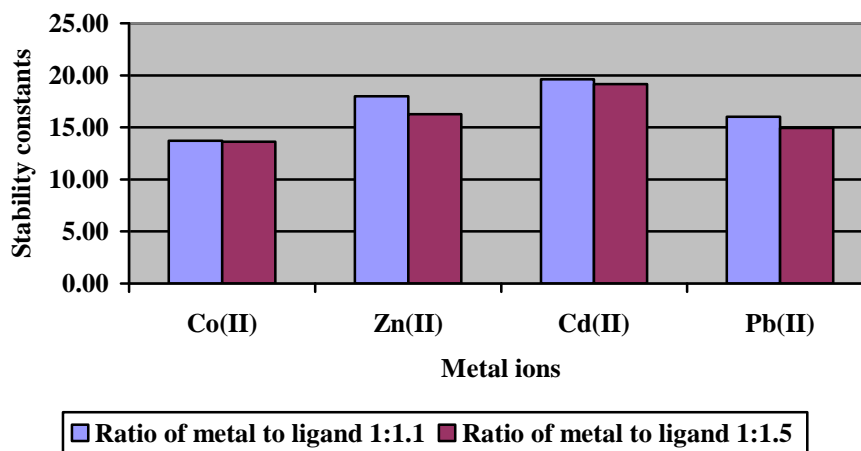


**Fig. 4.1** The stability constants of THTD with various transition metal ions; two different mol ratios were used.

#### 4.4.1.1 $Pb^{2+}$

The stability constant of  $Pb^{2+}$  with THTD is 15.47. The parent molecule, [10]-ane- $N_3$ <sup>67</sup> has a value of 10.0. The values for THETAC<sup>44, 67</sup> and TETA<sup>67</sup> are 12.00 and 14.55. There is a significant increase of almost 5.4 log units in the stability of the complex from the parent ligand to THTD. The pendant arms give extra stability to the complex in comparison to the parent molecule. The fact that there are three extra neutral oxygen donor atoms makes this complex substantially better with  $Pb^{2+}$  than with the parent ligand. Also, the pendant arms form 3 five-membered chelate rings which improve stability with the relatively larger  $Pb^{2+}$  metal ion. THETAC has a slightly lower formation constant than THTD. The inductive effect of the methyl groups on the pendant arms of THTD gives this complex a higher formation constant than THETAC.

#### 4.4.1.2 $Zn^{2+}$

THTD is compared to [9]-ane- $N_3$ ,<sup>44, 67, 68</sup> [10]-ane- $N_3$ , THETAC and TETA. The respective values are 15.5, 11.4, 12.1 and 16.62. THTD

has a value of 14.82. There is an increase of about 3.4 log units in the stability from the parent molecule, [10]-ane-N<sub>3</sub>, to THTD. THTD is only slightly less stable than [9]-ane-N<sub>3</sub> and TETA. It is more stable though than [10]-ane-N<sub>3</sub> and THETAC. It can be concluded that the pendant arms allow for greater complexing stability to the ligand when coordinated to Zn<sup>2+</sup> than just the parent molecule.

#### 4.4.1.3 Cd<sup>2+</sup>

THTD is compared to [10]-ane-N<sub>3</sub>, THETAC and TETA. THETAC has a value of 10.6, TETA a value of 18.25 and THTD shows a value of 19.38. The stability constant for the parent molecule, [10]-ane-N<sub>3</sub>, is 9.1. The stability of THTD more than doubled (logK value) when compared to [10]-ane-N<sub>3</sub>. The average standard deviation is 0.052 and the average R-factor is 0.018 (Table 4.2). It is thus clear that THTD forms a very stable and strong complex with Cd<sup>2+</sup>. It is remarkable that TETA which has eight donor atoms is slightly less stable with Cd<sup>2+</sup> compared to THTD which is hexadentate. Cd<sup>2+</sup> is considered to be medium to large in size ( $r^+ = 0.95 \text{ \AA}$ ).<sup>76, 77, 78</sup> It is thus conceivable that the Cd<sup>2+</sup> ion is too large to coordinate properly with the [10]-ane-N<sub>3</sub>. The ring is probably too small and the Cd<sup>2+</sup> coordinates outside the plane of the cavity and this will mean that the nitrogen atoms cannot bind properly because the angles (N-Cd<sup>2+</sup>-N) will be greatly distorted. On the other hand, the pendant arms though can fold around to donate electrons from the oxygen atoms, stabilizing the complex. Cd<sup>2+</sup> will prefer to form 5-membered rings. Although the macrocyclic ring can form two 5-membered rings and one 6-membered ring, the three nitrogen atoms are fairly close to one another. The bonds between the nitrogen atoms and the metal ion might be weakened due

---

<sup>76</sup> L.F. Lindoy in *The Chemistry of Macrocyclic Ligand Complexes*, Cambridge University Press, Cambridge, 1990, p. 42

<sup>77</sup> J.E. Huheey, E.A. Keiter and R.L. Keiter in *Inorganic Chemistry: Principles of Structure and Reactivity*, Harper Collins College Publishers, New York, 1993, pp. 114, 349

<sup>78</sup> C. Giacobozzo, H.L. Monaco, D. Viterbo, F. Scordari, G. Gilli, G. Zanotti and M. Catti in *Fundamentals of Crystallography*, Oxford University Press, Oxford, 1992, p 420



to the strain in the macrocyclic ring. The distorted bond angle between the nitrogen donors and the metal ion and the fact that  $\text{Cd}^{2+}$  is above the plane of the 3 nitrogen donors and not in the cavity, can also contribute to the weakening of the bonds between the nitrogen and the metal ion. The other three rings that form from the donating oxygen donors on the pendant arms supply enough stability to compensate for the weakening in the  $\text{N-Cd}^{2+}$  bonds to form a very strong complex. As with  $\text{Pb}^{2+}$ , there are three extra neutral oxygen donor atoms and three extra 5-membered chelate rings which appear to stabilize this complex. THTD coordinates to  $\text{Cd}^{2+}$  to form the most stable complex, compared to all the ligands that have been compared. The pendant arms of the THTD will fold over to produce just the right bond angles and bond distances to form a stable complex with  $\text{Cd}^{2+}$ . The methyl groups on the pendant arms will further stabilize the complex due to the induction effect that causes the oxygen donor atoms to become more basic.

#### **4.4.1.4 $\text{Co}^{2+}$**

TETA is an octadentate ligand and has a stability constant of 16.62 with  $\text{Co}^{2+}$ . THTD on the other hand is a hexadentate ligand and has a value of 22.22. This is by far the strongest complex which THTD forms with the metal ions that were used.  $\text{Co}^{2+}$  is relatively small and there is not enough space to accommodate the eight donating groups of TETA.<sup>11</sup> TETA contains four nitrogen atoms in the ring and is thus bigger than THTD which contains only three nitrogen atoms in the ring. In this instance the size of the metal ion seems to play a role in the stability of the complex. Although TETA (4 nitrogen atoms in the macrocyclic ring) is more flexible than THTD (3 nitrogen atoms in the macrocyclic ring), the distances between the donor atoms and the metal ion are longer than in THTD.  $\text{Co}^{2+}$  appears to have the right size to fit into the hollow space that is being created by the ring of THTD and the pendant arms which can fold over into the optimal position to supply the maximum stability. Because the bond lengths are shorter in THTD than in TETA, the bonds between the donor atoms and the

metal ion will be stronger and thus more stable. Although  $\text{Co}^{2+}$  would prefer to form 6-membered rings, the size of the ligand and the rings that form when coordinated to the  $\text{Co}^{2+}$ , forms just the right bond lengths and angles for  $\text{Co}^{2+}$  to fit. The induction effect of the methyl groups on the pendant arms will provide extra stability to the oxygen donors and strengthen the donating capabilities of the oxygen donor atoms.

**Table 4.2** Stability constants, the standard deviation and the R-factor for each value of the different metal ion to ligand ratio. M = metal and L = ligand (THTD).

M(NO <sub>3</sub> )	M:L 1:1.1	STDEV	R-factor	M:L 1:1.5	STDEV	R-factor
Co <sup>2+</sup>	21.92	0.20	0.07	22.51	0.04	0.03
Zn <sup>2+</sup>	13.37	0.16	0.04	15.53	0.12	0.05
Cd <sup>2+</sup>	19.61	0.07	0.03	19.14	0.03	0.01
Pb <sup>2+</sup>	16.01	0.27	0.03	14.93	0.04	0.02

#### 4.4.2 THTUD with a series of metal ions

From Fig. 4.2 and Table 4.3 it can be seen that with different mol ratios, the stability constants of the ligand with the various metal ions are virtually the same.

##### 4.4.2.1 Pb<sup>2+</sup>

THETAC has a  $\log(K)$  value of 12.00 and TETA a value of 14.55. THTUD has a stability constant of 14.63 and compares well with TETA. The standard deviation and R-factor in this case are 0.035 and 0.015 respectively. There is a slight increase in the stability (2.63 log units) of THTUD with  $\text{Pb}^{2+}$  compared to THETAC, most likely due to the induction effects from the methyl groups of the pendant donors compared to that of THETAC.

#### 4.4.2.2 $Zn^{2+}$

The stability constant,  $\log(K)$ , of THTUD with  $Zn^{2+}$  is 16.20. This value was compared to [9]-ane- $N_3$  – 15.5, [11]-ane- $N_3$  – 10.4, THETAC - 12.1. From the stability constant it is clear that THTUD forms the strongest complex of the three ligands in question. The standard deviation and R-factor for THTUD are respectively 0.043 and 0.018. There is an improvement of 6 log units in the stability constant when THTUD and [11]-ane- $N_3$  are compared. The pendant arms that fold around the  $Zn^{2+}$ , has the induction effect of the methyl groups to help stabilize the complex. THETAC does not have these additional groups to help with stabilization, and therefore cannot form such a strong complex with  $Zn^{2+}$ . [9]-ane- $N_3$  has a stability constant of 15.5 which is similar to that of THTUD.  $Zn^{2+}$  lies out of the plane of the 3 donor atoms as was confirmed by the crystal structure in Chapter 5.

#### 4.4.2.3 $Co^{2+}$

The stability constant for TETA is 16.62. For THTUD it is 17.52. The standard deviation is 0.035 and the R-factor is 0.018. By comparing the values of TETA and THTUD it is clear that there is very little difference between the two ligands, although the stability constant of THTUD is slightly higher.  $Co^{2+}$  is a relatively small metal ion which means that 6-membered rings are preferred. Both TETA and THTUD provide 5- and 6-membered rings. The only difference is the induction effect of the methyl groups on the pendant arms of the THTUD.

#### 4.4.2.4 $Cd^{2+}$

[11]-ane- $N_3$ , THETAC and TETA were used to compare the values of the stability constants against that of THTUD. These  $\log(K)$  values were respectively 8.6, 10.6 and 18.25. For THTUD the value is 18.05 and the standard deviation is 0.039 and the R-factor is 0.018. The complexing ability of TETA and THTUD is for all practical purposes

the same. It is clear though that THTUD is a much stronger complexing agent than THETAC. It is possible that THTUD has the correct dimensions for complexing optimally to  $\text{Cd}^{2+}$ . The cavity formed between the macrocycle and the pendant arms accommodates  $\text{Cd}^{2+}$  the best. [11]-ane- $\text{N}_3$  has a very low stability constant of 8.6 while THTUD is 18.05. This is an improvement of  $\pm 9.5$  log units.

**Stability constants of THTUD with various metal ions**

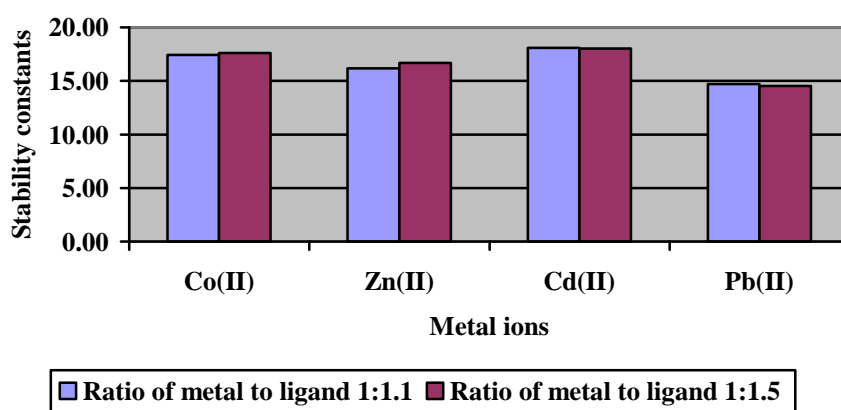


**Fig. 4.2** The stability constants of THTUD with various transition metal ions; two different mol ratios were used.

The pendant arms form rings that accommodates the  $\text{Cd}^{2+}$  at just the correct distance while the induction effects of the methyl groups provide the extra stability.  $\text{Cd}^{2+}$ , being large, will prefer to form 5-membered ring complexes, and with THTUD there is an extra three rings as well as three neutral oxygen donors which assist in making this ligand much more stable with  $\text{Cd}^{2+}$ .

**Table 4.3** Stability constants, the standard deviation and the R-factor for each value of the different metal ion to ligand ratio. M = metal and L = ligand (THTUD).

M( $\text{NO}_3$ )	M:L 1:1.1	STDEV	R-factor	M:L 1:1.5	STDEV	R-factor
$\text{Co}^{2+}$	17.43	0.033	0.018	17.61	0.036	0.018
$\text{Zn}^{2+}$	16.17	0.033	0.017	16.69	0.052	0.020
$\text{Cd}^{2+}$	18.09	0.033	0.015	18.02	0.043	0.020
$\text{Pb}^{2+}$	14.72	0.031	0.013	14.54	0.038	0.017

## 4.5 Conclusion

The stability constants of THTD increases in the following order:  $\text{Pb}^{2+}$ ,  $\text{Zn}^{2+}$ ,  $\text{Cd}^{2+}$ ,  $\text{Co}^{2+}$ . The stability constants for THTUD increases in the following order:  $\text{Pb}^{2+}$ ,  $\text{Zn}^{2+}$ ,  $\text{Co}^{2+}$ ,  $\text{Cd}^{2+}$ .

From the perspective of size-match selectivity, the radius of the different metal ions, -  $\text{Co}^{2+}$  (0.65 Å),  $\text{Zn}^{2+}$  (0.74 Å),  $\text{Cd}^{2+}$  (0.95 Å),  $\text{Pb}$  (1.19 Å)<sup>79</sup> –it looks like size does not play as marked a role in the stability of THTD and THTUD with the metal ions. The stability constants of THTD and THTUD suggest that there is no specific order when the size of the metal ion is taken into consideration.

From the Irving-Williams series it can be seen that Co(II) and Zn(II) have almost the same stability constants with THTUD. Co(II) and Zn(II) show a huge difference when THTD is used as the ligand. It is clear that the stability constants are much higher with the new ligands compared to the ligands used in the Irving-Williams series, because with the new ligands, we have the chelate effect, macrocyclic effect, pendant donor arms, different-sized chelate rings, different numbers and type of donor atoms.

Other factors that are definitely influencing the effectiveness of the ligand are the induction effects of the carbon bridges in the ring as well as the induction effect of the pendant arms.

Why THTD and THTUD form such stable complexes with Cd(II) is very intriguing. This would be explored further using molecular mechanics studies. We are at present trying to obtain single crystals of Cd(II) with these ligands to determine the bonding mode and other structural details of these complexes.

In conclusion, THTD compares favourably with other ligands of the same size with similar pendant arms. Both THTD and THTUD have very high stability constants with Cd(II) compared to any of these other ligands.

---

<sup>79</sup> R.D. Shannon, *Acta Cryst.*, **A32**, 1976, 751-767.

## Chapter 5

### *The Determination of Crystal Structures*

#### 5.1 Introduction

Zompa and Margulis determined the crystal and molecular structure of [9]-ane-N<sub>3</sub><sup>79</sup> with Ni<sup>2+</sup>. [9]-ane-N<sub>3</sub> functions as a tri-dentate ligand. Because Ni(II) can be six coordinate, it binds to two [9]-ane-N<sub>3</sub> ligands. The two ligands are positioned in such a way that they are opposite each other with the metal ion centre halfway between the two ligands.

Thermodynamic and spectroscopic properties of transition metal ions with triazamacrocycles are not so generally available. The stability of the complexes has been ascribed to the cyclic nature of the ligand and the associated large configurational entropy contribution. The unusual spectroscopic behaviour is due to the sizeable trigonal distortion along the C<sub>3</sub> axis. X-ray diffraction studies confirmed this distortion.<sup>79</sup>

Hammershøi and Sargeson<sup>80</sup> determined and investigated in detail the cage structures of hexaamine ligands with Co<sup>2+</sup>. The preparation of the ligands they used is analogous to the method we employed.

#### 5.2 Aim

The motivation for trying to obtain crystals of the free ligands is to establish their pre-organization prior to complexation.

---

<sup>79</sup> L.J. Zompa and T.N. Margulis, *Inorg. Chim. Acta*, 1978, **28**, L157-L159

<sup>80</sup> A. Hammershøi and A.M. Sargeson, *Inorg. Chem.*, 1983, **22**, 3554-3561

THTD and THTUD can form both 5- and 6-membered chelate rings when coordinated to a metal centre. We planned to investigate the crystal structures of these ligands with a series of transition metals in the oxidation state (II) as well as with Pb(II). Taking the size of the metal ions into consideration, it would also give insight as to whether the metal ion will be situated within or outside the cavity in other words, to what extent size-match selectivity drives the complex stability. The metal ions that were used range from relatively hard, to large soft whereas the ligand contains hard donor atoms.

### 5.3 Experimental procedures

#### 5.3.1 General preparation of the complexes

**CAUTION:** Care must be taken when working with organic perchlorates as they could be explosive. Small quantities should be used.

THTD  $M_r = 317.467$

THTUD  $M_r = 331.494$

In all the reactions with the different metals, a mole ratio of 1:1 (ligand:metal) was used. THTD (0.030g,  $9.5 \times 10^{-5}$  mol) and THTUD (0.030g,  $9.1 \times 10^{-5}$  mol) were respectively used in each of the reactions. The THTD and THTUD were dissolved in a minimum amount of ethanol. The  $M(\text{ClO}_4)_x$  was also dissolved in a minimum amount of ethanol. The metal perchlorate solution was then added dropwise by means of a Pasteur pipette to the ligand solution. The reaction mixture was placed in an oil bath and heated to 80°C under reflux conditions for approximately 8 hours while stirring.

The reaction mixture was filtered through a no. 4 filter paper and the precipitate washed with ethanol to rid the product of any unreacted metal perchlorate. The precipitate (product) was then dissolved in distilled water and the water boiled off until small crystals began to precipitate. These crystals were redissolved in distilled water and it was allowed to evaporate slowly in order to produce good quality crystals.

The procedures for the preparation of the complexes for crystallization were the same for both THTD and THTUD.

### 5.3.2 Methods used in the crystallization of the complexes

Crystallization was a problem and different methods were used in order to obtain crystals suited for single crystal X-ray diffraction studies. Some of the techniques that we were employing showed some very promising results.

Different methods of crystallization were attempted:<sup>81</sup>

1. Slow evaporation of the solvent
2. Slow cooling of the saturated solution
3. Liquid diffusion
4. Vapour diffusion
5. Different solvents
  - 5.1 water
  - 5.2 water (70%) : ethanol (30%)
  - 5.3 acetone
  - 5.4 hexane
  - 5.5 acetonitrile
  - 5.6 acetonitrile (50%) : methanol (50%)
6. Various size crystallization tubes

The use of metal nitrates rather than metal perchlorates did not assist in producing better quality crystals. On the contrary, less crystallization occurred with the metal nitrates compared to the metal perchlorates. Better crystals were obtained by using metal perchlorates.

---

<sup>81</sup> P.G. Jones, *Chem. Brit.*, 1981, **17**, 222-225



### 5.3.3 THTD with a Series of Metal Ions

#### 5.3.3.1 *Manganese(II) perchlorate hexahydrate* [Mn(ClO<sub>4</sub>)<sub>2</sub>·6H<sub>2</sub>O] Mr = 253.84

(Supplied by Sigma-Aldrich and the formula mass used as given on container)

Mn(ClO<sub>4</sub>)<sub>2</sub>·6H<sub>2</sub>O (0.023 g) was dissolved in a minimum amount of ethanol and added to the solution containing the ligand. The solution turned dark brown on addition of the metal ion and a dark brown precipitate formed almost immediately.

The dark brown crystals were obtained by slow evaporation of the water from the solution. The crystals were block shaped. The crystal is described in section 5.4.

#### 5.3.3.2 *Iron(III) perchlorate hexahydrate* [Fe(ClO<sub>4</sub>)<sub>3</sub>·6H<sub>2</sub>O] Mr = 354.20

(Supplied by Sigma-Aldrich and the formula mass used as given on container.)

Fe(ClO<sub>4</sub>)<sub>3</sub>·6H<sub>2</sub>O (0.032 g) was dissolved in a minimum amount of ethanol and added to the solution containing the ligand. The solution immediately formed an orange/red precipitate on addition of the metal ion.

As the water evaporated, only an orange precipitate appeared. We were not able to obtain any crystals from this solution.

#### 5.3.3.3 *Cobalt(II) perchlorate hexahydrate* [Co(ClO<sub>4</sub>)<sub>2</sub>·6H<sub>2</sub>O] Mr = 365.93

(Supplied by Sigma-Aldrich and the formula mass used as given on container)

Co(ClO<sub>4</sub>)<sub>2</sub>·6H<sub>2</sub>O (0.033 g) was dissolved in a minimum amount of ethanol and added to the solution containing the ligand. The solution formed a dark shade of pink on addition of the metal ion and a purple precipitate formed after about 3 minutes.

Although crystals did form, the quality was not good enough to obtain data of the crystal structure of the complex.

**5.3.3.4 Nickel(II) perchlorate hexahydrate**  $[\text{Ni}(\text{ClO}_4)_2 \cdot 6\text{H}_2\text{O}]$  Mr = 365.70

(Supplied by Sigma-Aldrich and the formula mass used as given on container)

$\text{Ni}(\text{ClO}_4)_2 \cdot 6\text{H}_2\text{O}$  (0.033 g) was dissolved in a minimum amount of ethanol and added to the solution containing the ligand. The solution turned light blue on addition of the metal ion and a blue precipitate formed after about 10 minutes.

The nickel complex did crystallize, but the quality of the crystals was too poor to yield any data on the crystal structure.

**5.3.3.5 Copper(II) perchlorate hexahydrate**  $[\text{Cu}(\text{ClO}_4)_2 \cdot 6\text{H}_2\text{O}]$  Mr = 370.53

(Supplied by Sigma-Aldrich and the formula mass used as given on container)

$\text{Cu}(\text{ClO}_4)_2 \cdot 6\text{H}_2\text{O}$  (0.034 g) was dissolved in a minimum amount of ethanol and added to the solution containing the ligand. The solution turned dark green on addition of the metal ion and a blue precipitate formed after about 10 minutes.

Blue crystals did form, but the quality was too poor to yield any data on the crystal structure.

**5.3.3.6 Zinc(II) perchlorate hexahydrate**  $[\text{Zn}(\text{ClO}_4)_2 \cdot 6\text{H}_2\text{O}]$  Mr = 372.36

(Supplied by Sigma-Aldrich and the formula mass used as given on container.)

$\text{Zn}(\text{ClO}_4)_2 \cdot 6\text{H}_2\text{O}$  (0.035 g) was dissolved in a minimum amount of ethanol and added to the solution containing the ligand. The solution immediately formed a white precipitate on addition of the metal ion. The white precipitate which formed was dissolved in a minimum amount of water.

Colourless, block shaped crystals formed, but they were too small to generate any data on the X-ray diffractometer.

#### 5.3.3.7 *Cadmium(II) perchlorate hydrate* [Cd(ClO<sub>4</sub>)<sub>2</sub>·H<sub>2</sub>O] Mr = 311.30

(Supplied by Sigma-Aldrich and the formula mass used as given on container.)

Cd(ClO<sub>4</sub>)<sub>2</sub>·H<sub>2</sub>O (0.028 g) was dissolved in a minimum amount of ethanol and added to the solution containing the ligand. The solution stayed colourless on addition of the metal ion. No precipitate formed over the course of the reaction.

Although no crystals were obtained, it still might be assumed that a complex did form when the stability constants are taken into consideration. According to the stability constants, a strong complex is formed. It is however unfortunate that no crystals were available for analysis at the time.

#### 5.3.3.8 *Lead(II) perchlorate hydrate* [Pb(ClO<sub>4</sub>)<sub>2</sub>·xH<sub>2</sub>O] Mr = 406.09

(Supplied by Sigma-Aldrich and the formula mass used as given on container.)

Pb(ClO<sub>4</sub>)<sub>2</sub>·xH<sub>2</sub>O (0.037 g) was dissolved in a minimum amount of ethanol and added to the solution containing the ligand. A white precipitate formed after a few minutes on addition of the metal ion. The white precipitate which formed was dissolved in a minimum amount of water and the solution turned colourless. The precipitate was very reluctant to dissolve in the water, and after a few days a white precipitate reoccurred in the polytop.

No crystals formed from the water phase and it was assumed that the white precipitate that formed might be Pb(OH)<sub>2</sub> since the precipitate was reluctant to dissolve in water.

### 5.3.4 THTUD with a Series of Metal Ions

#### 5.3.4.1 *Manganese(II) perchlorate hexahydrate* [Mn(ClO<sub>4</sub>)<sub>2</sub>·6H<sub>2</sub>O] Mr = 253.84

(Supplied by Sigma-Aldrich and the formula mass used as given on container.)

Mn(ClO<sub>4</sub>)<sub>2</sub>·6H<sub>2</sub>O (0.023 g) was dissolved in a minimum amount of ethanol and added to the solution containing the ligand. The solution turned dark

brown on addition of the metal ion and a dark brown precipitate formed almost immediately.

Brown crystals formed, but the quality was not good enough to collect any data from the X-ray diffractometer.

#### **5.3.4.2 Iron(III) perchlorate hydrate** $[\text{Fe}(\text{ClO}_4)_3 \cdot x\text{H}_2\text{O}]$ Mr = 354.20

(Supplied by Sigma-Aldrich and the formula mass used as given on container.)

$\text{Fe}(\text{ClO}_4)_3 \cdot x\text{H}_2\text{O}$  (0.032 g) was dissolved in a minimum amount of ethanol and added to the solution containing the ligand. The solution turned orange on addition of the metal ion and an orange precipitate formed almost immediately.

No crystals formed, only an orange precipitate occurred after a few weeks. The precipitate was again dissolved, but the same result occurred, so unfortunately no crystal structure could be obtained for  $\text{Fe}^{3+}(\text{THTUD})$ .

#### **5.3.4.3 Cobalt(II) perchlorate hexahydrate** $[\text{Co}(\text{ClO}_4)_2 \cdot 6\text{H}_2\text{O}]$ Mr = 365.93

(Supplied by Sigma-Aldrich and the formula mass used as given on container.)

$\text{Co}(\text{ClO}_4)_2 \cdot 6\text{H}_2\text{O}$  (0.033 g) was dissolved in a minimum amount of ethanol and added to the solution containing the ligand. The solution turned to a darker shade of pink (than the original cobalt solution) on addition of the metal ion and a dark pink precipitate formed after about 3 minutes.

The crystals were obtained using slow evaporation from water. The crystals were dark pink and block-like in shape.

#### **5.3.4.4 Nickel(II) perchlorate hexahydrate** $[\text{Ni}(\text{ClO}_4)_2 \cdot 6\text{H}_2\text{O}]$ Mr = 365.70

(Supplied by Sigma-Aldrich and the formula mass used as given on container.)

$\text{Ni}(\text{ClO}_4)_2 \cdot 6\text{H}_2\text{O}$  (0.033 g) was dissolved in a minimum amount of ethanol and added dropwise to the solution containing the ligand. The solution turned pale

blue on addition of the metal ion and a light blue precipitate formed after about 10 minutes.

Light blue, block shaped crystals formed, but the quality and size made it impossible to collect any data of these crystals.

#### **5.3.4.5 Copper(II) perchlorate hexahydrate** $[\text{Cu}(\text{ClO}_4)_2 \cdot 6\text{H}_2\text{O}]$ Mr = 370.53

(Supplied by Sigma-Aldrich and the formula mass used as given on container.)

$\text{Cu}(\text{ClO}_4)_2 \cdot 6\text{H}_2\text{O}$  (0.034g) was dissolved in a minimum amount of ethanol and added to the solution containing the ligand. The solution turned dark green on addition of the metal ion. A blue precipitate formed after about 10 minutes.

Blue crystals formed, but the quality was not good enough to collect any data.

#### **5.3.4.6 Zinc(II) perchlorate hexahydrate** $[\text{Zn}(\text{ClO}_4)_2 \cdot 6\text{H}_2\text{O}]$ Mr = 372.36

(Supplied by Sigma-Aldrich and the formula mass used as given on container.)

$\text{Zn}(\text{ClO}_4)_2 \cdot 6\text{H}_2\text{O}$  (0.034g) was dissolved in a minimum amount of ethanol and added to the solution containing the ligand. The solution immediately formed a white precipitate on addition of the metal ion. This white precipitate turned colourless when redissolved in water. Rectangular, colourless crystals formed after a few days.

A colourless, rectangular block shaped crystal was used to determine the crystal structure of  $\text{Zn}^{2+}(\text{THTUD})[\text{2}(\text{ClO}_4)^-]$ .

#### **5.3.4.7 Cadmium(II) perchlorate hydrate** $[\text{Cd}(\text{ClO}_4)_2 \cdot \text{H}_2\text{O}]$ Mr = 311.30

(Supplied by Sigma-Aldrich and the formula mass used as given on container.)

$\text{Cd}(\text{ClO}_4)_2 \cdot 4\text{H}_2\text{O}$  (0.028g) was dissolved in a minimum amount of ethanol and added to the solution containing the ligand. The solution stayed colourless on addition of the metal ion and no precipitate formed throughout the entire reaction.

Although no crystals were obtained, it still might be assumed that a complex did form when the stability constants are taken into consideration. According to the stability constants,  $\log(K) \approx 18$ , a strong complex is formed. It is however unfortunate that no crystals were obtained for analysis.

#### 5.3.4.8 Lead(II) perchlorate hydrate [Pb(ClO<sub>4</sub>)<sub>2</sub>.xH<sub>2</sub>O] Mr = 406.09

(Supplied by Sigma-Aldrich and the formula mass used as given on container.)

Pb(ClO<sub>4</sub>)<sub>2</sub>.H<sub>2</sub>O (0.037g) was dissolved in a minimum amount of ethanol and added to the solution containing the ligand. The solution stayed colourless on addition of the metal ion. A white precipitate formed after a few minutes.

The precipitate was very reluctant to dissolve in water. If the complex did form, it should be able to dissolve in water. It is believed that Pb(OH)<sub>2</sub> formed during the reaction, but further investigations should be carried out to confirm this prediction. No crystals were obtained from the water phase.

### 5.3.5 Instrumentation

A Bruker-Nonius SMART Apex I diffractometer equipped with a Mo fine-focus sealed tube and a 0.5 mm MonoCap collimator was used to determine the crystal structure. A Cryostat: Oxford Cryogenics Cryostat (700 Series Cryostream Plus) was used to cool the crystals to 100K. The structure was solved and refined using the programs SHELXS-97<sup>82</sup> and SHELXL-97<sup>83</sup> respectively. The program X-Seed<sup>84</sup> was used as an interface to the SHELX programs, and to prepare the figures.

## 5.4 Results and discussion

### 5.4.1 Attempted structure determination of the free ligands

THTD did not produce crystals of any kind. The only result was a white precipitate that formed after each attempt.

---

<sup>82</sup> G.M. Sheldrick, *Acta Cryst.*, 1990, **A46**, 467–473

<sup>83</sup> G.M. Sheldrick, *SHELXL97.*, 1997, University of Göttingen, Germany

<sup>84</sup> L.J. Barbour, *J. Supramol. Chem.*, 2001, **1**, 189-191

THTUD formed crystals when dissolved in hot hexane. These crystals were needle-like, colourless and extremely thin. These crystals were too thin and no results could be obtained from the X-ray analysis. A different solvent was used to try to produce better crystals. The best results were yielded from acetonitrile, but the quality of the crystals remained unsatisfactory for any data collection.

#### 5.4.2 The unusual complexation during the crystallisation of compound X - $[\text{Mn}_2(\text{THTD})(\text{THTD-H}^+)\cdot 3(\text{ClO}_4)^-]$

The X-complex crystallised in the orthorhombic crystal system, space group  $P2_12_12_1$  with no solvent molecule present in the unit cell.

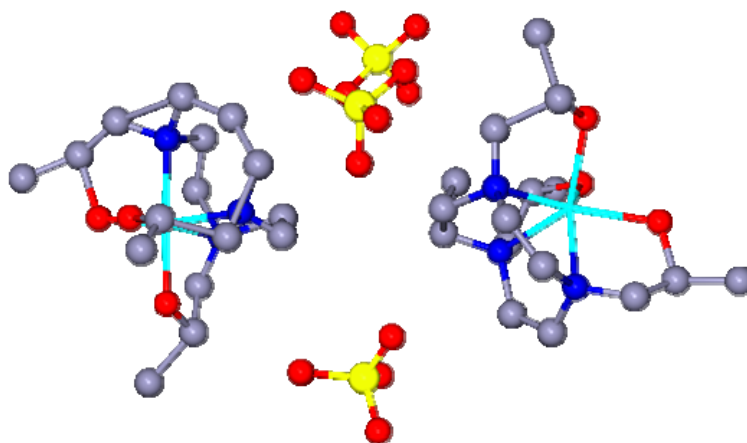


**Fig 5.1** The two metal complexes with three perchlorate counter ions between them.

Two molecules occur per asymmetric unit cell, but there are only three perchlorate anions present (Fig. 5.1), which means that one of the OH-groups was possibly deprotonated, resulting in a charge of +1 on the complex. It is however not possible to prove or predict which OH-group was deprotonated. The methyl groups on the pendant arms all face in the same direction because of the chiral carbons of the pendant arms. The N-atoms in the ring binds in a facial coordination on the one side of the metal centre and the O-donors form a second facial coordination on the opposite side of the octahedral part.

One of the molecules in the unit cell has a distorted octahedral structure. The other molecule is trigonal prismatic. There is one 6-membered ring and five 5-membered rings present in the chelates formed (Table 5.1).

The structure of the octahedral part of the compound X is shown in Fig. 5.2. Perchlorate anions and hydrogen atoms are omitted for clarity.

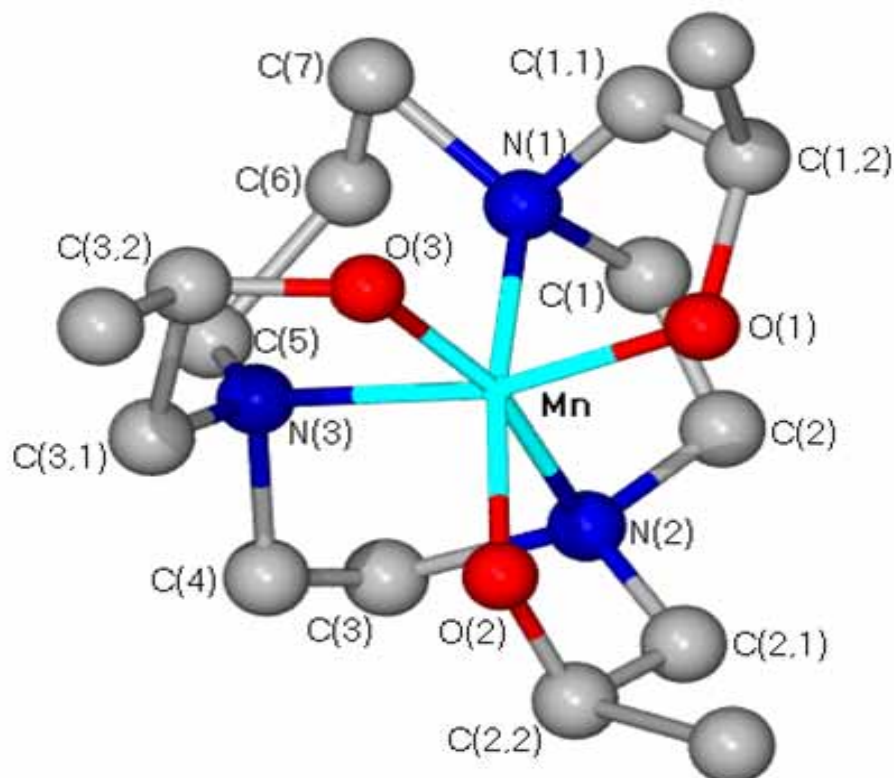


**Fig.5.2** Structure of the octahedral part of compound X with no perchlorate anions shown. The facial coordination of the N-donor atoms and the O-donor atoms are shown.

It is clear from the structure that the Mn(II) is above the cavity, and not inside the macrocycle. The macrocyclic ring bends away from the metal centre, forcing the N-donors towards the metal ion while the pendant arms reach around to bind to the metal ion, and pulling the metal away from the ring.

Mn<sup>2+</sup> is a  $d^5$  system. Normally, with weak field ligands, Mn<sup>2+</sup> is a high spin complex due to the dominant loss of exchange energy compared to the concomitant gain in CFSE when the electrons are forced to pair up. The radius of Mn<sup>2+</sup> (high



spin) is  $0.830\text{\AA}^{78}$  and  $\text{Mn}^{2+}$  (low spin) is  $0.67\text{\AA}^{78}$  and it is thus considered to be a small metal ion. Small metal ions prefer six-membered rings. Because  $\text{Mn}^{2+}$  is quite small and it would seem that the metal ion could fit in the cavity of the ligand in the absence of pendant arms.

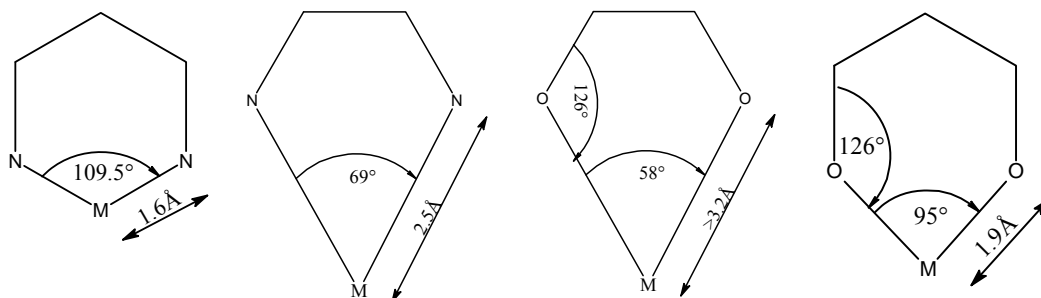


**Fig. 5.3** The ideal geometry for five and six-membered rings bonded to nitrogen and oxygen atoms.<sup>41</sup>

The ideal bond lengths are shown in Fig.5.3. The ideal bond length between the metal centre of a small metal ion ( $\text{Mn}^{2+}$ ), and the N-donors of a macrocyclic ring is  $1.6\text{\AA}$ . The average Mn(II)-N bond length from the literature is  $2.306\text{\AA}$ .<sup>85</sup> The Mn(II)-N bond lengths in the present structure vary between  $2.020(10)\text{\AA}$  and  $2.069(12)\text{\AA}$ . It is thus clear that these bond lengths are significantly longer than the ideal lengths, but shorter than the average bond lengths. The ideal bond lengths between Mn and O, would be about  $1.9\text{\AA}$ , and in the case of the octahedron, the bond lengths are between  $1.813(8)\text{\AA}$  and  $1.864(5)\text{\AA}$  which is close to the ideal distances. For the trigonal prismatic part, the Mn(II)-N bond distances are between  $2.215(15)\text{\AA}$  and  $2.238(8)\text{\AA}$ . The Mn and O bond distances in the trigonal part are between  $2.104(5)\text{\AA}$  and  $2.169(11)\text{\AA}$ . The average separation reported in the literature for Mn(II)-O is  $2.223\text{\AA}$ .<sup>85</sup> The bond lengths between the nitrogen and the metal centre are slightly longer than that of the oxygen metal bond lengths.

<sup>85</sup> A.G. Orpen, I. Brammer, F.H. Allen, O. Kennard, D.G. Watson and R. Taylor, *J.Chem. Soc., Dalton Trans.*, 1989, S37

**Table 5.1** The bond lengths and bond angles of the octahedral part of the X-complex are shown. The \* indicates where the 6-membered ring is situated (Fig. 5.2).

Bond Lengths (Å)		Bond Angles(°)	
Mn-O(1)	1.813(8)	N(1)-Mn-N(3)	89.5(6)
Mn-O(2)	1.864(8)	N(2)-Mn-N(3)*	93.9(5)
Mn-O(3)	1.864(5)	N(1)-Mn-N(2)	84.4(8)
Mn-N(1)	2.020(10)	N(3)-Mn-O(1)	167.0(5)
Mn-N(2)	2.054(11)	N(2)-Mn-O(3)	169.7(5)
Mn-N(3)	2.069(12)	N(1)-Mn-O(2)	170.4(6)

The ideal angle (Fig. 5.3) for an N-Metal-N 6-membered ring is  $109.5^\circ$ .<sup>41</sup> In our octahedral structure, the bond angle to the metal ion of the 6-membered N-Metal-N ring is only  $93.9(5)^\circ$  which means that there is certainly a lot of strain in the ring. The ideal angle for the 5-membered N-Metal-N ring is  $69^\circ$ .<sup>41</sup> In the octahedral part of compound X, the angles are much larger at  $84.4(8)^\circ$  and  $89.5(6)^\circ$  respectively (Table 5.1). These angles are forced upon the structure by the carbon-carbon bridges which keep their bond angles, which means that the bond angles between the Mn(II) and the N- and the O-donors has to change to accommodate the metal ion.

The inductive effect of the methyl groups is responsible for stronger bonding by the oxygen atoms despite some strain in the rings.

The following, more detailed discussion pertains to the trigonal prismatic complex in the crystalline compound X. Selected bond lengths and bond angles are tabulated in Table 5.2 and the molecular structure is shown in Fig. 5.4.

**Table 5.2** The bond lengths and bond angles of the trigonal prismatic part of the X-complex are shown. The \* indicates where the 6-membered ring is situated (Fig. 5.4).

Bond Lengths (Å)		Bond Angles(°)	
Mn-O(1)	2.104(5)	N(1)-Mn-O(1)	76.4(6)
Mn-O(2)	2.140(8)	N(2)-Mn-O(2)	79.1(5)
Mn-O(3)	2.169(11)	N(3)-Mn-O(3)	77.1(3)
Mn-N(1)	2.215(15)	N(1)-Mn-N(3)	83.9(6)
Mn-N(2)	2.224(12)	N(2)-Mn-N(3)*	84.2(8)
Mn-N(3)	2.238(8)	N(1)-Mn-N(2)	82.0(7)

The bond lengths between the O(2)-Mn 2.140 (8)Å and O(3)-Mn 2.169(11)Å are the closest to each other in this structure. The bond length between O(1)-Mn is shorter at 2.104(5)Å and could in all probability indicate the deprotonated hydroxy

group. There is some insignificant variation in the bond lengths between the Mn and the N as can be seen from Table 5.2. As expected, the nitrogen bond lengths are slightly longer than those of the oxygen bond lengths to the Mn(II) centre.

**Table 5.3** Crystal data of  $[\text{Mn}_2(\text{THTD})(\text{THTD-H}^+)](\text{ClO}_4)_3$  that was obtained in this study.

Compound	[Mn(THTD)]
Empirical Formula	$\text{C}_{16} \text{H}_{32} \text{C}_{11} \text{Mn N}_3 \text{O}_9$
Mr	518.56
Crystal habit	block
Crystal size/mm	0.04×0.03×0.02
Crystal system	orthorhombic
Space group	$P2_12_12_1$
a[Å]	10.0979(11)
b[Å]	13.5373(16)
c[Å]	32.138(4)
$\alpha/^\circ$	90.00
$\beta/^\circ$	90.00
$\gamma/^\circ$	90.00
$V/\text{Å}^3$	4393.3(9)
$Z, D_c/\text{Mg m}^{-3}$	8
$\mu(\text{MoK}\alpha)/\text{mm}^{-1}$	0.836
Number of reflections, unique	23592 9007
$R_{im}$	0.0467
$hkl$ index range	$h\pm 12$ $k\pm 16$ $l-16\rightarrow$ 40
Data	5864
Restraints, Parameters	30 553
$F(000)$	2172
$R_b, wR_2^a[I]>$	0.1073
$2\sigma(I)$	0.2802
$R_1, wR_2$ (all data)	0.1462 0.1462
Goodness-of-fit	1.029

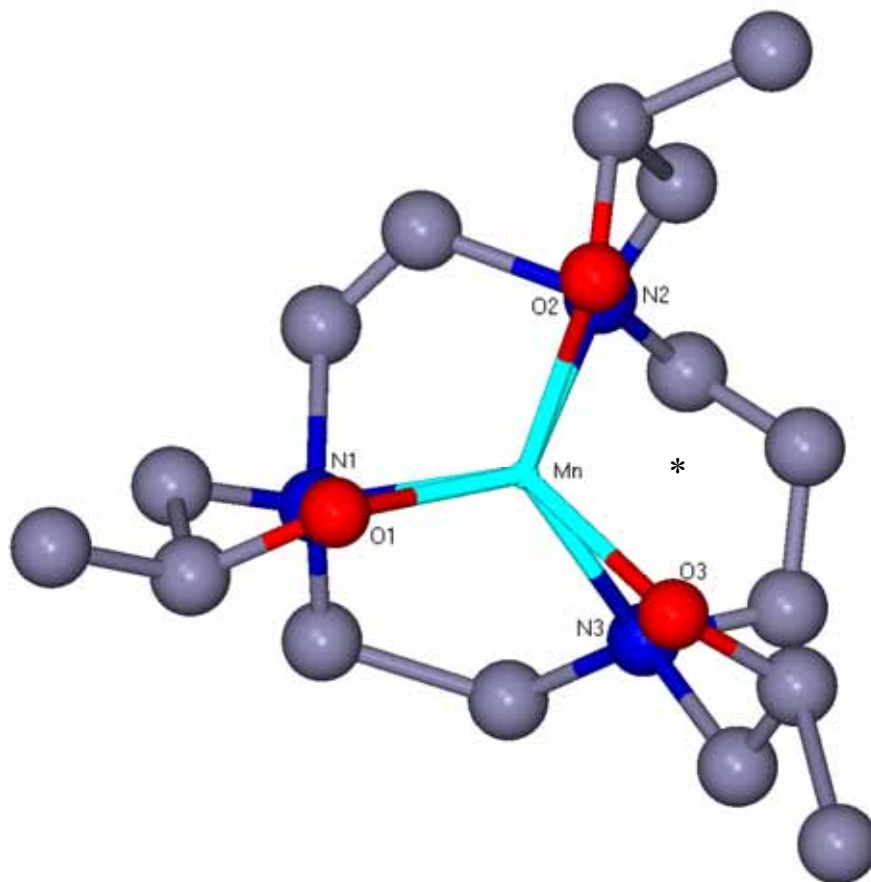


**Fig.5.4** The structure of the trigonal prismatic part of compound X with no perchlorate anions shown as observed along the  $C_3$ -axis.

Some smaller variations are observed in the bond angles between the nitrogen atoms and the metal centre. The biggest angle is the N(2)-Mn-N(3) [ $84.2(8)^\circ$ ] which forms the 6-membered ring of the complex. The 5-membered rings are formed by N(1)-Mn-N(3) [ $83.9(6)^\circ$ ] and N(1)-Mn-N(2) [ $82.0(7)^\circ$ ] of the macrocycle.

The packing of  $[Mn_2(THTD)(THTD-H^+)](ClO_4)_3$  along the a-axis is represented by Fig. 5.5. There are no short distance interactions between the counter ions and Mn(II)THTD or between the Mn(II)THTD units itself. The packing appears to be very chaotic with no apparent order in the arrangement of the molecules. There are no solvent molecules present in the structure. No intermolecular hydrogen bonding is observed.

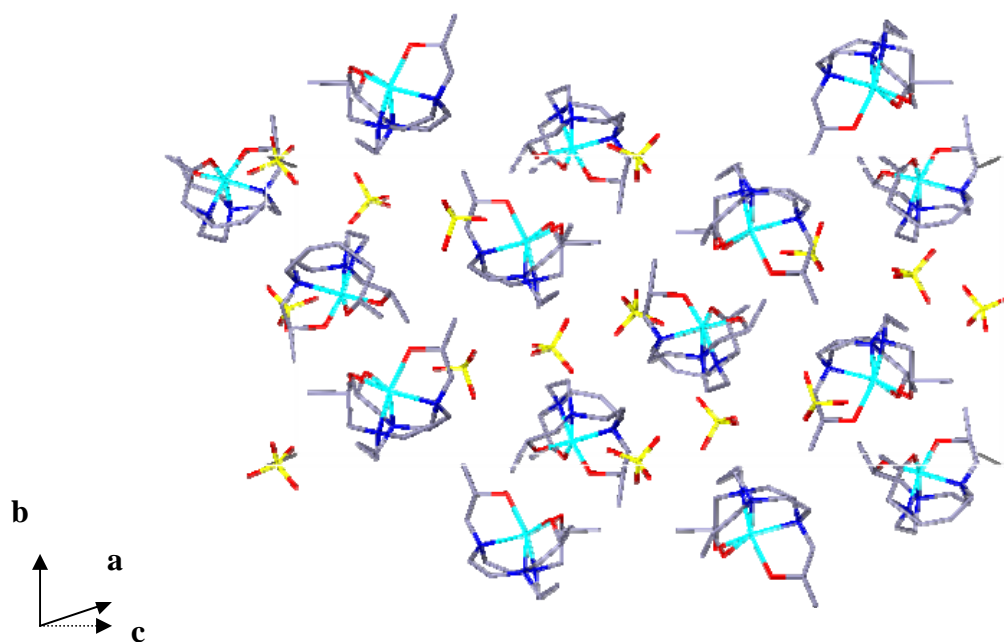


**Fig 5.5** Packing of the  $Mn_2[(THTUD)(THTUD-H^+)](ClO_4)_3$  along the a-axis is shown.

### 5.4.3 The crystal and molecular structure of $[Co(THTUD)](ClO_4)_2$

The compound crystallised in the trigonal crystal system, space group  $P3_1$ . No solvent molecules were present in the structure.

The molecular structure and atomic numbering scheme is shown in Fig. 5.7. Selected bond lengths and angles are shown in Table 5.4.

3 Co(II), 3 THTUD and 6  $ClO_4$  are contained in the asymmetric unit cell (Fig. 5.6). No noteworthy internal interactions were observed in the structure.

It is clear from the structure that the Co metal centre does not lie in the plane of the ring, but almost halfway between the N-donors and the O-donors.  $[Co(THTUD)](ClO_4)_2$  is distorted octahedral. The ligands arrange themselves in such a way that the nitrogen donors of the macrocycle coordinate in a facial orientation (Fig 5.7). The pendant arms fold over and arrange the oxygen donors to

coordinate in a facial manner to the metal ion centre. The coordination of the OH-groups can clearly be seen in this structure (Fig 5.7).

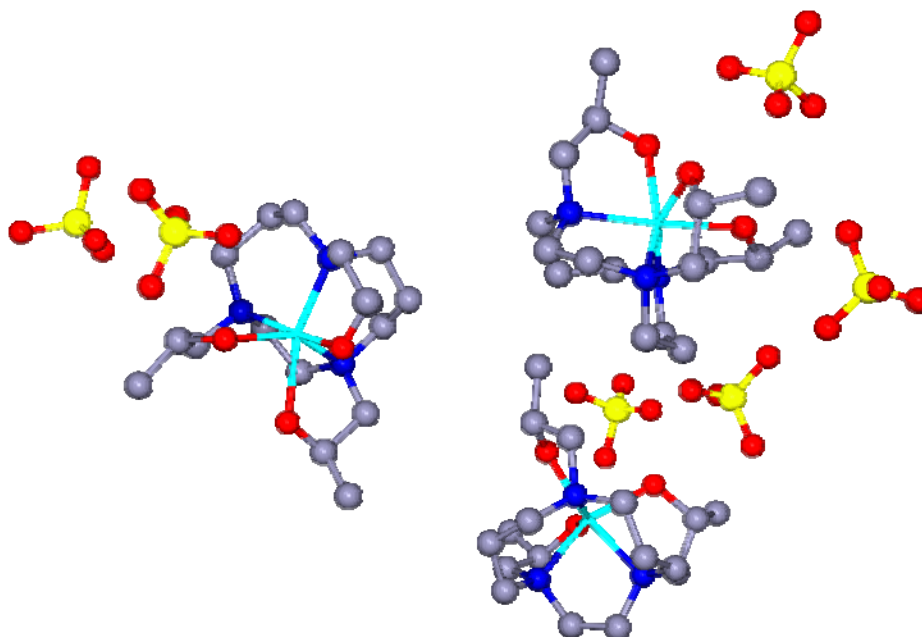


**Fig 5.6** The asymmetric unit cell of  $[\text{Co}(\text{THTUD})](\text{ClO}_4)_2$  showing the three complexes with their perchlorate counter ions.

A similar structure,  $[(\text{Co}\{\text{H}_3\text{L}^2\}_2(\text{NO}_3)_2)](\text{PF}_6)_2$ , was investigated by Al-Sagher *et al.*<sup>16</sup> The structure that they discussed, crystallised as a dimer with trigonal prismatic coordination geometry. The present  $[\text{Co}(\text{THTUD})](\text{ClO}_4)_2$  crystallised as a monomer with distorted octahedral coordination geometry. The bond lengths between the oxygen donors and the Co(II) in our structure (Fig. 5.7) are slightly longer than in the reported structure of Al-Sagher *et al.* The bond lengths between the nitrogen donors and the Co(II) in our structure are slightly shorter than in the reported structure of Al-Sagher *et al.*

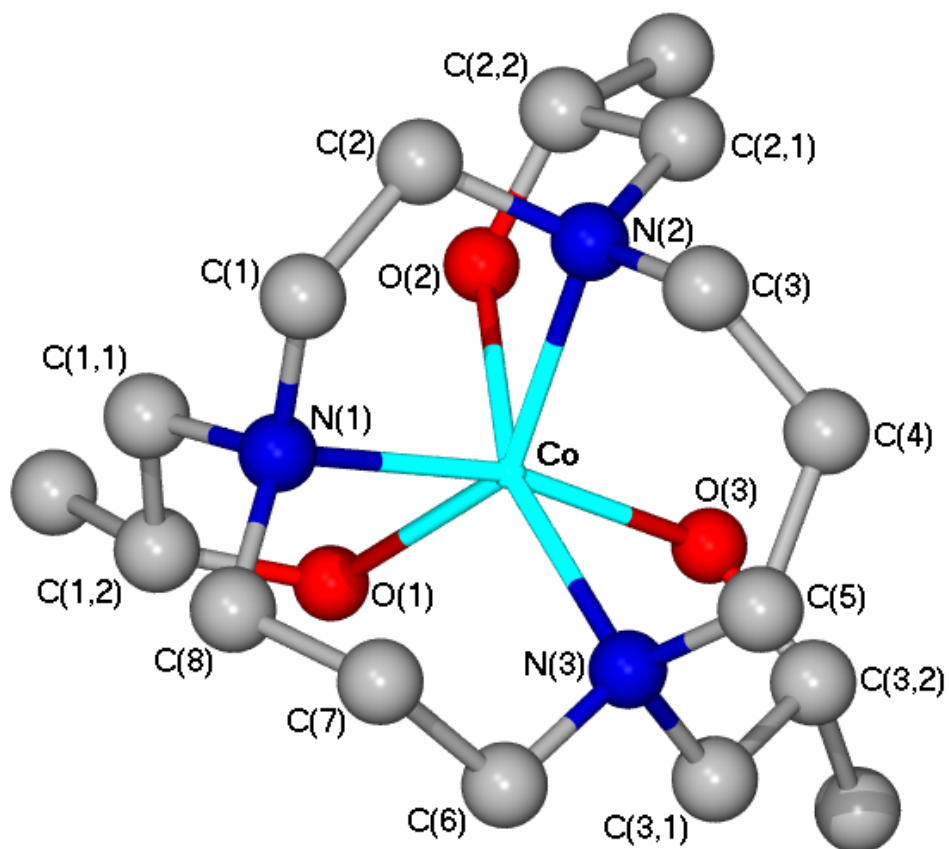


**Fig. 5.7** Structure of  $[\text{Co}(\text{THTUD})](\text{ClO}_4)_2$  showing atomic numbering scheme. The facial coordination of the N-donor atoms and the O-donor atoms is shown.

**Table 5.4** Bond lengths and the bond angles of the  $[\text{Co}(\text{THTUD})](\text{ClO}_4)_2$ . The \* indicates where there are 6-membered rings in the structure. Table 5.4 refers to Fig. 5.7.

Bond Lengths (Å)		Bond Angles(°)	
Co-O(1)	2.049(5)	N(1)-Co-N(2)	96.5(3)
Co-O(2)	2.114(8)	N(2)-Co-N(3)*	104.5(3)
Co-O(3)	2.133(6)	N(1)-Co-N(3)*	103.7(3)
Co-N(1)	2.154(7)	N(1)-Co-O(3)	171.4(3)
Co-N(2)	2.159(7)	N(3)-Co-O(2)	159.9(3)
Co-N(3)	2.237(6)	N(2)-Co-O(1)	159.8(3)

The ideal bond lengths for a 6-membered ring that is formed with nitrogen atoms are considered to be about  $1.6\text{Å}$  with all atoms being about the size of C/N (Fig. 5.3). The average bond length from the literature between Co(II) and N is  $2.216\text{Å}$ .<sup>87</sup> For oxygen atoms bonded to the Co(II), it is ideally  $1.9\text{Å}$ .<sup>41</sup> The average bond length from the literature between Co(II) and OH is  $2.089\text{Å}$ .<sup>87</sup> We observe that the oxygen metal bond lengths are somewhat longer than the ideal bond lengths, but in line with the average bond lengths. In this structure all three Co-O

bond lengths are significantly different from each other with Co-O(1) the shortest at 2.049(5)Å. The longest bond is Co-O(3) with a length of 2.133Å. For a 5-membered ring, the ideal bond length between nitrogen and a metal would be 2.5Å (Fig.5.3). The bond lengths in this structure between the nitrogen and the metal ion centre are somewhat shorter than that of the ideal bond length. There is also a difference between the N-Co bonds in the structure itself. The shortest bond distance is Co-N(1) with a distance of 2.154Å. Co-N(2) has a distance of 2.159(7)Å and the longest separation seen between Co-N(3) is 2.237(6)Å. Co<sup>2+</sup> is slightly larger than Mn<sup>2+</sup>, which means that the pendant arms cannot reach as far around as was the case with the Mn-complex.

Unfortunately the R-factor for this structure was high due to disorder from the perchlorate counter ions in the crystal and, therefore, we are not able to compare bond distances and bond angles to similar structures in more detail.

The bond angles between the N-Co-N in [Co(THTUD)](ClO<sub>4</sub>)<sub>2</sub> are smaller than those found in the previously published structure.<sup>16</sup> The ideal angle between the metal centre and the nitrogen atoms is 109.5° for small atoms (Fig. 5.3). In this structure N(4)-Co-N(8) is the closest with an angle of 104.5(3)° which shows that the ligand is already under some strain. For a 5-membered ring the ideal bond angle should be 69° for small atoms (Fig 5.3).<sup>41</sup> The bond angles in [Co(THTUD)](ClO<sub>4</sub>)<sub>2</sub> are far greater at 96.5(3)° (Table 5.4). The reason for these bigger angles is that the carbon bridges keep their preferred angles which now force the rest of the ring into a strained conformation.

The packing of [Co(THTUD)](ClO<sub>4</sub>)<sub>2</sub> along the a-axis is shown in Fig. 5.8. The molecules are stacked in layers with the counter ions packed between these layers. No hydrogen bonding occurred between the complex and the counter ions or between the complexes themselves. There are no intermolecular hydrogen bonds in this structure. The counter ions do not participate in any bonding to the metal complex. No further intermolecular interactions can be described.



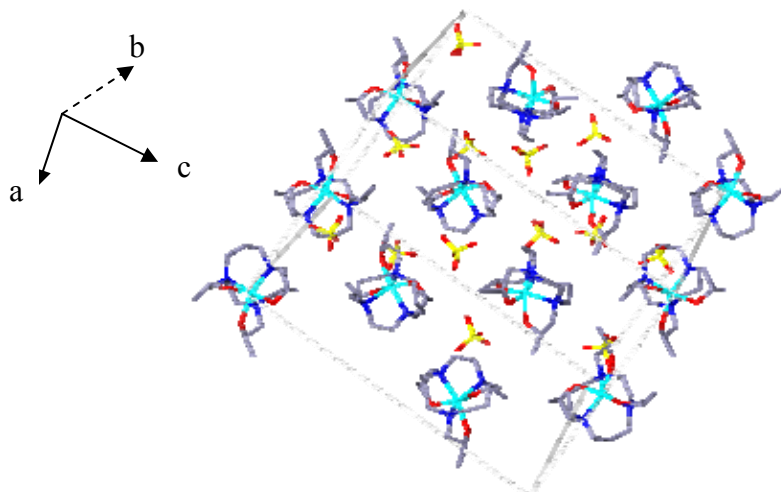


**Fig 5.8** The packing of  $[\text{Co}(\text{THTUD})](\text{ClO}_4)_2$  along the b-axis.

#### 5.4.4 The crystal and molecular structure of $[\text{Zn}(\text{THTUD})](\text{ClO}_4)_2$

The compound crystallised in the monoclinic crystal system, space group  $P2_1$ . No solvent molecules were present in the structure.

The R-factor for this structure was again high owing to disordered perchlorate counter ions.

The molecular structure and atomic numbering scheme is shown in Fig. 5.9. All the hydrogen atoms have been omitted for clarity. Selected bond lengths and bond angles are shown in Table 5.5.

No angle in the structure is close to  $180^\circ$  which encompasses the Zn(II) as part of the axis. Looking in the facial direction ( $C_3$ -axis), no  $60^\circ$  angles are observed between the facial atoms, and the angle between the oxygen and the nitrogen atoms does not define the complex clearly as an octahedral structure. The pendant arms are not very long (average length =  $4.39\text{\AA}$ ) and this leads to a distorted octahedron because the arms cannot reach far enough around to reach the optimal position. The nitrogen atoms and the oxygen atoms are also not lying on top of each other when viewed down the  $C_3$  axis, and therefore the structure cannot be classified as trigonal prismatic. This complex can therefore be best described as a distorted octahedron.

The are 6 Zn(II), 6 THTUD and 12 ClO<sub>4</sub> present in the asymmetric unit cell. The ligands arrange themselves in such a way so that the nitrogen donors of the macrocycle will coordinate in a facial orientation. The pendant arms fold over and arrange to coordinate in a facial manner to the metal ion centre. The counter ions do not participate in any bonding to the metal complex. A similar structure, [Fe<sub>2</sub>(THETAC)<sub>2</sub>H<sub>3</sub>](ClO<sub>4</sub>)<sub>3</sub>, was discussed by Luckay and co-workers.<sup>44</sup> In the structure of Luckay and co-workers, it was found that the crystal forms a dimer and that the ligand lost three protons.<sup>44</sup> In the [Zn(THTUD)](ClO<sub>4</sub>)<sub>2</sub> structure, there is no intermolecular hydrogen bonding and the ligands remained neutral.

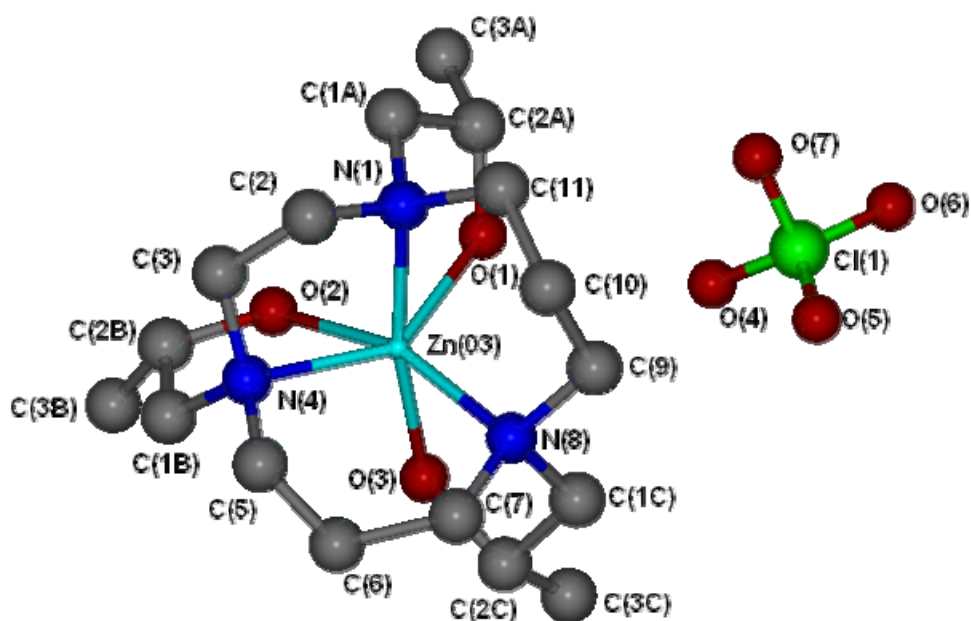


**Fig 5.9** The structure of [Zn(THTUD)](ClO<sub>4</sub>)<sub>2</sub>, with only one perchlorate anion shown for clarity.

Shannon<sup>86</sup> stated that zinc is of medium size and it should not be too much of a problem to coordinate to a metal centre to form either the 5- or the 6-membered chelate rings. There are two 6-membered rings and four 5-membered rings in this complex. The three pendant arms form three 5-membered rings. The fourth 5-membered ring is part of the macrocycle. From the crystal structure it is very clear that the Zn<sup>2+</sup> ion does not enter the cavity of the macrocycle. It lies out of the plane, between the N-donors and the O-donor atoms of the molecule.

<sup>86</sup> R.D. Shannon, *Acta Cryst.*, 1976, **A32**, 751-767

The average bond lengths from the literature between Zn(II) and R-OH is 2.122Å and between Zn(II) and N is 2.171Å.<sup>87</sup> The bond lengths between the metal centre and nitrogen varies between 2.154(10)Å and 2.170(11)Å. The separation between the oxygen donors and the metal centre varies between 2.052(8)Å, 2.132(9)Å and 2.260(11)Å. The reason for this longer bond [Zn-O(2)] is most likely because the pendant arm is positioned between the ethylene bridge and a propylene bridge of the ring. The arm must now bend in such a way to form a bond, that the angle will cause a lot of strain that will pull the arm away from the metal centre.

The bond angle between the N(1)-Zn-O(1)\* is 78.4(4)°, N(4)-Zn-O(2) is 72.9(5)° and between N(8)-Zn-O(3) it is 78.9(4)°. The angle between the Zn(II) and the nitrogen atoms varies significantly as can be seen from Table 5.5. The two 6-membered rings will not have to bend to such an extent as the 5-membered rings and this will lead to less strain and bigger bond angles. The two propylene bridges are longer than the ethylene bridge and the angles that form with the Zn are larger; N(4)-Zn-N(8) = 102.1(5)° and N(1)-Zn-N(8) = 97.8(5)°.

**Table 5.5** The most important bond lengths and bond angles of the molecule in Fig. 5.7 are shown.

Bond Lengths (Å)		Bond Angles(°)	
Zn-O(1)	2.052(8)	N(1)-Zn-O(1)*	78.4(4)
Zn-O(2)	2.260(11)	N(4)-Zn-O(2)*	72.9(5)
Zn-O(3)	2.132(9)	N(8)-Zn-O(3)*	78.9(4)
Zn-N(1)	2.170(11)	N(1)-Zn-N(4)*	87.5(5)
Zn-N(2)	2.164(12)	N(4)-Zn-N(8)**	102.1(5)
Zn-N(3)	2.154(10)	N(1)-Zn-N(8)**	97.8(5)

\* - 5-membered ring

\*\* - 6-membered ring

**Table 5.6** The table shows the crystal data for the three crystals that were obtained in this study.

Compound	[Co(THTUD)]	[Zn(THTUD)]
Empirical Formula	C <sub>17</sub> H <sub>34</sub> C <sub>12</sub> Co N <sub>3</sub> O <sub>11</sub>	C <sub>18</sub> H <sub>33</sub> C <sub>12</sub> N <sub>3</sub> O <sub>11</sub> Zn
Mr	586.3	595.77
Crystal habit	block	block
Crystal size/mm	0.04×0.03×0.01	0.03×0.02×0.015
Crystal system	trigonal	monoclinic
Space group	<i>P</i> 3 <sub>1</sub>	<i>P</i> 2 <sub>1</sub>
a[Å]	16.639	16.8629(12)
b[Å]	16.639	19.3643(13)
c[Å]	23.379	23.6268(17)
α/°	90.00	90.00
β/°	90.00	90.270(2)
γ/°	120.00	90.00
<i>V</i> /Å <sup>3</sup>	5605.5	7715.0(9)
<i>Z</i> , <i>D</i> <sub>c</sub> /Mg m <sup>-3</sup>	9	12
μ(MoKα)/mm <sup>-1</sup>	0.963	1.220
Number of reflections, unique	33740 17133	49119 32431
<i>R</i> <sub>int</sub>	0.0449	0.0428
<i>hkl</i> index range	<i>h</i> -11→ 21 <i>k</i> -21→ 17 <i>l</i> -29→ 30	<i>h</i> ±21 <i>k</i> -24→ 25 <i>l</i> -21→ 30
Data	11001	14239
Restraints, Parameters	1 930	1 1492
<i>F</i> (000)	2754	3596
<i>R</i> <sub>i</sub> , w <i>R</i> <sub>2</sub> <sup>a</sup> [ <i>I</i> >	0.0941	0.1098
2σ( <i>I</i> )	0.2302	0.2705
<i>R</i> <sub>i</sub> , w <i>R</i> <sub>2</sub> (all data)	0.1245 0.2473	0.2099 0.3536
Goodness-of-fit	0.994	0.998

The packing of [Zn(THTUD)](ClO<sub>4</sub>)<sub>2</sub> along the *c*-axis is shown by Fig. 5.10. The molecules are stacked in layers with the counter ions arranged around the metal complexes. There are no solvent molecules present. No further intermolecular hydrogen bonding and no further intermolecular interactions are present.

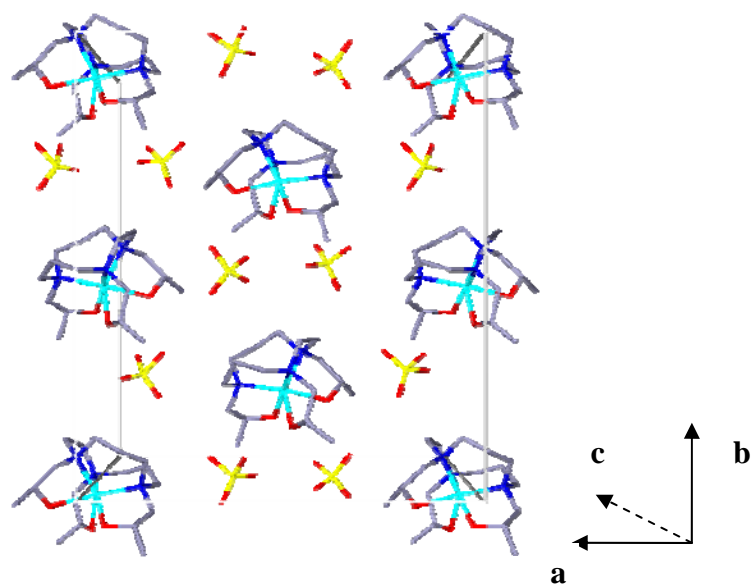


**Fig. 5.10** The packing of the  $[\text{Zn}(\text{THTUD})](\text{ClO}_4)_2$  along the c-axis.

## 5.5 Conclusion

These novel ligands form both 5- and 6-membered rings when co-ordinated to metal ions. In theory, there should be very little discrimination between small and medium sized metal ions. Based on size-match selectivity, the large metal ions are much too big for the small radii of THTD and THTUD.

Although most of the metal ion ligand complexes afforded crystals, we were unable to determine their crystal structures owing to poor crystal quality. What is clear from the three crystal structures obtained is that the metal ion does not occupy the cavity of the macrocyclic ring, it lies out of the plane, almost equidistant between the nitrogen and oxygen donor atoms of the ligands. There is unfortunately disorder due to the large perchlorate counter ions. Due to the strain in the propylene bridges in the macrocyclic ring, the centre carbon of these propylene bridges occupies more than one position when coordinated to the metal ion. This is a feature in all three structures, causing further disorder in the crystal structures.

THTD and THTUD form stable complexes with various size metal ions such as  $\text{Co}^{2+}$ ,  $\text{Zn}^{2+}$  and  $\text{Mn}^{2+}$ . Other methods for crystalization are currently being investigated to produce better quality crystals for all the metal ions that were studied. THTD with

Mn(II) crystallized in an unusual fashion since both octahedral and trigonal prismatic complexes occur in the unit cell. One of the ligands seemed to be deprotonated, but it is not possible to determine which one.

THTUD yielded crystals with both Co(II) and Zn(II). The unit cells have quite a large number of atoms and this caused the R-factors to be high. There was also disorder due to the perchlorate counter ions.

## Chapter 6

### *Conclusion*

The aim of this investigation was to synthesize two novel medium sized triazamacrocyclic ligands with pendant arms. The parent macrocycle has been known for a long time, but by adding the pendant arms we wanted to “fill the gap” between the [9]-ane-N<sub>3</sub> and the [12]-ane-N<sub>3</sub> and see how selectivity is affected by having both 5- and 6-membered rings in the same macrocycle. We characterized the ligands by means of NMR, elemental micro-analysis, mass spectrometry, melting point determination and X-ray crystallography. Although crystals of the free ligands were obtained, they were not big enough to collect data on the X-ray diffractometer.

Secondly, we determined the protonation constants of these two ligands by means of potentiometric titrations, using a glass electrode with an in-built standard. These results were discussed and compared with the parent ligands and other similar ligands with pendant arms. The potentiometric data yielded very consistent results when compared to other similar ligands. The standard deviations and the R-factors are within acceptable limits.

The third aim was to determine some formation constants of the complexes that formed using the two novel ligands THTD and THTUD. The formation constants were determined by means of potentiometric titration using a glass electrode with an in-built standard.

The formation constants were determined with enough certainty to confirm that very stable complexes were formed with the metal ions that were used. These values were also compared to complexes of similar ligands with the same metal ions that were reported in the literature. Some interesting results were obtained. Cd(II) showed an unusual high stability with both THTD and THTUD.

The fourth and final objective was to determine crystal structures of the novel ligands with a series of metal ions, mostly in the first row of the transition metals, as well as with cadmium and lead to see whether (if at all) the size of the ion would play a role in the complexation with the ligands. The structures also gave information on coordination geometry, bond lengths, angles and strain in the rings.

Most of the metal ions did crystallize, but unfortunately not all the crystals were suitable for X-ray crystallography. The structures that were determined, confirmed not only the structures of the ligands, but also the structure of some of the complexes that were formed.

Future work would include further exploration of some of the interesting results which were obtained. The crystal structure of the  $[\text{Mn(II)THTUD}](\text{ClO}_4)_2$  should be investigated further to see whether there is a change in the oxidation state of the Mn(I)-Mn(II). The stability constants for Ni(II) and Cu(II) could not be determined very accurately using potentiometry, hence alternatively this could be done using UV-VIS spectroscopy and working at an ionic strength of  $0.5 \text{ mol dm}^{-3}$ . Crystal structures of the HBr-salts of the free ligands are another possibility to explore, which might shed some light on the pre-organization of the ligand. Although we would in fact be changing the ligand, crystallography could give us information on the  $\log(K_1)$  values for both ligands. Other methods need to be employed to determine the third protonation constants of the ligands. Molecular mechanics could be a further tool which can be used on some of the structures which were obtained. This could indirectly shed some light on why Cd(II) forms such stable complexes with these ligands.